

University of Trento

Daniele Casagrande

STUDY OF TIMBER-FRAME BUILDING SEISMIC
BEHAVIOUR BY MEANS OF NUMERICAL MODELLING
AND FULL-SCALE SHAKE TABLE TESTING

Prof. Maurizio Piazza

Prof. Roberto Tomasi

April, 2014

UNIVERSITY OF TRENTO

Engineering of Civil and Mechanical Structural Systems - XXVI Cycle

Final Examination 10/04/2014

Board of Examiners

Prof. Maurizio Piazza (University of Trento)

Prof. Andrea Prota (University of Napoli, Federico II)

Prof. Carmelo Gentile (Polytechnic University of Milan)

Prof. Helmut Wenzel (BOKU, University of Vienna)

ACKNOWLEDGEMENTS

I would like to thank my supervisors prof. M. Piazza and prof. R. Tomasi for giving me the possibility to work within the Timber Research Group of University of Trento and for supporting me during these three years. It was a great pleasure to collaborate with all the staff. A particular acknowledgement goes to Tiziano Sartori, Ivan Giongo, Paolo Grossi, Cristiano Loss and Simone Rossi.

A particular acknowledgement to Rubner Haus company and FederLegnoArredo federation for partially funding my PhD grant.

I am really grateful to undergraduate students for their important help: Alessandro Armanini, Gianluca Mischi, Marco Pedrotti, Simone Rossi, Federico Pederzoli, Alessandro Franciosi, Mirko Testoni and Michele Zanotelli.

The staff of Eucentre TreesLab is gratefully acknowledged for their assistance during the seismic tests.

A particular thank to technical staff of the Material and Structural testing laboratory of the Department of Civil, Environmental and Mechanical Engineering of the University of Trento: Alfredo Pojer, Tiziano Dallatorre, Ivan Brandolise and Luca Corradini.

The work presented in this thesis is part of the CHI-Quadrato research project in which the Department of Civil, Mechanical and Structural Engineering of University of Trento was involved. This project was financed by the Autonomous Province of Trento. The investigation of the structural behaviour of timber frame buildings was directly supported by LegnoCase company.

SUMMARY

Timber frame constructive system can be considered one of the most important and most spread worldwide. In many countries, such as U.S.A., Canada, New Zealand, Germany and Scandinavia, the constructive process of timber buildings is characterized by a strong tradition and experience, so that most of low-rise residential houses are generally constructed using wood-based materials. On the contrary, in Italy the timber frame construction system do not belong to the residential building tradition. In fact, the majority of residential houses is characterized by masonry structures (typically if built before the 70's) or by reinforced concrete ones. However, during the last decade, the timber construction system has been characterized by a significant growth in the Italian market. The increasing sensitivity to environmental issues and the need to reduce the construction time in situ, in addition to the importance of the design details, have given Italian timber buildings a leading role in the constructive market also in European Subalpine countries (historically not associated with such construction technology).

The timber-frame structural type has not been put on the Italian market referring to the North American constructive system but to the European one and in particular to the constructive system of those countries characterized by high tradition and experience in this field (Scandinavia, Germany and Austria). The European constructive system differs from the American one mainly for the considerable prefabrication process. This makes the building similar to an industrial product. Moreover, larger sizes of the elements constituting the walls themselves are used. The traditional American "plat-form frame" system is generally made up with "two by four" studs (39 by 89 mm) whereas in European countries larger cross section elements (usually 60-100 mm by 100-140 mm) are used.

The development of the timber-frame buildings in subalpine countries, such as Italy, has required a specific investigation about their seismic performance. Unlike the countries of Northern Europe and Germany, the Mediterranean Area is in fact characterized by high seismic hazard. Nevertheless the researches and the studies about timber-frame buildings seismic behaviour are rather limited; a direct demonstration of this is the limited number of design rules which European Standards (Eurocode 8) require for timber building seismic design. Many studies and researches have been conducted on the European timber frame system, concerning with different engineering topics, but very few of them concerned with their seismic capacity. For this reason, during the last years, many research projects, aimed at the investigation of the timber buildings seismic behaviour, have been financed in Europe.

One of these has been the *CHI-QUADRATO* industrial research project whose objective has been the study of structural, thermic and constructive matters for a typical Italian timber-frame constructive system. Within this project, the Department of Civil, Mechanical and Structural Engineering of University of Trento has been involved to investigate the seismic behaviour of such buildings. The research program has been characterized both by a wide experimental campaign and by the proposal of numerical and analytical models for the analysis and the design of timber buildings under seismic loads. Some of these topics are deeply investigated and described by the work presented in this thesis.

The work has been divided in three different but closely related phases.

In the first part, the behaviour of a single timber-frame wall under a horizontal force is discussed. The main objective is the proposal of some simplified analytical expressions aimed to describe both its linear and its non-linear behaviour. Depending on the mechanical and geometrical properties of the structural components, an analytical model for the prediction of the stiffness, strength and ductility of the wall is presented. This model may be used both for the implementation of a simplified numerical model of the wall and for the definition of the relationship between the local mechanical properties (structural members and connection devices) to the wall ones. This aspect is crucial in the traditional approach of seismic engineering and represents an innovative issue for timber buildings.

In the second part of the thesis, a linear numerical modelling for the analysis of multi-storey timber-frame buildings under seismic loads is presented. In common practice the seismic analysis models for timber buildings are very simple and based on strong hypotheses. The wall stiffness is usually considered linear dependent on the wall length and the lateral force method is often used, without taking account of the dynamic properties of the structure. However, in many cases a more advanced analysis should be performed, (i.e. modal response spectrum analysis) requiring a suitable numerical model capable to consider all significant deformation contributions of timber frame walls. In the first part of the thesis in fact, is demonstrated that the wall stiffness cannot be considered a priori linearly proportional to the wall length. For these reasons an innovative numerical modelling, based on the single wall numerical model and a new analysis approach are discussed. The analysis model is defined “unified” because it can be used for different timber structural types and not only for the timber frame building, objective of this thesis.

The third and last part of thesis describes a full scale three-story building shaking table test performed at the Eucentre laboratory in Pavia (Italy). This test represents the last phase of the experimental campaign conducted by the Timber Research Group of the

University of Trento about the investigation of the seismic behaviour of a typical Italian timber frame building within the CHI-QUADRATO project. Many interesting issues about the seismic performance of a full scale timber building, designed in accordance with Eurocode 8, were investigated. The interaction between the structural components were in particular analysed. More than one hundred instruments were used to monitor the behaviour of the building during the seismic tests measuring accelerations, displacements and forces. The main results and conclusions are reported.

INDEX

ACKNOWLEDGEMENTS.....	5
SUMMARY	7
INDEX.....	11
1 INTRODUCTION.....	17
1.1 Objectives and thesis layout	24
2 STRUCTURAL DESIGN OF TIMBER-FRAME WALLS.....	27
2.1 Vertical load path.....	30
2.2 Out-of-plane horizontal loads	33
2.3 In-plane horizontal force.....	34
2.4 Seismic horizontal force distribution.....	41
2.5 Timber-frame building behavior factor q	43
3 LINEAR ANALYSIS OF A TIMBER-FRAME WALL UNDER A HORIZONTAL FORCE	47
3.1 Elastic horizontal displacement of a timber frame wall under a horizontal force	47
3.1.1 Rigid-body rotation.....	48
3.1.2 Sheathing panel shear deformation.....	49
3.1.3 Sheathing-to framing fastener deformation	50
3.1.4 Rigid-body translation	54
3.1.5 Total elastic horizontal displacement.....	55
3.2 Horizontal stiffness of a timber frame wall	56

3.3	Parametric study of the wall stiffness.....	60
3.4	Finite element modelling of a timber-frame wall	62
3.4.1	Complete model.....	62
3.4.2	Simplified model.....	63
4	ELASTO-PLASTIC ANALYSIS OF A TIMBER -FRAME WALL UNDER A HORIZONTAL FORCE	67
4.1	Rheological model for the assessment of the non-linear behavior of a timber-frame wall	68
4.2	Mechanical properties of sources of deformation	69
4.2.1	Rigid body rotation	69
4.2.2	Friction block.....	71
4.2.3	Horizontal non-linear spring for the rigid-body rotation of the wall	71
4.2.4	Rigid-body translation contribution	73
4.2.5	Sheathing-to-framing fastener contribution.....	75
4.3	Definition of the idealized elasto-plastic behavior of a timber-frame wall	78
4.4	Elasto-plastic behaviour of a fully anchored timber-frame wall.....	87
4.4.1	Elasto-plastic analysis of a fully anchored wall with E.A.T.W.-1.0.....	90
4.5	Case study	101
4.6	Performance based seismic design of a timber-frame wall	108
4.6.1	Design Example.....	111
5	LINEAR ANALYSIS OF TIMBER-FRAME MULTI-STOREY WALLS UNDER HORIZONTAL FORCES.....	121

5.1	A backup numerical modelling for multi-storey walls under horizontal forces	122
5.1.1	Backup numerical modelling for a vertically-aligned wall (m x 1)	122
5.1.2	Study of 1-storey series of walls (1 x n)	124
5.1.3	Case study	126
5.1.4	Modelling for a series of walls (m x n)	130
5.1.5	Case study	131
5.2	Linear seismic analysis of timber frame walls	135
5.2.1	Lateral force method	135
5.2.2	Modal Response Spectrum analysis	136
5.2.3	Case study	140
6	3-STOREY TIMBER-FRAME BUILDING SHAKE TABLE TEST	147
6.1	Geometry and Design of the specimen	147
6.2	Specimen assembly and description of instrumentation	152
6.3	Test design	157
6.4	Analysis of results	164
6.4.1	Global hysteretic response	173
6.4.2	Modal testing	175
6.5	Analysis of results	183
7	CONCLUSIONS	187
7.1	Linear backup numerical modelling (a)	187

7.2 Analytical analysis model of 1-storey timber frame wall nonlinear behaviour (b).
.....189

7.3 Full scale 3-storey timber frame building shake table test (c).....190

REFERENCES193

PUBLICATIONS199

1 INTRODUCTION

Timber frame constructive system can be considered as one of the most important and most spread worldwide. In many countries, such as U.S.A., Canada, New Zealand, Germany and Scandinavia (Figure 1.1), this constructive process is characterized by a strong tradition and experience, so that most of low-rise residential houses are generally constructed using wood-based materials.



Figure 1.1: *Swedish Timber Frame House*

Up until not so long ago, the majority of timber-frame houses were built based on experience and tradition rather than on specific design rules. In concrete and steel constructions there were extensive experimental campaigns in the past and several

Standards and Line Guides are nowadays available. Conversely, for timber constructions, many aspects have not yet been investigated and the gap with other materials has not still been bridged. In spite of this shortcoming, a lot of construction handbooks exist, representing the cultural baggage of the timber-frame structures. Based on a strong tradition, they describe exhaustively the realization phases, the details and the materials which should be used in order to satisfy the structural and serviceability requirements.

During last 30 years there has been a significant increase of tests and research programs aimed to the technological development of new devices or wood based materials and to the improvement of timber-frame building structural performances. The significant damages from earthquakes and high wind loads has created a need to examine the current design practice. As reported in next chapters, the horizontal load design is without any doubts the most significant and relevant part of the design process for a timber frame building because it greatly influences the choice of structure elements and number of the connection devices (angle brackets, hold-down, etc.). The results of these studies and researches have permitted to get a new design philosophy which, added to the tradition and experience, has been needed to improve the timber-framed building performances, in particular under seismic loads. However, as reported above, the gap with others types of construction is still to be bridged: nowadays many research programmes have started in several countries characterized by a high seismic hazard.

Concerning with the Italian market, the timber frame construction system does not belong to the residential building tradition. In fact, the majority of residential houses is characterized by masonry structures (typically if built before the 70's) or by reinforced concrete ones. The use of timber as structural material was highly reduced and confined to the roof construction in the Dolomite Area. However, during the last decade, the timber construction system has been characterized by a significant growth. The increasing sensitivity to environmental issues and the need to reduce the construction time in *situ*, have given timber buildings a leading role in the constructive market also in European Subalpine countries (historically not associated with such construction technology). The development of new manufacturing technologies (i.e. new types of connectors, connection devices, sheathing panels, etc.), and, in particular, the production of the Cross Laminated Timber (CLT) panels have contributed significantly to the timber building exponential growth in Italy.

The timber-frame construction system has not been put on the Italian market referring to the North American structural type but to the European one, and in particular to the constructive system of those countries characterized by high tradition and experience in this field (*i.e.* Scandinavia, Germany and Austria). The strict performances required by Italian Guidelines and Standards about thermal insulation, sound insulation, vibration and durability, make the European constructive system, without any doubts, the most suitable for Italy. In order to optimize the constructive process and to guarantee definite construction times *in situ*, the European constructive system is characterized by a considerable prefabrication process, making the building similar to an industrial product (Figure 1.2, Figure 1.3). The assembly in the factory of the framed-walls, which constitute the primary structural element, guarantee to reduce significantly the work phases *in situ* (joining the walls, laying the floors and making the final finishes) and thus to reduce both the constructive times and the mistakes in progress. Hence, it is clear how the whole construction process must be supported by a careful design phase in order to produce in the factory all structural elements and to make them ready for their placing *in situ*. A resulting increase of the production quality is expected: all details must be designed and built on purpose.

A further reason for which the European timber-frame constructive system differs from the North American one is the size of the elements constituting the walls themselves. The traditional "plat-form frame" system generally is characterized in fact the so-called "two by four" studs whereas in Italy and in European countries larger cross section elements (usually 60-100 mm by 80-160 mm section) are used. This guarantees the possibility of interposing a thicker material insulation layer in the walls. Moreover a higher robustness of the construction is obtained.

The development of the timber frame buildings also in subalpine countries, such as Italy, needed to investigate the seismic performance of timber buildings made by European constructive system technology. Unlike the countries of Northern Europe and Germany, the Mediterranean Area is in fact characterized by a high seismic hazard, requiring special construction details, which are not necessary in the common design for static loads.

However, the researches and the studies about the seismic behaviour of European timber frame constructive system have been not many; a direct demonstration is the limited number of design rules and requirements for timber building seismic design in European Standards (Eurocode 8). Many studies and research programs have been

INTRODUCTION

conducted on the European timber framed system, dealing with different interesting topics, but very few of them have been concerned with the performance of timber buildings under seismic loads. The main reason is that European countries with a high tradition in timber constructions cannot be considered significant seismic areas.



Figure 1.2: *Timber frame wall assembling in the factory*

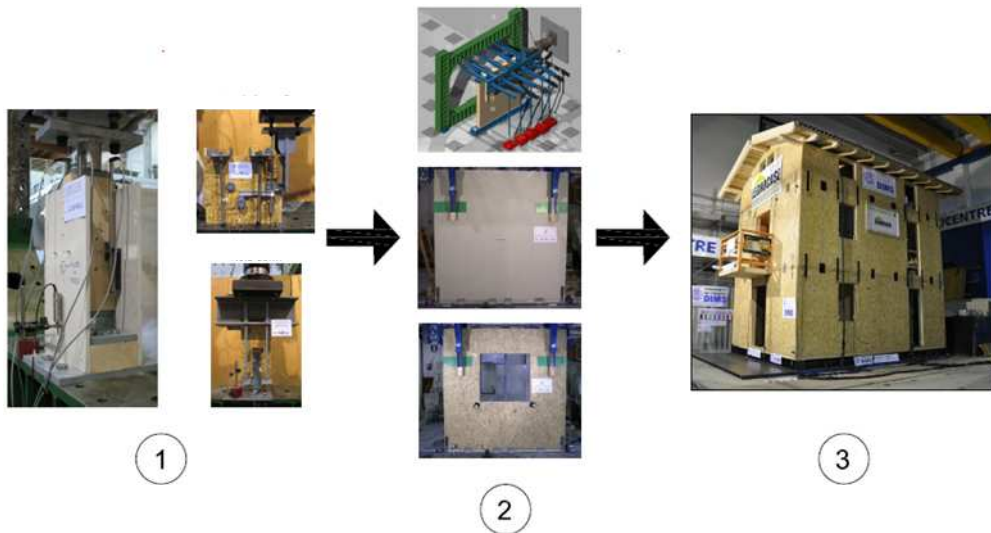


Figure 1.3: *Prefabricated wall placing in situ*

However, it is important to highlight how the seismic behaviour of timber buildings has been deeply investigated in other countries, such as U.S.A and New Zealand, which, as known, are characterized by a very high seismic hazard. The most important international research projects have been conducted in these countries, improving significantly the seismic timber buildings behaviour knowledge. Nevertheless the North American constructive system, as mentioned previously, differs from the European one, both for the prefabrication process and for the size of the wall elements.

For this reason in the last years many research projects, aimed at the study of the timber buildings seismic behaviour, have been financed in Europe in order to propose new design rules and Standards requirements, and to develop new useful technologies and devices for timber buildings in seismic areas.

One of these has been the Chi-Quadrato industrial research project whose main objective has been the study of structural, thermic and constructive matters for a typical Italian timber frame constructive system. Within this project, the Department of Civil, Mechanical and Structural Engineering of University of Trento has been involved to investigate the seismic behaviour of such buildings. The research program has been characterized both by a wide experimental campaign and by the proposal of numerical and analytical models for the analysis and the design of timber buildings under seismic loads.



The research has been divided in three different, but sequential and closely related, working phases (Figure 1.4).

The first phase has been concerned with the study of the structural components which guarantee the stability of a timber frame under a horizontal force. The study focused in particular both on the wall connections to the ground (used in order to prevent the rigid motion of the wall, Figure 1.5) and on the sheathing-to-framing connection by means of fasteners.



Figure 1.5: *Hold Down Load Test*

The second phase studied the behaviour of a single timber frame wall. By means of the data collected during the first phase an experimental campaign has been designed and performed in order to investigate the behaviour of a timber frame wall subjected to a horizontal force (Figure 1.6). In addition, numerical and analytical analyses have been developed for the prediction of the wall behaviour, depending on the mechanical and geometrical properties of the structural components.



Figure 1.6: *Timber Frame Wall Load Test*

The third and last phase focused on the seismic behaviour of the whole building. The main objective has been in particular the study of the interaction between the structural components. A full scale shake table test was performed and a numerical prediction analysis model was proposed.

1.1 Objectives and thesis layout

The work of this thesis focuses on the second and the third phase of the research program described in the previous section and is concerned with both the experimental campaign and the numerical analyses.

Chapter 2 reports the common structural verifications required for a timber frame wall under vertical and horizontal loads. The role of each structural component (wood members and connection devices) is described. Moreover some aspects of the common-in-practice design methods and the related assumptions are discussed.

In chapters 3 and 4 the behaviour of a single wall under a horizontal force is investigated. Several analytical expressions are proposed in order to describe the linear and the non-linear behaviour of a timber frame wall subjected to a horizontal load. Depending on the mechanical properties of each structural component, an analytical prediction model capable to evaluate the strength, stiffness and ductility of the wall is presented and a simplified numerical modelling is described. The proposed analysis method defines the analytical relationship between the local mechanical properties (strength, stiffness and ductility), related to the structural components and to the connection devices, and the wall's ones. This matter is crucial in the traditional approach of seismic engineering and represents an innovative issue for timber building seismic design. As known, in fact, the seismic design should be referred not only to structure strength but also to its stiffness (fundamental for serviceability limit states) and to its ductility (required for the definition of the behaviour factor). Both Italian and European Standards [*NTC08*, *Eurocode 8*] are nowadays quite lacking in requirements for the seismic design of timber buildings. A direct proof is that the design rules which are to be satisfied in order to guarantee a high behaviour factor, and hence a high energy dissipation during a seismic event, are very few, as described in chapter 2. Moreover no specific rule for the application of the capacity design of a timber structure is suggested

Chapter 5 is concerned with the proposal of a linear back-up numerical modelling for the seismic analysis of multi-storey timber frame buildings. In common practice the wall stiffness is usually considered linear dependent on the wall length and simple lateral force method is used, without taking account of the dynamic properties of the structure. However, in many cases, a more advanced analysis should be performed, such as modal response spectrum analysis, requiring a suitable numerical model capable to

consider all significant deformation contributions of timber framed walls. In the first part of the thesis, it is demonstrated that the wall stiffness cannot be considered a priori linearly proportional to the wall length. For these reasons an innovative numerical modelling, based on the single wall numerical model, and a new analysis approach are presented.

Chapter 6 describes a full scale three-story building shaking table test at the Eucentre laboratory in Pavia (Italy). Several interesting aspects about the seismic performance of a full scale timber building, designed in accordance with Eurocode 8, were investigated. The interaction between the structural components was in particular analysed. More than one hundred instruments were used to monitor the behaviour of the building during the seismic tests measuring accelerations, displacements and forces. The main results and conclusions are reported. The design phase, the execution tests and the results are described.

In chapter 7 the discussion of results and the main conclusions for each part of the thesis work are presented.

2 STRUCTURAL DESIGN OF TIMBER-FRAME WALLS

Timber frame buildings are characterized mainly by a “wall” structure. Unlike “frame” structure, both vertical and horizontal loads are absorbed by timber-frame walls. Therefore, the timber-frame wall represents the fundamental structural element of the building as it transmits gravity loads to the foundations and guarantees the stability of the whole structure against lateral forces (wind or earthquake).

Walls are defined “framed” in relation to their inner structure, formed precisely by a timber frame (Figure 2.1). Each wall is characterized by two horizontal beams, the bottom one and the top one, and by vertical studs. In order to guarantee the lateral stability of the frame, lateral sheathing panels are connected to the frame by means of metallic fasteners (nails or staples). For a typical Italian constructive system studs are generally characterized by a thickness ranging between 100 mm and 160 mm and their spacing along the wall is usually between 60 cm and 70 cm. They are made of solid construction timber or finger-jointed solid construction timber (KVH). Particle composite (OSB), Particleboard, Fiberboard (MDF), Plytimber or Gybsum-fiber panels are used as sheathing panels. The metallic fasteners are usually ring nails, with a diameter ranging

from 2.5 mm to 3.1 mm, or staples. Fastener spacing ranges between 50 mm and 150 mm along the beams and the outer studs of each panel. In order that the centre stud may be considered to constitute a support for a sheet, the spacing of fasteners in the centre stud should not be greater than twice the spacing of the fasteners along the edges of the sheet.

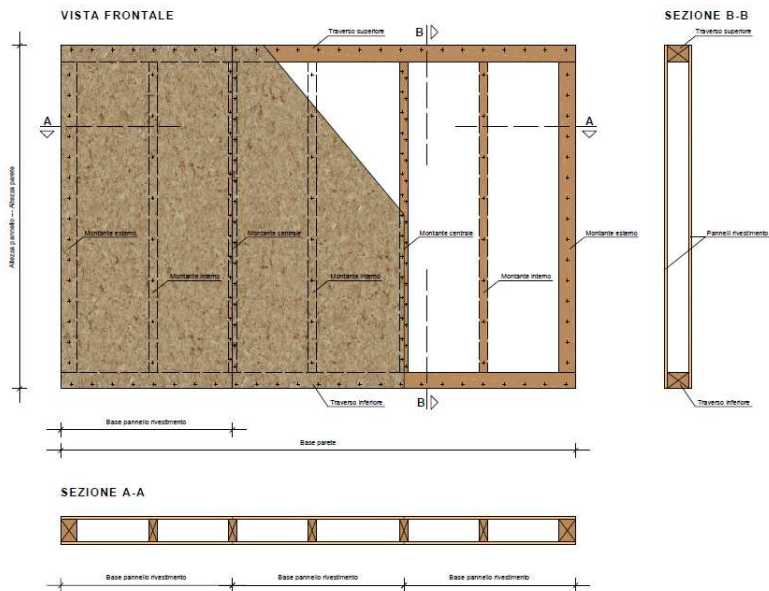


Figure 2.1: Timber-frame wall [Rossi, S. 2012]

The wall anchorage to the foundations, or to lower walls in multi-storey buildings, is usually achieved by means of metallic devices or screws. In order to prevent the wall rigid rotation, one or more metallic devices, called Hold-Down, are displaced at each wall corner (Figure 2.2); the wall rigid translation is generally prevented by angle brackets (Figure 2.3), steel plates or inclined screws (Figure 2.4). The metallic devices are connected directly to the wooden frame by means of ring nails and to the foundation elements by appropriate anchor bolts (Figure 2.5).



Figure 2.2: *Hold-downs*



Figure 2.3: *Angle brackets*

Horizontal floors are generally made up by box section elements or by wooden joists. In both cases in order to achieve a diaphragm behaviour of the floor, timber panels should be superimposed. An efficient floor connection to the underlying walls is also required in order to transfer seismic loads to the structural bracing system, represented by the walls themselves.

In the next sections the more significant verifications for a timber frame wall are reported. The expressions are referred to Eurocode 5. Vertical load, out-of-plane horizontal loads and in-plane horizontal force are considered. Moreover the horizontal force distribution of the walls for wind or seismic loads is explained, referring to the common-in-practice method. Lastly, the most significant aspects of seismic design of timber frame buildings are summarized.

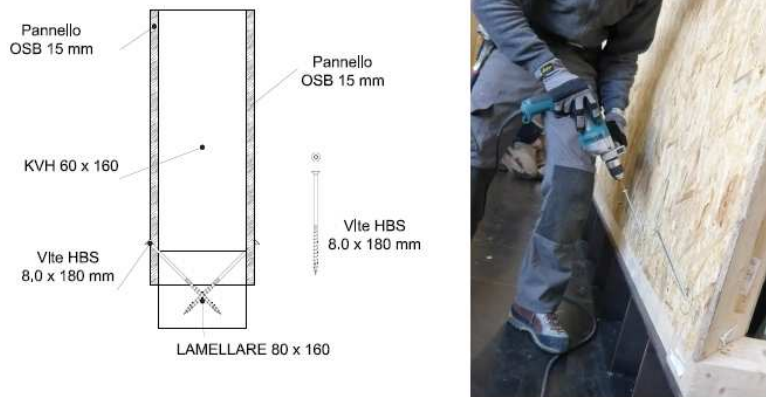


Figure 2.4: *Bottom beam Inclined screws*



Figure 2.5: *Hold-down and Angle brackets positioning*

2.1 Vertical load path

As reported in previous section, vertical loads may be absorbed by the walls, whose task is to transmit the dead and live loads from the floors to the foundations. In some cases, however, for architectural reasons, timber columns, designed to transmit the loads carried by beams to the ground, might be used. This solution is particularly efficient in order to guarantee a considerable freedom in the flat space distribution. Inner

walls can thus be neglected from a structural point of view; they play only the role of partition walls.

Timber-frame walls are characterized by the presence of a top timber beam on which are generally connected the floor elements by means of vertical screws. The top beam is supported in turn by equally spaced (60-80 cm) vertical timber studs. In case of openings (windows or doors, Figure 2.6), orthogonal wall joints or significant concentrated loads on the top beam, the insertion of additional studs or the use of larger section studs may be required. It is important to highlight that the frame wall prefabrication is particularly efficient and cost-effective if the structure is regular. In this case, in fact, an excessive insertion of additional elements (studs or lintels) is not necessary. Wall modularity represents a significant advantage in the prefabrication phase.



Figure 2.6: *Openings in a prefabricated timber-framed wall*

The verification for the gravity load is to be performed for all structural wood elements. Concerning the top beam, the bending and shear stresses are to be calculated, assuming the top beam as a multiple span continuous beam. In the event that openings are larger than the stud spacing, a reinforcing timber lintel may be required. According to the Eurocode 5 the bending and shear verification should be satisfied:

$$\sigma_{m,d,ub} \leq f_{m,d,ub} \quad (2.1)$$

$$\tau_{v,d,ub} \leq f_{v,d,ub} \quad (2.2)$$

where:

- $\sigma_{m,d,ub}$ is the design bending stress for the upper beam
- $f_{m,d,ub}$ is the design bending strength for the upper beam
- $\tau_{v,d,ub}$ is the design shear stress for the upper beam
- $f_{v,d,ub}$ is the design shear strength for the upper beam

The section size of studs should be selected in order to satisfy the stability verification. Stud section is usually rectangular: the base section is parallel to the wall length direction and whereas the section height is equal to the wall thickness. Since in both directions studs may be assumed as a vertical pinned beam, the z-z axes (Figure 2.7) should be considered as the axis with the greater slenderness. Nevertheless the presence of a good connection between the sheathing panel and the stud guarantees a considerable reduction of the stud effective length along the z-z axis. For this reason the stud stability verification is carried only referring to the y-y axis according to the equation (2.3), as reported in section 6.3.2 of Eurocode 5:

$$\sigma_{c,0,d,stud} \leq k_{c,y-y} \cdot f_{c,0,d,stud} \quad (2.3)$$

where:

- $\sigma_{c,0,d,stud}$ is the design compressive stress along the grain
- $f_{c,0,d,stud}$ is the strength compressive stress along the grain

A further important verification concerns the load transmission from the studs to the bottom timber beam which is compressed perpendicular to the grain. This check, especially in the case of multi-story buildings, may be very limiting and may influence significantly the choice of the structural element dimensions. According to the section 6.1.4 of Eurocode 5 the following expression should be satisfied:

$$\sigma_{c,90,d,lb} \leq k_{c,90} \cdot f_{c,90,d,lb} \quad (2.4)$$

Where:

- $\sigma_{c,90,d,bb}$ is the design compressive stress perpendicular the grain for the bottom beam
- $f_{c,0,d,bb}$ is the strength compressive stress perpendicular the grain for the bottom beam

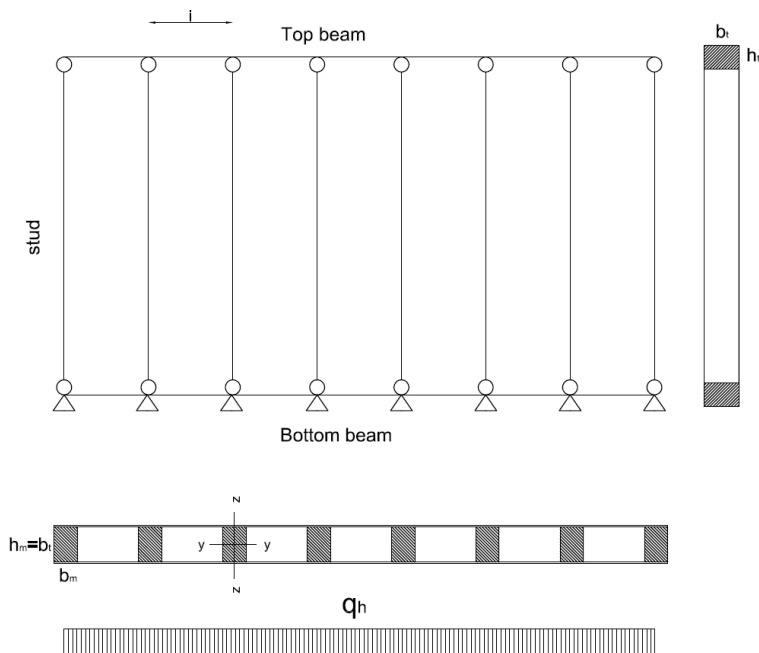


Figure 2.7: Timber-frame wall model loaded by uniform vertical load q_v and wind out-of-plane horizontal load q_h

2.2 Out-of-plane horizontal loads

In the case of horizontal transverse load q_h (such as wind load for outer walls, Figure 2.7) the stability verification of the studs must be corrected, because the combined

effect of the wind out of plane bending and of the vertical load q_v compression is to be considered. Also in this case each stud is assumed a simple pinned beam. The expression for a column subjected to combined bending and compression, according to EC5, should be satisfied:

$$\frac{\sigma_{c,0,d,stud}}{k_{c,y} \cdot f_{c,0,d,stud}} + \frac{\sigma_{m,y,d,stud}}{f_{m,y,d,stud}} \leq 1 \quad (2.5)$$

2.3 In-plane horizontal force

The calculation model used for the wall verifications against vertical loads assumes the studs as simple pinned vertical elements, connected superiorly and inferiorly by a continuous beam. Hence, it is evidence how the wall cannot support horizontal actions in its plane and a bracing, capable to guarantee the lateral stability of the frame, is required (Figure 2.8).

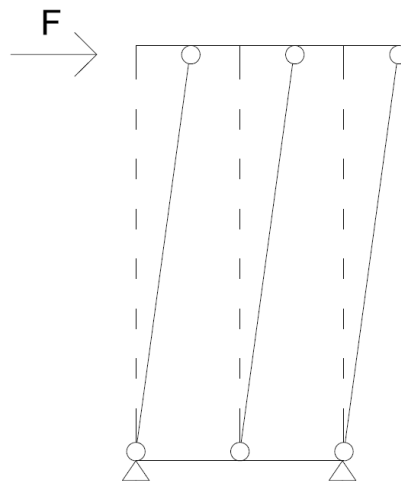


Figure 2.8: Labile frame loaded by a horizontal force F

The wall bracing is made up with wood-based panels (OSB, plywood or gypsum-fibre) connected to the timber frame by means of metallic cylindrical fasteners (ring nails in the

case of wooden panels and staples in the case of gypsum-fibre panels). The panel length should be equal to twice stud spacing to guarantee a regular nailing spacing on the panel edge. The panel should also be nailed to the central stud (usually the spacing is twice the spacing required on the edge of the panel) in order to prevent the panel shear instability.

The shear transmission between the sheathing panel and the timber frame may be analysed using in first approximation the lower bound theorem limit analysis, assuming a rigid-perfectly plastic behaviour of the cylindrical fasteners and an infinite stiffness of the wooden frame and of the panel. Supposing a constant shear stress distribution on the panel edge, it is possible to calculate, by simple equilibrium, the shear stress magnitude. Considering a wall with length l equal to the length b of a single panel (the distance between the studs is therefore equal to $b/2$) and considering a regular fastener spacing s along the panel edge (Figure 2.9), the shear stress v_d on the edge of the panel is given by:

$$v_d = \frac{F_d}{b} \quad (2.6)$$

where F_d is the horizontal force acting on the wall. The shear force $F_{c,d}$ on each fastener is therefore equal to:

$$F_{c,d} = v_d \cdot s = \frac{F_d}{b} \cdot s \quad (2.7)$$

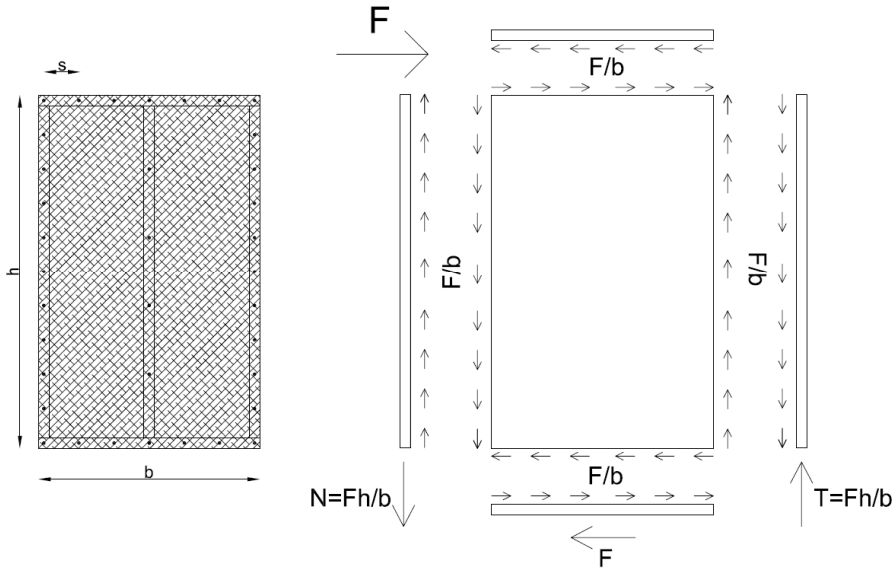


Figure 2.9: Sheathing panel shear stresses

In order to prevent the wall rigid rotation a compression force N and a force traction T are to be transferred to the foundation:

$$T_d = N_d = \frac{F_d \cdot h}{b} \quad (2.8)$$

where h is the height of the wall.

If the compression force can be transmitted directly to the ground by the simple contact of the stud with the foundation element, for the transmission of the vertical tensile force a specific connection device is required. This device, called hold-down, is positioned on each corner of the wall and connected to the outer studs by means of ring nails and to the foundation by means of anchor bolts.

In order to prevent the horizontal rigid body translation of the wall angle brackets or screws are used. Their spacing is usually uniform and equal to s_a . The design force for each of them $F_{a,d}$ for each device is thus given by:

$$F_{a,d} = \frac{F_d}{b} \cdot s_a \quad (2.9)$$

If the horizontal force F and the traction force T are to be transmitted from an upper wall to a lower one, suitable devices should be used, such as steel plates nailed to the wall (Figure 2.10).



Figure 2.10: *Nailed steel plates for upper wall connection*

In most cases the walls are subjected by a uniform load (dead load and live load) as described in section 2.1: the equilibrium of the wall thus should take into account its stabilizing effect (Figure 2.11). Assuming the centre of rotation of the wall is placed at one of the bottom corner of the wall, the vertical load q_v is transmitted only to two outer studs; the compressive force is equal to:

$$N_q = \frac{q \cdot l}{2} \quad (2.10)$$

The presence of the vertical load does not change, on the contrary, the stress distribution related to the sheathing-to-framing connection and the rigid body translation

one. This force is to be added and subtract respectively from the tensile and compressive force of the outer studs

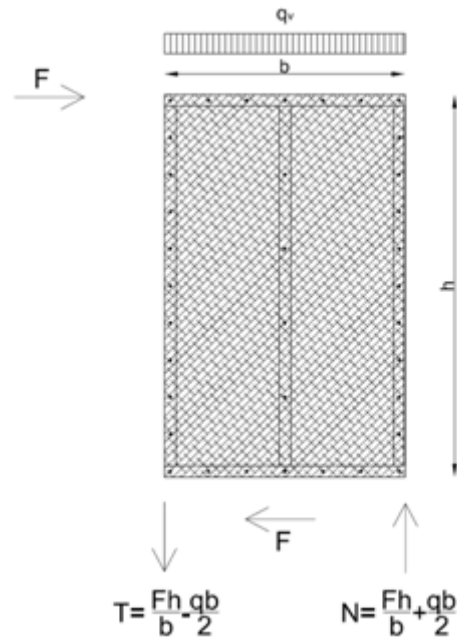


Figure 2.11: Timber frame wall under a horizontal force and a uniform distributed vertical load

The verifications required for a timber-frame wall loaded by a horizontal force F_d , are reported in the following equations, according to Eurocode 5 and taking account of all possible failure mechanisms.

For the verification of the sheathing-to-framing fastener connection the design force acting on each fastener $F_{c,d,fastener}$ should be lower than the fastener lateral design capacity $F_{c,rd}$:

$$F_{c,d,fastener} = \frac{F_d \cdot s \cdot c}{b} \leq F_{c,rd} \quad (2.11)$$

where c is equal to 1 if the length panel b is greater than $h/2$, $2b/h$ if b is within $h/4$ and $h/2$, 0 if b is less than $h/4$. Experimental campaigns in fact demonstrated how the shear capacity of the wall is reduced if the geometrical ratio h/b is greater than 2 and it should be neglected if greater than 4.

The outer stud tensile force produce a tensile tension $\sigma_{t,0,d,externalstud}$ that should be lower than the design tensile strength along the grain $f_{t,0,d,externalstud}$

$$\sigma_{t,0,d,externalstud} = \frac{\frac{F_d \cdot h}{b} - \frac{q \cdot b}{2}}{A_{stud}} \leq f_{t,0,d,externalstud} \quad (2.12)$$

The outer stud stability is verified as in the case of the static load, taking account of the contribution of both the seismic and the static axial force:

$$\sigma_{c,0,d,externalstud} = \frac{\frac{F_d \cdot h}{b} + \frac{q \cdot b}{2}}{A_{stud}} \leq k_{c,y} \cdot f_{c,0,d,externalstud} \quad (2.13)$$

Also for the bottom beam perpendicular to the grain compression the same expression of static load can be considered:

$$\sigma_{c,90,d,bottombeam} = \frac{\frac{F_d \cdot h}{b} + \frac{q \cdot b}{2}}{A_{eff}} \leq k_{c,90} \cdot f_{c,90,d} \quad (2.14)$$

Lastly, the sheathing panel design shear $\tau_{d,panel}$ should be lower than the panel shear strength $f_{v,d}$. The coefficient k_c is used to consider the panel slenderness. The verification is expressed as:

$$\tau_{d,panel} = \frac{F_d}{b \cdot t} \leq k_c \cdot f_{v,d} \quad (2.15)$$

If the wall length l is greater than the single panel length b , more sheathing panels are used. The horizontal stability of the frame is guaranteed by the shear force transfer by

the panels to the frame itself. Also in this case, in order to know the magnitude of the force effecting on each fastener it is possible to apply the lower bound theorem limit analysis. It is simple to demonstrate how the shear force v_d on the edge of the panel in this case is equal to:

$$v_d = \sum_{i=1}^N \frac{F_d}{b_i \cdot c_i} \quad (2.16)$$

where N is the number of sheathing panels whose height is greater than $h/4$. As for a single panel wall sheathing panels characterized by a ratio h/b greater than 2 cannot transfer efficiently the flow of shear stress. For this reason also in this case the a coefficient c_i is used. where N is the number of sheathing panels whose height is greater than $h/4$.

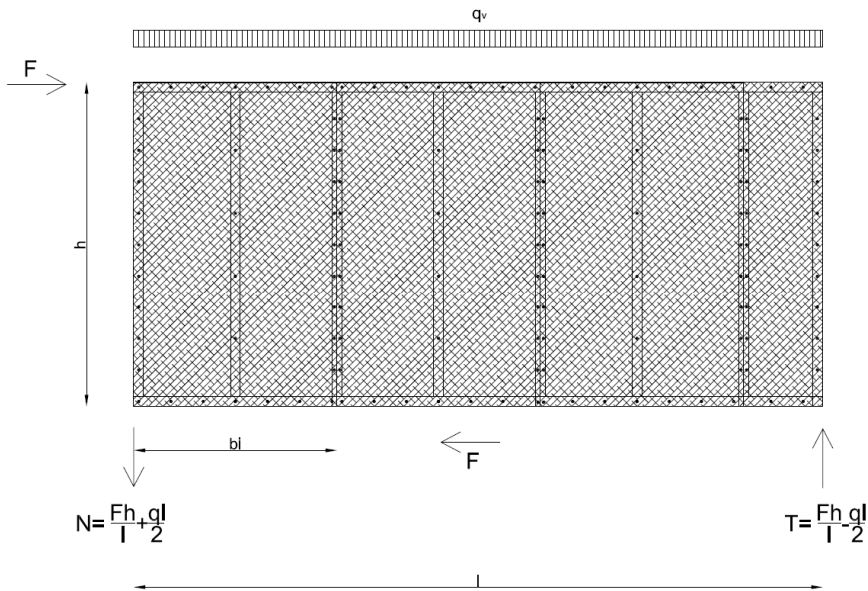


Figure 2.12: Timber frame wall with length l

According to Eurocode 5 the verification of fasteners is rewritten as:

$$F_{c,d,fastener} = F_d \cdot s \cdot \sum_{i=1}^N \frac{1}{b_i c_i} \leq F_{c,r,d} \quad (2.17)$$

where c_i is equal to 1 if the length panel b is greater than $h/2$, $2b/h$ if b is within $h/4$ and $h/2$, 0 if b is less than $h/4$

Also in this case the rotation and the translation of the wall are prevented respectively by hold-downs and angular brackets (or screws). As for a single panel wall, the tensile and compression forces on the outer studs is calculated considering the wall total length:

$$N = \frac{F \cdot h}{l} + \frac{q \cdot l}{2} \quad (2.18)$$

$$T = \frac{F \cdot h}{l} - \frac{q \cdot l}{2} \quad (2.19)$$

If the uniform vertical load q_v is significant, the hold-down tensile force T may be negative and the analysis model is not consistent any more. The wall, in fact, does not rotate and the vertical load q_v is not transferred just to the two outer stud but to all studs. In this case hold-downs would not be required because the wall overturning is prevented by the vertical load.

2.4 Seismic horizontal force distribution

In seismic areas the most significant horizontal load may be given by seismic action. Seismic action is usually represented by some equivalent static horizontal forces acting at each storey of the building. If the floors can be considered as rigid diaphragms the seismic force is assumed to be concentrated in the centre of mass of the floor. Its magnitude is given, in the elastic range, by the product of the mass of the floors and their horizontal acceleration. Admitting a structural damaging, the seismic force can be reduced depending on the ductility of the structure, avoiding global and local failure mechanisms.

The floor horizontal forces are transmitted to the timber frame walls proportionally to their horizontal stiffness. Therefore, the seismic horizontal force F_d acting on each timber wall depends on its mechanical and geometrical properties. For this reason a correct distribution of horizontal forces would require a suitable analysis model capable of taking account of all significant deformation sources of the walls.

In the common practice, the seismic analysis of timber-frame buildings is usually carried out by means of simplified methods. In most cases, the lateral force method of analysis (as suggested by the Eurocode 8) is used and the wall stiffness is assumed directly proportional to the wall length. Hence, the analysis model can be reduced to a simple spreadsheet. This method is without any doubt very simple and intuitive but generally cannot be universally accepted.

Firstly, the lateral force method of analysis should be applied only when building dynamic response is not significantly affected by contributions from modes of vibration higher than the fundamental one (typically when the building can be assumed as regular in elevation). Otherwise a modal response spectrum analysis should be carried out, considering the contribution of all significant vibration modes. The seismic demand of the building is in fact strongly influenced by their dynamic behaviour of the structure and for this reason a static force equivalent distribution cannot be thorough.

Secondly, in the common evaluation of the wall stiffness, the deformation contribution of the connection devices is totally neglected. Nevertheless, as demonstrated by the results of the experimental campaign of the *CHI-QUADRATO* research project [Conte *et al.*, 2011; Conte *et al.*, 2010; Sartori *et al.*, 2012, Sartori *et al.*, 2013, Tomasi and Sartori, 2013], the influence of the connections is not negligible and should be adequately considered in the analysis of the structure.

For these reasons, a key part of this thesis (presented in chapter 3) is represented by the analysis of the linear behaviour of a timber frame wall subjected to a horizontal load. An analytical expression for the assessment of the wall stiffness is suggested considering four different sources of deformation due to the sheathing-to-framing connection, the hold downs, the angle brackets and sheathing panel. The influence of each deformation component is then analysed by means of a parametric study, demonstrating the importance of the role of the connections. Moreover, a backup numerical modelling of a single wall, based on the obtained results, is proposed. Thanks

to its simplicity, this model can be used to develop numerical models for a series of walls or an entire building, as reported in Chapter 5, and hence to carry out the correct distribution of horizontal seismic forces between the timber walls.

2.5 Timber-frame building behavior factor q

The seismic design of a structure is generally carried out referring to a force-based seismic design method, as reported in European Standard [EN 1998-1/A1, 2013]. The seismic action is represented by the peak inertial forces to which the structure is subjected during a seismic event. The capacity of the structure to support the seismic action is obtained from dissipating the seismic energy via its structural damaging and hence assuming a nonlinear structural behaviour. For economic reasons, in fact, because earthquake is a very intense but rare phenomenon, a damaging of the structure is accepted. However seismic linear analyses are usually carried out, dividing the elastic seismic forces by the behaviour factor q , depending on the global structural ductility. The global behaviour of a structure, and in particular its ductility strongly depends both on the mechanical properties of structural components and on the global failure mechanism. For this reason, in order to achieve high values of q , brittle failure mechanism should be prevented. Moreover, the ductility of the structural components where the energy dissipation occurs should be related to the ductility demand of the entire structure. Standards [i.e. EN 1998-1/A1, 2013; NTC08, 2008] suggest the values of q -factor for several structural types. In order to guarantee an adequate global ductility, preventing brittle failure mechanisms, some design criteria and structural details are reported for several types of buildings.

In timber buildings the structural ductility cannot be reached in timber elements because, as known, are characterized by a brittle behaviour. The capability of the structure to dissipate the seismic energy is hence obtained from the yielding of the metallic connection devices. Referring to timber-frame buildings three are the main sources where the energy dissipation may occur, namely sheathing-to-frame fasteners, hold-downs and angle brackets (or screws). The first contribution is commonly considered as the most important because in timber-frame buildings the number of fasteners is usually very large. In addition, their small diameter guarantees a high local ductility. For this reason a high capacity to dissipate energy is assumed for this structural type.

Referring to European Standards for design of structure for earthquake resistance [EN 1998-1/A1,2013] an upper limit value of the behaviour factor q equal to 5 is suggested (Figure 2.13), setting this structural type in the high ductility class (DCH).

Table 8.1: Design concept, Structural types and upper limit values of the behaviour factors for the three ductility classes.

Design concept and ductility class	q	Examples of structures
Low capacity to dissipate energy - DCL	1,5	Cantilevers; Beams; Arches with two or three pinned joints; Trusses joined with connectors.
Medium capacity to dissipate energy - DCM	2	Glued wall panels with glued diaphragms, connected with nails and bolts; Trusses with doweled and bolted joints; Mixed structures consisting of timber framing (resisting the horizontal forces) and non-load bearing infill.
	2,5	Hyperstatic portal frames with doweled and bolted joints (see 8.1.3(3)P).
High capacity to dissipate energy - DCH	3	Nailed wall panels with glued diaphragms, connected with nails and bolts; Trusses with nailed joints.
	4	Hyperstatic portal frames with doweled and bolted joints (see 8.1.3(3)P).
	5	Nailed wall panels with nailed diaphragms, connected with nails and bolts.

Figure 2.13: EC8 upper limit values of behaviour factor for timber structures

(3)P In order to ensure that the given values of the behaviour factor may be used, the dissipative zones shall be able to deform plastically for at least three fully reversed cycles at a static ductility ratio of 4 for ductility class M structures and at a static ductility ratio of 6 for ductility class H structures, without more than a 20% reduction of their resistance.

(4) The provisions of (3)P of this subclause and of 8.2(2) a) and 8.2(5) b) may be regarded as satisfied in the dissipative zones of all structural types if the following provisions are met:

a) in doweled, bolted and nailed timber-to-timber and steel-to-timber joints, the minimum thickness of the connected members is $10 \cdot d$ and the fastener-diameter d does not exceed 12 mm;

b) In shear walls and diaphragms, the sheathing material is wood-based with a minimum thickness of $4d$, where the nail diameter d does not exceed 3.1 mm.

If the above requirements are not met, but the minimum member thickness of $8d$ and $3d$ for case a) and case b), respectively, is assured, reduced upper limit values for the behaviour factor q , as given in Table 8.2, should be used.

Table 8.2: Structural types and reduced upper limits of behaviour factors

Structural types	Behaviour factor q
Hyperstatic portal frames with doweled and bolted joints	2.5
Nailed wall panels with nailed diaphragms	4.0

Figure 2.14: Seismic design criteria and details for timber structures (EC8)

In order to guarantee a global high ductility of the structure, it is required that the ductility of the components where the energy dissipation occurs must be greater than 6 (Figure 2.14). The observance of this requirement, however, does not seem to be enough to guarantee completely the global structural ductility defined by the behaviour factor q . Unlike what for other material structural types (concrete or steel), no detailed suggestion about the failure mechanism that should be achieved is reported, and thus it is not clear which connection type should be selected (fasteners, hold-down or angle brackets) as the weakest element where the ductility capacity of the structure is concentrated. Moreover, very few specific structural details are suggested (Figure 2.14) and no expression about capacity design rule is reported. For these reasons current standards for seismic design of timber structures may be considered lacking if compared to other types of structures.

During last twenty years several research projects have been carried out with the aim to validate the high value of the behaviour factor for timber frame buildings and investigate the seismic behaviour of timber structures. Shake table tests and non-linear numerical analysis (static and dynamic) were in particular performed [Christovallis et al., 2007; Daudeville et al., 2004; Dujic and Zaranic, 2004; Filiatrault et al., 2003; Filiatrault et al.,

2001; Filiatrault and Fischer., 2001; Filiatrault et al., 2000; Folz and Filiatrault., 2002; Judd and Fonseca, 2005; Kasal et al., 1994; Kesse and Kammer, 2004; Salenicovich, 2000, Tarabia and Itani, 1997; Van de Lindt et al.,2006]. The obtained results have demonstrated good seismic performances of timber-frame wall buildings. However an analytical model capable to correlate the local ductility of connections, where energy dissipation occurs, to the global structure ductility has not proposed yet. As explained previously this relationship is crucial because defines the local ductility demand of the components in relation to the global ductility capacity.

With this purpose, a predictive analytical model for the elasto-plastic behaviour of a timber-frame shear wall under horizontal loading is presented in Chapter 4. The main goal of this model is in particular to link the local properties (e.g. ductility) of each component to the global properties of a single wall. This does not define complete the sought relationship but it represents the first fundamental step. The obtained results in fact may be used to relate the properties of a single wall to the properties of an entire timber frame building

3 LINEAR ANALYSIS OF A TIMBER-FRAME WALL UNDER A HORIZONTAL FORCE

As reported in chapter 2, one of the most important aspect that should be investigated in order to perform a correct distribution of elastic horizontal forces in timber frame buildings is the definition of a suitable model for the elastic behaviour of walls. In this chapter an analytical expression for the calculation of the horizontal displacement of a timber frame wall under a horizontal force is proposed considering four different deformation sources. A parametric study of the wall stiffness is shown, demonstrating as a linear relationship between the stiffness and the length of the wall cannot be assumed. Moreover a simplified numerical model of the wall is proposed.

3.1 Elastic horizontal displacement of a timber frame wall under a horizontal force

The elastic horizontal displacement of a timber-frame wall under a horizontal force can be calculated considering four difference sources of deformation, namely rigid-body

rotation, sheathing panel shear deformation, sheathing-to-framing fastener deformation, and rigid-body translation. In this section the horizontal displacement Δ of a timber frame wall under a horizontal force is calculated. In the analysis a timber frame with length l and height h is considered. The external loads are represented by the uniform vertical load q and a horizontal force F (Figure 3.1).

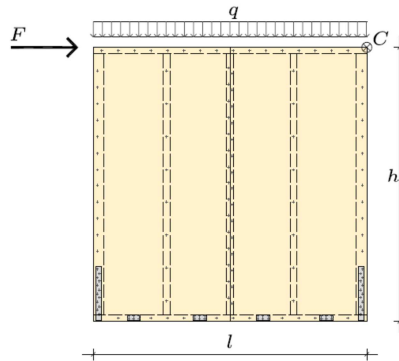


Figure 3.1: Timber frame wall subjected to a horizontal force [Rossi, S.]

3.1.1 Rigid-body rotation

The source of deformation caused by the rigid-body rotation (see, Figure 3.3, l) of the wall is related to the tensile force of hold-downs, placed at each corner of the wall, for effect of the overturning moment produced by the force F . Considering also that a uniform vertical load may be acting on the wall, the hold-down vertical elongation v can be calculated as:

$$v = \left(\frac{F \cdot h}{l} - \frac{q \cdot l}{2} \right) \cdot \frac{1}{k_h} \quad (3.1)$$

where k_h is the hold-down stiffness.

The rigid rotation angle γ is obtained dividing v by the length l to:

$$\gamma = \frac{v}{l} = \left(\frac{F \cdot h}{l^2} - \frac{q}{2} \right) \cdot \frac{1}{k_h} \quad (3.2)$$

Thus, the horizontal displacement Δ_h caused by the rigid-body rotation of the wall is:

$$\Delta_h = \gamma \cdot h = \left(\frac{F \cdot h}{l^2} - \frac{q}{2} \right) \cdot \frac{h}{k_h} \quad (3.3)$$

When the vertical load q is enough to prevent the wall rigid rotation and hence the overturning moment is lower than the stabilizing moment due to the vertical load, the hold-down elongation v must be assumed equal to zero. Consequently, Eq. (3.3) is rewritten as:

$$\Delta_h = \begin{cases} 0 & \text{when } F \leq \frac{q \cdot l^2}{2 \cdot h} = F_q \\ \frac{h}{l \cdot k_h} \cdot \left(\frac{F \cdot h}{l} - \frac{q \cdot l}{2} \right) & \text{when } F > \frac{q \cdot l^2}{2 \cdot h} = F_q \end{cases} \quad (3.4)$$

3.1.2 Sheathing panel shear deformation

The horizontal displacement Δ_p (see, Figure 3.3, II) caused by the sheathing panel shear deformation contribution can be calculated deferring to the shear deformation ζ . This results equal to:

$$\zeta = \frac{dx}{dy} = \chi \cdot \frac{F}{G_p \cdot A_p} = \chi \cdot \frac{F}{G_p \cdot (t_p \cdot l \cdot n_{bs})} \quad (3.5)$$

where:

- A_p is the shear area of the sheathing panel;

- G_p is the shear modulus of the sheathing panel;
- t_p is the sheathing panel thickness.

The displacement Δ_p can be obtained multiplying ζ by the wall height h , assuming a shear factor χ equal to one.

$$\Delta_p = \zeta \cdot h = \frac{F \cdot h}{G_p \cdot n_{bs} \cdot t_p \cdot l} \quad (3.6)$$

3.1.3 Sheathing-to framing fastener deformation

A timber framed wall is characterized by a timber frame made with solid timber studs and beams. The frame is braced against horizontal loads by sheathing panels connected to the frame itself by means of fasteners (nails or staples). For a single panel wall (the length wall l is equal to the panel length b) the horizontal displacement Δ_{sh} caused by the deformation of fastener (see, Figure 3.3, III) can be evaluated, according to [Girhammar and Kallsner, 2009] as follows:

$$\Delta_{sh} = \frac{F \cdot h^2}{k_c} \cdot \left[\frac{1}{\sum_{i=1}^n x_i^2} + \frac{1}{\sum_{i=1}^n y_i^2} \right] \quad (3.7)$$

where:

- F : is the external horizontal force;
- h : is the height of the wall. The height of the sheathing panel is assumed in the analysis equal to the height of the wall;
- k_c : is the elastic stiffness of each fastener;

- x_i, y_i are the fasteners' coordinates with respect to a reference system with the origin in the centre of the panel;
- n : is the number of fasteners;

Assuming a constant spacing of fasteners along the beams s_p , on the perimeter studs s_{ps} and on the inner studs, we obtain:

$$\sum_{i=1}^n x_i^2 \cong \frac{1}{6} \cdot \left(1 + 3 \cdot \frac{s_p}{s_{ps}} \cdot \frac{h}{b} \right) \cdot \frac{b}{s_p} \cdot b^2 \quad (3.8)$$

$$\sum_{i=1}^n y_i^2 \cong \frac{1}{12} \cdot \left(6 + 2 \cdot \frac{s_p}{s_{ps}} \cdot \frac{h}{b} + \frac{s_p}{s_{is}} \cdot \frac{h}{b} \right) \cdot \frac{b}{s_p} \cdot h^2 \quad (3.9)$$

The ratio between the panel height h and the panel length b is defined as the panel geometrical parameter α . It is obtain as:

$$\alpha = \frac{h}{b} \quad (3.10)$$

The fastener spacing on the inner stud s_{is} is assumed usually double than the fastener spacing on the perimeter studs s_{ps} and on the beams s_p . For this reason a reference fastener spacing s_c can be defined as:

$$s_c = s_{ps} = s_p = \frac{s_{is}}{2} \quad (3.11)$$

Moreover the parameters η and ξ are defined:

$$\eta = \frac{1}{6} \cdot (1 + 3 \cdot \alpha) \quad (3.12)$$

$$\xi = \frac{\alpha^2}{12} \cdot \left(6 + \frac{5}{2} \cdot \alpha \right) \quad (3.13)$$

Hence, equations (3.8) and. (3.9) can be rewritten as:

$$\sum_{i=1}^n x_i^2 \cong \eta \cdot \frac{b^3}{s_c} \quad (3.14)$$

$$\sum_{i=1}^n y_i^2 \cong \xi \cdot \frac{b^3}{s_c} \quad (3.15)$$

Therefore, the horizontal displacement Δ_{sh} is:

$$\Delta_{sh} = \frac{F \cdot b^2}{k_c} \cdot \alpha^2 \cdot \left[\frac{1}{\eta} + \frac{1}{\xi} \right] \cdot \frac{s_c}{b^3} \quad (3.16)$$

At this stage we can define a new parameter λ depending on α , as:

$$\lambda = \alpha^2 \cdot \left[\frac{1}{\eta(\alpha)} + \frac{1}{\xi(\alpha)} \right] = \lambda(\alpha) \quad (3.17)$$

The displacement Δ_{sh} becomes:

$$\Delta_{sh} = \frac{F}{k_c} \cdot \lambda(\alpha) \cdot \frac{s_c}{b} \quad (3.18)$$

Equation (3.18) represents to the horizontal displacement due to the sheathing-to-framing fastener deformation for a wall whose length is equal to the panel (“single panel wall”). When a wall is characterized by several sheathing panels, eq. (3.18) can be rewritten as:

$$\Delta_{sh} = \frac{F}{k_c} \cdot \lambda(\alpha) \cdot \frac{s_c}{l} \quad (3.19)$$

The eq. (3.19) is developed assuming that the sheathing panels superimposition occurs only on one side of the wall. Therefore a more general expression can be obtained, considering also the case for which sheathing panels are superimposed on both sides of wall. Hence we get:

$$\Delta_{sh} = \frac{F \cdot \lambda(\alpha) \cdot s_c}{k_c \cdot l \cdot n_{bs}} \quad (3.20)$$

where n_{bs} is the number of the sides of the wall where sheathing panels are superimposed (equal to 1 or 2).

The shape function λ , function of α is plotted in Figure 3.2. For values of $1 < \alpha < 6$, λ , can be approximated by the linear equation (3.21).

$$\lambda(\alpha) = 0,81 + 1,85 \cdot \alpha \quad (3.21)$$

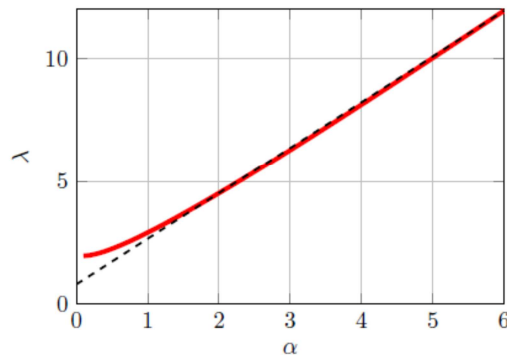


Figure 3.2: Shape function vs panel geometrical ratio

For the value of $\alpha = 2$, λ is equal to 4.52 as obtained by [Girhammar and Kallsner, 2009].

3.1.4 Rigid-body translation

A timber-framed wall is usually connected to the foundation by means of angle-brackets or screws in order to prevent its rigid-body translation, see

Neglecting the friction, the deformation source due to the rigid-body translation Δ_a can be calculated (see, Figure 3.3, IV) intuitively as:

$$\Delta_a = \frac{F}{k_a \cdot n_a} \quad (3.22)$$

where:

- k_a : is the stiffness of each angle-brackets (or screw);
- n_a : is the number of angle-brackets (or screws).

When the angle-brackets spacing i_a is constant

$$n_a = \frac{l}{i_a} \quad (3.23)$$

Equation (3.22) can be rearranged as:

$$\Delta_a = \frac{F \cdot i_a}{k_a \cdot l} \quad (3.24)$$

3.1.5 Total elastic horizontal displacement

The elastic horizontal displacement (Point C, Figure 3.1) of a timber frame wall subjected to a horizontal force shear wall can be obtained by adding the displacements caused by the four sources previously described. We get:

$$\Delta = \Delta_{sh} + \Delta_h + \Delta_a + \Delta_p \quad (3.25)$$

$$\Delta = \frac{\lambda \cdot F \cdot s_c}{l \cdot n_{bs} \cdot k_c} + \left[\frac{h}{l \cdot k_h} \cdot \left(\frac{F \cdot h}{l} - \frac{q}{2} \right) \right] + \frac{F \cdot i_a}{k_a \cdot l} + \frac{F \cdot h}{l \cdot G_p \cdot n_{bs} \cdot t_p} \quad (3.26)$$

In equations (3.26) the contribution due to the wall rigid-body rotation must be considered only when greater or equal to zero (hold-down in tension). Otherwise it must be neglected.

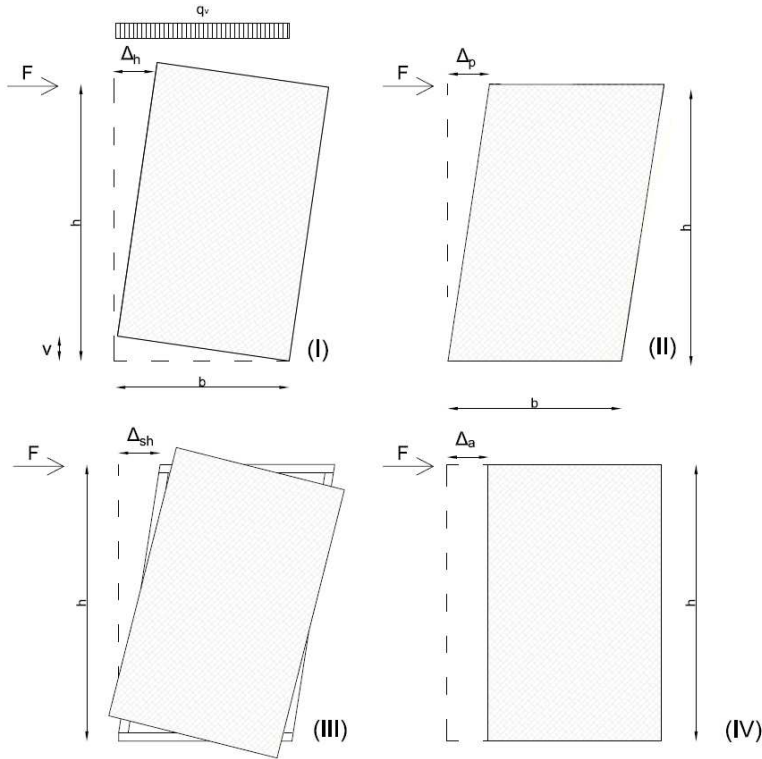


Figure 3.3: Timber frame deformation contribution: rigid-body rotation (I), Sheathing-panel shear deformation (II), Sheathing-to-framing connection (III) and Rigid body translation (IV)

3.2 Horizontal stiffness of a timber frame wall

From eq. (3.26) the force vs displacement curve can be plotted, as shown in Figure 3.4. Because the deformation contribution caused the hold-down must be considered only if it is positive, a bi-linear curve is obtained. Two regimes are hence to be assumed. The first one is when the hold-down is not in tension ($F < F_{q_v}$), since the stabilizing moment is greater than the overturning moment. The wall stiffness in this case is defined as $K_{tot,nt}$. The second regime occurs when the hold-down is in tension ($F > F_{q_v}$). The related stiffness is defined as K_{tot} . If the vertical load q is zero only the second regime occurs.

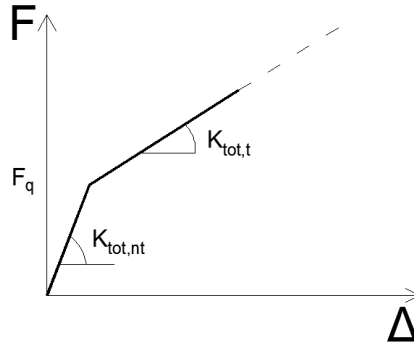


Figure 3.4: Force vs displacement curve

Referring to the second regime, the total horizontal displacement Δ , see Eq. (3.26), can be rewritten to highlight the contribution of the external force F , as shown by eq. (3.27):

$$\Delta = \frac{F}{K_{SH}} + \frac{F}{K_P} + \frac{F}{K_A} + \frac{F}{K_H} - \frac{N \cdot h}{l \cdot k_h} \quad (3.27)$$

where:

- the sheathing panel global stiffness is:

$$K_P = \frac{G_p \cdot n_{bs} \cdot t_p \cdot l}{h} \quad (3.28)$$

- the sheathing-to-framing fastener stiffness is:

$$K_{SH} = \frac{n_{bs} \cdot k_c \cdot l}{\lambda \cdot s_c} \quad (3.29)$$

- the rigid body translation stiffness is:

$$K_A = \frac{k_a \cdot l}{i_a} = k_a \cdot n_a \quad (3.30)$$

- the rigid body rotation stiffness is:

$$K_{HD} = \frac{k_h \cdot l^2}{h^2} \quad (3.31)$$

- the vertical load acting on the outer studs is:

$$N = \frac{q \cdot l}{2} \quad (3.32)$$

The global stiffness K_{tot} of the wall is hence defined as:

$$\frac{1}{K_{tot}} = \frac{1}{K_{SH}} + \frac{1}{K_P} + \frac{1}{K_A} + \frac{1}{K_H} \quad (3.33)$$

while the backwards horizontal displacement Δ_N of the wall due to the vertical load is :

$$\Delta_N = \frac{N \cdot h}{l \cdot k_h} \quad (3.34)$$

Thus, the horizontal displacement of the wall can be expressed as:

$$\Delta = \frac{F}{K_{tot}} - \Delta_N \quad (3.35)$$

Similarly, the external force F can be expressed as:

$$F = K_{tot} \cdot (\Delta + \Delta_N) = K_{tot} \cdot \Delta + F_N \quad (3.36)$$

where F_N is the equivalent horizontal force due to the vertical load.

A representation of the Equation (3.36) is shown in Figure 3.5. The elastic behaviour of a timber frame wall is represented by a rheological model characterized by four elastic springs in series subjected to an external total force equal to $F - F_N$.

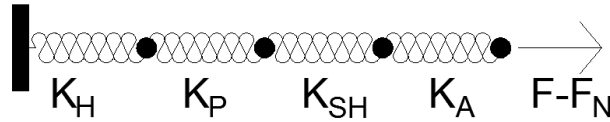


Figure 3.5: Wall rheological model for the elastic behaviour of a timber frame wall in the second regime

Equations (3.35) and (3.36) prompt the following two considerations

1. The horizontal displacement produced by the horizontal force F is decreased at a rate caused by the vertical load equal to Δ_N , which is constant.
2. The force F depends on two different quantities: the elastic force $K_{TOT} \cdot \Delta$ and the force to counteract the vertical load $K_{tot} \cdot \Delta_N$.

The first regime (when the hold-down is not in tension), may be considered as a subcase of the first regime, setting the hold-down stiffness k_h equal to infinity. Hence, the global stiffness $K_{tot,nt}$ of the wall is rewritten as:

$$\frac{1}{K_{tot,nt}} = \lim_{k_h \rightarrow \infty} \frac{1}{K_{tot}} = \frac{1}{K_P} + \frac{1}{K_{SH}} + \frac{1}{K_A} \quad (3.37)$$

The horizontal displacement due to the vertical load Δ_N also becomes 0. Hence, the global displacement Δ is given by:

$$\Delta = \frac{F}{K_{tot,nt}} \quad (3.38)$$

In this case the rheological model is represented by three springs in series, neglecting the contribution due to the rigid rotation. The acting force is equal to F (Figure 3.6).

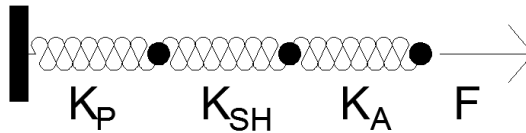


Figure 3.6: Wall rheological model for the elastic behaviour of a timber frame wall in the first regime

3.3 Parametric study of the wall stiffness

In common practice, as explained in Chapter 2, the stiffness is assumed is linearly proportional to the wall length. In order to demonstrate that this assumption cannot be taken for granted, a dimensionless parametric study was performed. Regarding the second regime the global wall stiffness can be rewritten as:

$$\frac{1}{K_{tot}} = \frac{h}{l} \cdot \frac{1}{G_p \cdot n_{bs} \cdot t_p} + \frac{\lambda \cdot s_c}{l \cdot n_{bs} \cdot k_c} + \frac{i_a}{k_a \cdot l} + \frac{h^2}{l^2 \cdot k_h} \quad (3.39)$$

Four new parameters are defined to isolate the contribution of the length of the wall , namely:

$$\frac{1}{\vartheta} = \frac{h}{G_p \cdot n_{bs} \cdot t_p} = \frac{l}{K_P} \quad (3.40)$$

$$\frac{1}{\beta} = \frac{s_c}{n_{bs} \cdot k_c} \cdot \lambda = \frac{l}{K_{SH}} \quad (3.41)$$

$$\frac{1}{\varphi} = \frac{i_a}{k_a} = \frac{l}{K_A} \quad (3.42)$$

$$\frac{1}{\delta} = \frac{h^2}{k_h} = \frac{l^2}{K_H} \quad (3.43)$$

Hence equation (3.39) becomes:

$$\frac{1}{K_{tot}} = \frac{1}{\vartheta \cdot l} + \frac{1}{\beta \cdot l} + \frac{1}{\varphi \cdot l} + \frac{1}{\delta \cdot l^2} \quad (3.44)$$

Equation (3.44) shows that the stiffness of the wall is not linearly proportional to the wall length. Unlike all other components the rigid-body rotation deformation is in fact linearly proportional to the square of the length influencing the relationship between the global stiffness and the length of the wall.

When the hold-down is not in tension, the parameter $\delta \rightarrow \infty$. The wall stiffness is hence given by:

$$K_{tot,nt} = \lim_{\delta \rightarrow \infty} K_{tot} = \frac{\vartheta \cdot \beta \cdot \varphi \cdot l}{\vartheta \cdot \beta + \vartheta \cdot \varphi + \beta \cdot \varphi} = \omega \cdot l \quad (3.45)$$

Equation (3.45) shows that the common in practice assumption is in this case correct. The deformation contributions related to sheathing panel, sheathing-to-frame fasteners and angle brackets are in fact linearly proportional to the length.

3.4 Finite element modelling of a timber-frame wall

Two numerical modelling suitable to investigate the linear elastic behaviour of timber wall under an horizontal external force are presented in this section. These are characterized by a different complexity and for this reason may be employed for different purposes.

The former was implemented in order to validate the results of the analytical predictive model (complete model) The latter, much simpler, is based on the results of the analytical predictive model and can be employed for global elastic linear analyses of series of walls or buildings (simplified model).

3.4.1 Complete model

The model is defined as “complete” since each significant deformation contribution is appropriately represented by an element (Figure 3.7).

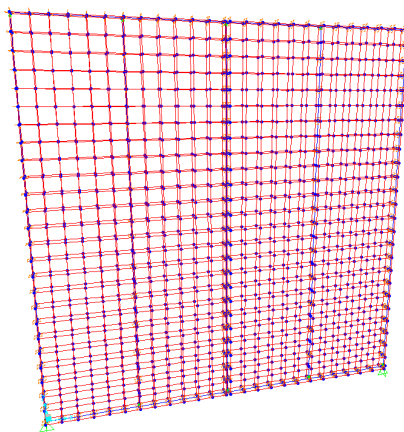


Figure 3.7: Complete numerical model

Pinned frame elements were used to model the timber frame while shell elements represented the sheathing panels. The frame and the studs of the pinned frame are linked to the shell elements with two perpendicular linear elastic springs simulating

fastener deformation contribution. The bottom beam is restrained by means of a vertical and a horizontal linear springs in order to represent respectively the in-tension hold-down and the angle brackets.

In order to validate the equation proposed for the calculation of the wall horizontal displacement, several analyses were performed changing the geometrical properties, the spacing of the fasteners and the stiffness of each connection device. An extensive description of the model and the results are reported in [Conte *et al.*, 2011].

3.4.2 Simplified model

The complete model is characterized by a large number of degrees of freedom because each fastener is represented by two perpendicular linear –elastic springs. Based on the predictive analytical model described in previous sections a simplified model is presented (Figure 3.8) in order to represent the contribution of deformation of all fasteners by means of a single horizontal spring, reducing considerably the number of degrees of freedom of the model. This may be really significant when a series of walls (or an entire building) is to be modelled. As an example, a 2.5 m (length l) x 2.5 m (height h) wall characterized by sheathing panels ($b=1.25$ m) on both sides ($n_{bs}=2$) with a fastener spacing (s) of 125 mm needs a number of fasteners equal to:

$$n_{fasteners} = \left(\frac{l}{s} \cdot 2 + \frac{l}{b} \cdot \frac{h}{s} \cdot 2 \right) \cdot n_{bs} = \left(\frac{2.5}{0.125} \cdot 2 + \frac{2.5}{1.25} \cdot \frac{2.5}{0.125} \cdot 2 \right) \cdot 2 = 240 \quad (3.46)$$

The number of degrees of freedom are hence equal to 480. For this reason the reduction factor r is equal to:

$$r = \frac{1}{480} = 0.0021 \quad (3.47)$$

The equivalent horizontal spring, characterized by a stiffness K_{SP} is defined by eq. (3.48) considering both the sheathing-to-frame fastener contribution K_{SH} and the sheathing panel deformation K_P .

$$K_{SP} = \frac{K_P \cdot K_{SH}}{K_P + K_{SH}} \quad (3.48)$$

The stiffness of the frame timber elements must be assumed as infinite in order to prevent its bending deformation.

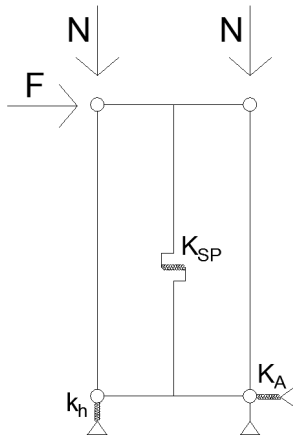


Figure 3.8: Simplified model for in-tension hold-down

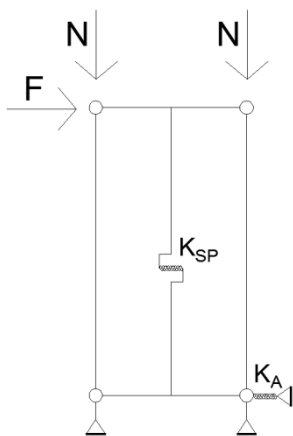


Figure 3.9: Simplified model for non in-tension hold-down

As for the complete model, a vertical spring with stiffness equal to k_r is used to represent the hold-down while a horizontal spring with stiffness K_A models the rigid body translation contribution.

When the hold-down is not in-tension (Figure 3.9), the vertical spring must be substituted by a vertical rigid-pinned beam. In fact if the stabilizing moment caused by vertical load q is greater than the overturning moment caused by the horizontal force F the rotation rigid body contribution is to be neglected. For this reason an iterative process of analysis must be performed in order to get a consistent solution considering the real state in-tension (or not in-tension) of the hold-down.

4 ELASTO-PLASTIC ANALYSIS OF A TIMBER -FRAME WALL UNDER A HORIZONTAL FORCE

In chapter 3 an approach for the linear behaviour of a timber frame wall under a horizontal force was described and a simplified backup numerical modelling, capable to take account of all significant deformation contributions, was proposed. In this chapter an analytical predictive model of the elasto-plastic behaviour of a timber frame wall under a horizontal load is presented. In this case three main sources of resistance have been considered (sheathing-to-frame fasteners, hold-down and angle brackets) neglecting the contribution of the sheathing panel (as reported in [Conte *et al.*,2011; Conte *et al*, 2010] its influence on the global response of the wall is not significant). For any load level, the ability to represent the total force carried by all fasteners (allowing for their sequential yielding) in one spring (as reported in the simplified model) is shown to be a key benefit, as this approach considerably reduces the number of degrees-of-freedom in the model. This aspect becomes really important for non-linear analyses for which the reduction of the number of degrees of freedom is a significant issue for an

acceptable time-consuming of the analysis. The development of this spring in the non-linear range was investigated via a parametric study in which the variables were the sheathing panel's aspect ratio and the fastener spacing. By also considering equivalent springs for the other components (as in the linear range), it has been possible to define a rheological model for elasto-plastic behaviour of a sheathed timber frame as function of the mechanical properties of the fasteners, hold-downs and angle brackets. Particular attention has been paid to the relationship between component (e.g. fastener) ductility and the global ductility of the wall. Use of this approach to underpin nonlinear numerical modelling of seismic response of multiple timber frame walls is discussed. This then feeds into assessment of seismic capacity of timber-frame walls and hence of timber buildings.

4.1 Rheological model for the assessment of the non-linear behavior of a timber-frame wall

According to the simplified model describe in Chapter 3 the behaviour of a timber-frame wall under a horizontal force F and a distributed vertical load q , can be represented by a simple pinned frame, braced by a horizontal spring of stiffness equal to K_{SH} representing the sheathing-to-framing connection (when the contribution of the sheathing panel K_P is neglected, K_{PS} is equal to K_{SH}). The contribution of the devices which prevent the horizontal translation of the wall is represented by horizontal spring of stiffness K_A connected to the ground, while the rigid body rotation, (hold-down contribution) is taken into account by means of a vertical spring of stiffness equal to k_r .

The implementation of this model in the non-linear range is quite simple and straightforward: each spring (sheathing-to-frame, rigid body translation and rigid body rotation) is not characterized simply by its linear stiffness but by a non-linear curve. In this thesis an elasto—plastic behaviour of each source is assumed: the force vs displacement curve of each spring is hence characterized simply by its stiffness, strength and ductility. In this case, the non-linear mechanical behaviour of the wall is therefore described by a bi-linear or tree-linear curve.

In order to obtain simple analytical expressions for the relationship between the behaviour of each individual source and the global behaviour of the wall, the backup numerical model of the wall was substituted by a simplified rheological model. This is characterized by two in-series horizontal springs (sheathing-to-frame source K_{SH} and

rigid translation K_A) and a third in-series element, made up by a horizontal spring K_H (representing the rigid body rotation) placed parallel to a friction block (F_q) representing the vertical load contribution (Figure 4.1).

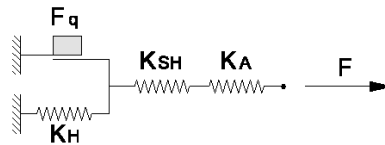


Figure 4.1 Timber frame rheological model

4.2 Mechanical properties of sources of deformation

In this section some analytical expressions are proposed for the definition of elasto-plastic behaviour of each component of the rheological model. The calculation is based on the knowledge of the mechanical properties of the fasteners and the connection devices of each source of deformation.

4.2.1 Rigid body rotation

The parameters that describe the rigid-body rotation contribution in the rheological model (represented by the non-linear horizontal spring K_H and by the friction block F_q , see Figure 4.2) can be obtained by geometrical and mechanical considerations from the simplified numerical model of the wall, depending on the vertical load q , on the geometry of the wall (height h and length l) and on the mechanical parameters which characterize each hold down (stiffness k_h , strength f_h and ductility μ_h),.

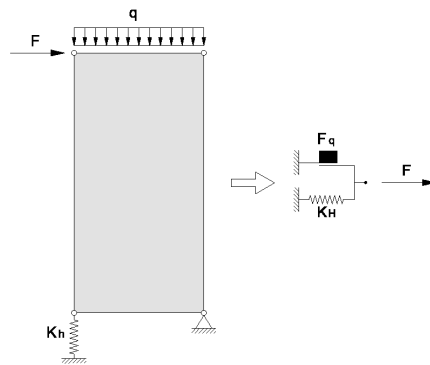


Figure 4.2: Rigid body rotation and vertical load component

The hold down device, used in order to prevent the rigid rotation of the wall, is loaded by a tensile force only when the overturning moment, caused by the horizontal force F is greater than the stabilizing moment, resulting from vertical load q . This condition occurs when:

$$M_{ovt} = F \cdot h \geq M_{stb} = \frac{q \cdot l^2}{2} \quad (4.1)$$

As described in chapter 3, the value F_q of the horizontal force for which the hold down is subjected to a tensile force is given by:

$$F_q = \frac{q \cdot l^2}{2 \cdot h} \quad (4.2)$$

For this reason the rigid body rotation source is represented by an horizontal spring with stiffness K_H , and a block friction placed in parallel with the spring itself. When F is lower than F_q (the force value required to overcome the friction of the block) the horizontal spring cannot be stretched and therefore no force and no deformation can be absorbed. On the contrary, when F is greater than F_q , the horizontal spring can increase its deformation and its internal force.

4.2.2 Friction block

The friction block is used in the rheological model to represent the stabilizing contribution of the uniform vertical load q and in particular the condition for the activation of the rigid rotation source. Its mechanical behaviour is described by a rigid indefinite perfectly plastic curve, as shown in Figure 4.3. The force for the yield of the block is equal to F_q .

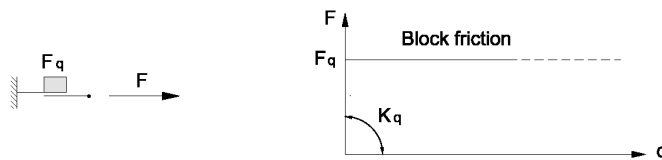


Figure 4.3: Block friction component

4.2.3 Horizontal non-linear spring for the rigid-body rotation of the wall

The horizontal non-linear spring is used in the rheological model to represent the hold-down contribution. According to the hypothesis of section 4.1 its mechanical behaviour can be defined by an elasto-plastic force vs displacement curve and hence by the stiffness K_H , the strength F_H and the ductility μ_H (Figure 4.4). The curve parameters can be obtained with some simple analytical expressions from the hold-down elasto-plastic curve, described by stiffness h_h , strength f_h , and ductility μ_H . The hold down curve can be obtained by the bi-linearization of the hold down experimental curve or by means of numerical analyses.

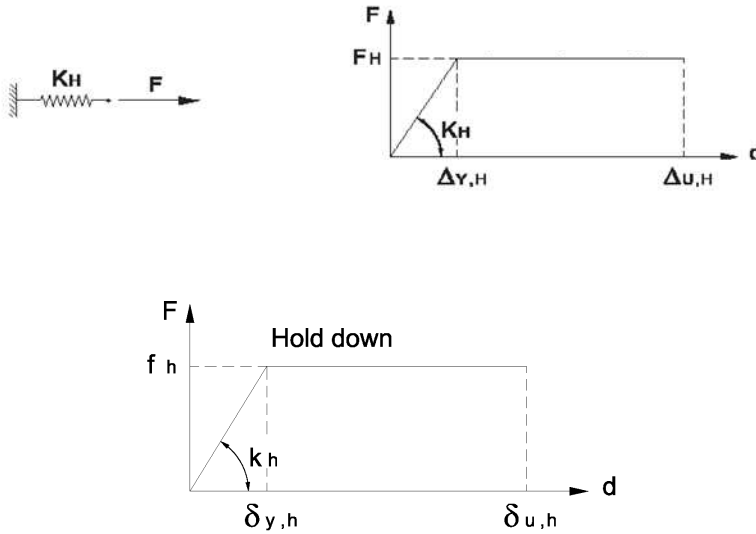


Figure 4.5: Hold down elasto-plastic behaviour

The analytical expressions for the calculation of the mechanical parameters that characterize the horizontal non-linear spring of the rheological model can be obtained by some geometrical and mechanical considerations, isolating the deformation contribution of the hold down. The strength F_H can be directly calculated from the strength of the hold-down strength f_h as:

$$F_H = n_h \cdot \frac{f_h \cdot l}{h} \quad (4.3)$$

where:

- f_h is the hold down strength;
- l is the length of the wall;
- h is the height of the wall;

- n_h is the number of hold downs for each corner of the wall.

The yield displacement $\Delta_{y,H}$ can be related to the hold down yield displacement $\delta_{y,h}$ by according to equation (4.4):

$$\Delta_{y,H} = \frac{\delta_{y,h}}{l} \cdot h \quad (4.4)$$

The stiffness K_H is therefore given by:

$$K_H = \frac{F_H}{\Delta_{y,H}} = n_h \cdot \frac{f_h \cdot l}{h} \cdot \frac{l}{\delta_{y,h} \cdot h} = n_h \cdot \frac{f_h}{\delta_{y,h}} \cdot \frac{l^2}{h^2} = n_h \cdot k_h \cdot \left(\frac{l}{h}\right)^2 \quad (4.5)$$

As for the yield displacement calculation, the ultimate displacement $\Delta_{u,H}$ can be obtained multiplying the hold down ultimate displacement $\delta_{u,h}$ by the ratio h/l :

$$\Delta_{u,H} = \frac{\delta_{u,h}}{l} \cdot h \quad (4.6)$$

As a results, the ductility μ_H is equal to the ductility of the hold down μ_h , according to the following expression:

$$\mu_H = \frac{\Delta_{u,H}}{\Delta_{y,H}} = \frac{\delta_{u,h}}{\delta_{y,h}} = \mu_h \quad (4.7)$$

4.2.4 Rigid-body translation contribution

The rigid body translation of the wall is usually prevented by means of metallic angle brackets (nailed or screwed to the wall) or inclined screws. If the devices are placed along the wall length with a constant spacing i_a the number of devices n_a can be calculated as:

$$n_a = \frac{l}{i_a} \quad (4.8)$$

The idealized elasto-plastic force vs. displacement curve of each device can be obtained by experimental tests or by numerical analyses, defining its strength f_a , its stiffness k_a and its ductility μ_a (Figure 4.6). The parameters which characterize the mechanical behaviour of the related horizontal non-linear spring in the rheological model (Figure 4.7) can be obtained by isolating the rigid translation source (Figure 4.8):

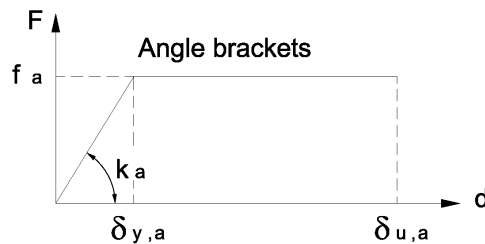


Figure 4.6: Angle brackets (or screws) elasto-plastic behaviour

$$\Delta_{Y,A} = \delta_{y,a} \quad (4.9)$$

$$\Delta_{U,A} = \delta_{u,a} \quad (4.10)$$

$$F_A = \frac{f_a \cdot l}{i_a} = f_a \cdot n_a \quad (4.11)$$

$$K_A = \frac{k_a \cdot l}{i_a} = k_a \cdot n_a \quad (4.12)$$

$$\mu_A = \frac{\delta_{u,a}}{\delta_{y,a}} = \mu_a = \frac{\Delta_{U,A}}{\Delta_{Y,A}} \quad (4.13)$$

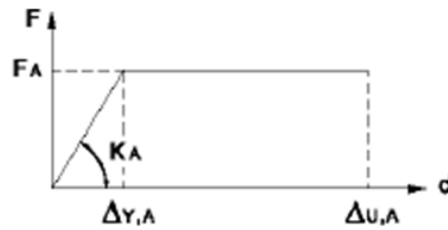


Figure 4.7: Rigid body translation component elasto-plastic behaviour

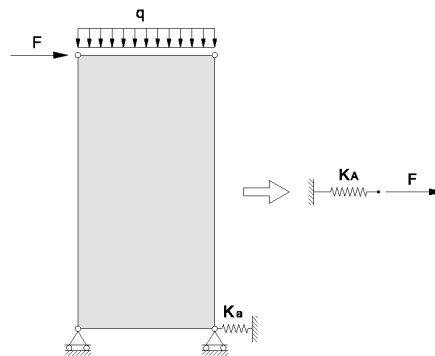


Figure 4.8: Rigid body translation component

4.2.5 Sheathing-to-framing fastener contribution

The sheathing-to-framing connection is represented by the horizontal non-linear spring K_{SH} and concerns the deformation contribution given by the fasteners slip (nails or staples). The mechanical behaviour of the spring (strength F_{SH} , the stiffness K_{SH} and the ductility μ_{SH}) does not depend only on the mechanical behaviour of each fastener (and hence on its strength f_c , the stiffness k_c and the ductility μ_c) but it is also strongly influenced by their geometrical disposition. Therefore, the global mechanical behaviour of the sheathing-to-framing connection cannot be assumed equal to the mechanical behaviour of the fasteners. Because fasteners are generally placed with a constant spacing along the edge of the panel, only the spacing s and the ratio between the height and the length of the panel α can be considered in the analysis.

The mechanical behaviour of a fastener, and hence its elasto-plastic curve, can be obtained also in this case by cheap experimental tests (monotonic or cyclic, in the same

way of angle brackets or hold-downs). On the contrary it might be burdensome and expensive to perform experimental tests on full-scale walls considering many several significant cases (with different fastener spacing s and geometrical ratios α). For this reason an analytical expression which relates global behaviour of the sheathing-to-frame connection to the mechanical behaviour of a single fasteners to, should be calculated.

In European Standard for timber structures (Eurocode 5) a relationship between the strength of fasteners f_c (Figure 4.9) and the strength of sheathing-to-frame fastener connection F_{SH} (Figure 4.10) is suggested. The expression was obtained by means of the application of the limit analysis static theorem assuming a constant distribution of the shear stresses on the edge of the panel fastener. The expression is given by:

$$F_{SH} = n_{bs} \cdot f_c \cdot \frac{l}{s} \cdot \tau \quad (4.14)$$

where¹:

- n_{bs} is the number (1 or 2) of the braced sides of the wall;
- $\tau=1$ se $\alpha < 2$ or $\tau= 2/ \alpha$ se $\alpha < 2$
- s the fasteners spacing.

¹ In equations 4.14 and 4.15, the wall length is equal to the effective wall length only if each sheathing panel length b is greater than $h/4$. On the contrary the wall length should be reduced, taking into account of the sheathing panels that respect the previous condition and a reduced length l_{red} should be used.

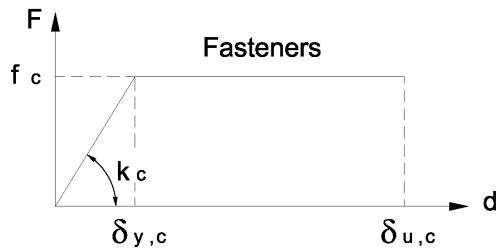


Figure 4.9: Fastener elasto-plastic behaviour

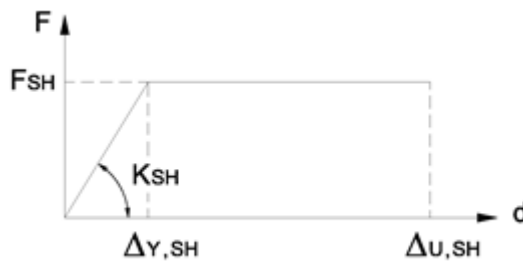


Figure 4.10: Sheathing-to-frame connection elasto-plastic behaviour

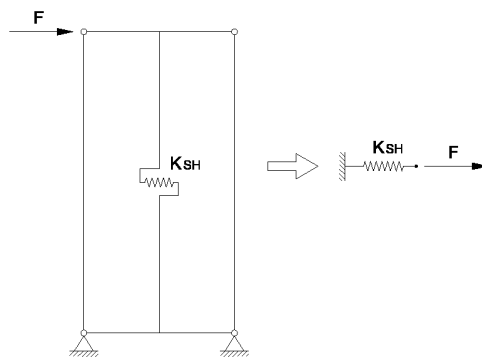


Figure 4.11: Sheathing-to-framing connection component

The stiffness K_{SH} can be obtained directly by expression suggested by eq. 3.29 , depending on the stiffness of fasteners k_c , the spacing s , the panel geometrical parameter α and the wall length l :

$$K_{SH} = \frac{n_{bs}}{\frac{1}{k_c} \cdot \lambda(\alpha) \cdot \frac{s}{l}} \quad (4.15)$$

where $\lambda(\alpha) = 0.810 + 1.855 \cdot \alpha$.

Therefore, referring to (14) and (15), the yield displacement $\Delta_{y,SH}$ can be calculated as:

$$\Delta_{y,SH} = \frac{F_{SH}}{K_{SH}} \quad (4.16)$$

whereas the ultimate displacement $\Delta_{u,SH}$ is given by:

$$\Delta_{u,SH} = \mu_{SH} \cdot \Delta_{y,SH} \quad (4.17)$$

However Standards and the literature suggest no expression for the calculation of the ductility μ_{SH} of the sheathing-to-frame connection from the ductility μ_c of the fasteners. As a consequence, the elasto-plastic mechanical behaviour of the connection cannot be completely defined.

For this purpose in section 4.4 an analytical expression is proposed. This was obtained by means of an elasto-plastic analysis of a fully anchored timber frame wall with a sequential yielding of the fasteners.

4.3 Definition of the idealized elasto-plastic behavior of a timber-frame wall

After defining the idealized elasto-plastic behaviour of each element of the rheological model (the three horizontal springs and the friction block), the elasto-plastic force vs. displacement curve of the entire wall can be obtained by means of simple mathematical expressions.

As shown in the Figure 4.12 the parameters that characterize the curve are:

- the yield force of the friction block F_q (the horizontal force required for the rotation of the wall);
- the wall strength F_W ;
- the wall stiffness $K_{tot,nt}$ when the rotation contribution is not considered;
- the wall stiffness $K_{tot,t}$ when the rotation contribution is considered;
- the wall secant stiffness K_W ;
- the wall displacement $\Delta_{q,W}$ when the friction block yields;
- the wall yield displacement $\Delta_{Y,W}$;
- the wall ultimate displacement $\Delta_{U,W}$.

The friction block yield force F_q can be calculated according to equation (4.2).

When the rotation contribution cannot be considered because the friction block is not yielded yet, the wall stiffness $K_{tot,nt}$ depends only on the contributions of the sheathing-to-framing connections and the rigid-body translation. It can be calculated as:

$$\frac{1}{K_{tot,nt}} = \frac{1}{K_{SH}} + \frac{1}{K_A} \quad (4.18)$$

Therefore, the displacement $\Delta_{q,W}$ for which the friction block yields results in:

$$\Delta_{q,W} = \frac{F_q}{K_{tot,nt}} = \frac{q \cdot l^2}{2 \cdot h} \cdot \left(\frac{1}{K_{SH}} + \frac{1}{K_A} \right) \quad (4.19)$$

The wall strength F_W is defined as the minimum value of the strength of each source (sheathing-to-panel fastener, rigid translation and rigid rotation) according to the following equation:

$$F_W = \min (F_H + F_q ; F_A ; F_{SH}) \quad (4.20)$$

The weakest source, which firstly yields because is characterized by the minimum strength, can be identified by the index i , defined as:

$$\begin{cases} i = H \rightarrow F_W = F_H + F_q \\ i = A \rightarrow F_W = F_A \\ i = SH \rightarrow F_W = F_{SH} \end{cases} \quad (4.21)$$

When the wall strength F_W is greater than the friction block yield force F_q , the wall curve is characterized by an additional stroke, describing a trilinear curve (Figure 4.12).

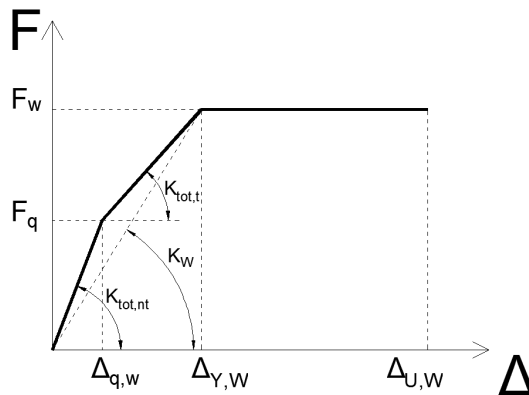


Figure 4.12: Trilinear elasto-plastic curve of a timber-frame wall

The wall secant stiffness K_{tot} when the rotation contribution is considered because the friction block is yielded, can be calculated considering all source of deformation (sheathing-to frame connection, rigid translation and rigid rotation):

$$\frac{1}{K_{tot}} = \frac{1}{K_{SH}} + \frac{1}{K_A} + \frac{1}{K_H} \quad (4.22)$$

Therefore the wall yield displacement $\Delta_{Y,W}$ can be obtained by:

$$\begin{aligned}
\Delta_{Y,W} &= \frac{F_q}{K_{tot,nt}} + \frac{F_W - F_q}{K_{tot}} = \\
&= F_q \cdot \left(\frac{1}{K_{SH}} + \frac{1}{K_A} \right) + (F_W - F_q) \cdot \left(\frac{1}{K_{SH}} + \frac{1}{K_A} + \frac{1}{K_H} \right) = \\
&= F_W \cdot \left(\frac{1}{K_{SH}} + \frac{1}{K_A} + \frac{1}{K_H} \right) - \frac{F_q}{K_H} = \\
&= \frac{F_W}{K_{tot}} - \frac{F_q}{K_H}
\end{aligned} \tag{4.23}$$

The wall secant stiffness K_W is defined as the ratio between the wall strength F_W and the yield displacement $\Delta_{Y,W}$, as reported in equation (4.24).

$$K_W = \frac{F_W}{\Delta_{Y,W}} = \frac{F_W}{\frac{F_W}{K_{tot}} - \frac{F_q}{K_H}} = \left(\frac{1}{K_{tot}} - \frac{F_q}{K_H \cdot F_W} \right)^{-1} \tag{4.24}$$

Defining the parameter β :

$$\beta = \frac{F_q}{F_W} \tag{4.25}$$

we get:

$$\frac{1}{K_W} = \frac{1}{K_{tot}} - \frac{\beta}{K_H} \tag{4.26}$$

It can be demonstrated that the wall secant stiffness K_W is greater than $K_{W,tot}$ and lower than $K_{tot,nt}$. In fact:

$$\frac{1}{K_{tot,nt}} < \frac{1}{K_W} < \frac{1}{K_{tot}} \quad (4.27)$$

$$\frac{1}{K_{SH}} + \frac{1}{K_A} < \frac{1}{K_W} < \frac{1}{K_{SH}} + \frac{1}{K_A} + \frac{1}{K_H} \quad (4.28)$$

Defining:

$$\frac{1}{K_{SH}} + \frac{1}{K_A} = C \quad (4.29)$$

we obtain:

$$C < C + \frac{1-\beta}{K_H} < C + \frac{1}{K_H} \quad (4.30)$$

Because $0 < \beta < 1$ (the yield force of the friction block F_q is lower than the strength of the wall F_W) equation (4.27) is satisfied.

When the wall strength F_W is lower than F_q ($\beta > 1$) the friction block does not yield. This condition usually occurs in case of a weak hold down or a high vertical load. The mechanical curve of the wall is therefore bi-linear (elasto-perfectly plastic), with stiffness $K_{W,na}$ (Figure 4.13).

$$\frac{1}{K_W} = \frac{1}{K_{tot,nt}} = \frac{1}{K_{SH}} + \frac{1}{K_A} \quad (4.31)$$

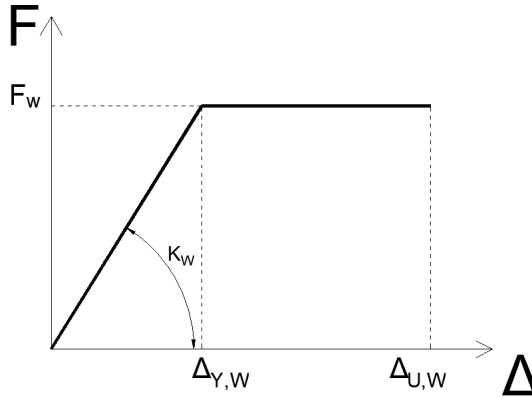


Figure 4.13: Bilinear elasto-plastic curve of a timber-frame wall

Therefore the wall yield displacement $\Delta_{Y,W}$ can be calculated as:

$$\Delta_{Y,W} = \frac{F_W}{K_{tot,nt}} = \frac{F_W}{\left(\frac{1}{K_{SH}} + \frac{1}{K_A} \right)^{-1}} \quad (4.32)$$

Considering the two different cases, the wall secant stiffness F_W and the wall yield displacement $\Delta_{Y,W}$ are defined by the following expressions:

$$\left\{ \begin{array}{l} \beta > 1 \rightarrow \frac{1}{K_W} = \frac{1}{K_{tot,nt}} \\ \beta < 1 \rightarrow \frac{1}{K_W} = \frac{1}{K_{tot}} - \frac{\beta}{K_H} \end{array} \right. \quad (4.33)$$

$$\Delta_{Y,W} = \frac{F_W}{K_W} \quad (4.34)$$

Referring to the assessment of the wall ductility μ_W , it can be shown as the global plastic displacement of the model is equal to the plastic displacement of the weakest (and hence yielded) spring. In fact, after that the external force F achieves the wall strength F_W , an increase of the external force F cannot be absorbed by the model. For this reason the increase of global displacement of the model is caused only by the stretch of the spring representing the yielded connection. In fact for the stretch of the springs which gave remained in the elastic range an increase of the external force F would be required. Therefore we get:

$$\Delta_{pl,W} = \Delta_{pl,i} \quad (4.35)$$

The wall ductility μ_W is defined as the ratio between the wall ultimate displacement $\Delta_{U,W}$ and the wall yield displacement $\Delta_{Y,W}$. Because the ultimate displacement $\Delta_{U,W}$ is given by the sum of the yield displacement $\Delta_{Y,W}$ and the plastic displacement $\Delta_{pl,W}$, the wall ductility can be rewritten as:

$$\mu_W = \frac{\Delta_{U,W}}{\Delta_{Y,W}} = \frac{\Delta_{Y,W} + \Delta_{pl,W}}{\Delta_{Y,W}} = 1 + \frac{\Delta_{pl,W}}{\Delta_{Y,W}} = 1 + \frac{\Delta_{pl,i}}{\Delta_{Y,W}} \quad (4.36)$$

The plastic displacement of the weakest spring $\Delta_{pl,i}$ can be related directly to yield displacement of the same source of deformation and to its ductility μ_i , according to the following expression:

$$\Delta_{pl,i} = \Delta_{U,i} - \Delta_{Y,i} = \Delta_{Y,i} \cdot \left(\frac{\Delta_{U,i}}{\Delta_{Y,i}} - 1 \right) = \Delta_{Y,i} \cdot (\mu_i - 1) = \frac{F_i}{K_i} \cdot (\mu_i - 1) \quad (4.37)$$

Substituting equations (4.35) and (4.37) in eq. (4.36), we get:

$$\mu_w = 1 + \frac{\frac{F_i}{K_i} \cdot (\mu_i - 1)}{\frac{F_w}{K_w}} \quad (4.38)$$

If the weakest element is represented by the sheathing-to-frame fastener contribution or by the rigid translation contribution, the wall strength F_w of the wall is given by:

$$F_w = F_i \quad (4.39)$$

where:

$$i = SH \text{ vel } A \quad (4.40)$$

Therefore the wall ductility μ_w , can be obtained by the following simplified equation:

$$\mu_w = 1 + \frac{K_w}{K_i} \cdot (\mu_i - 1) = 1 + \kappa \cdot (\mu_i - 1) \quad (4.41)$$

We can show that the parameter κ is lower than 1 and hence the ductility of the weakest contribution μ_i is always greater than the wall ductility μ_w .

In case of $\beta > 1$ we get:

$$\frac{1}{K_i} < \frac{1}{K_W} \rightarrow \frac{1}{K_i} < \frac{1}{K_{SH}} + \frac{1}{K_A} \quad i = SH, A \quad (4.42)$$

Whereas in case of $0 < \beta < 1$ we obtain:

$$\frac{1}{K_i} < \frac{1}{K_W} \rightarrow \frac{1}{K_i} < \frac{1}{K_{SH}} + \frac{1}{K_A} + \frac{1-\beta}{K_H} \quad i = SH, A \quad (4.43)$$

If the weakest source is represented by the rigid-body rotation of the wall, we get:

$$i = H \quad (4.44)$$

$$F_w = F_H + F_q > F_H \quad (4.45)$$

In this case the wall ductility μ_w can be calculated by means of the following expression:

$$\mu_w = 1 + \frac{F_H}{F_H + F_q} \cdot \frac{K_w}{K_H} \cdot (\mu_i - 1) = 1 + \iota \cdot \kappa \cdot (\mu_i - 1) \quad (4.46)$$

Because both κ and ι are lower than one, also in this case the weakest connection ductility is greater than the wall ductility. For this reason in order to maximize the wall ductility, the stiffness of the stronger sources of deformation, which remain in the elastic range, should be as great as possible so that the parameter κ tends to 1.

After calculating the wall ductility, the wall ultimate displacement $\Delta_{u,w}$ can be obtained by:

$$\Delta_{u,w} = \mu_w \cdot \Delta_{y,w} \quad (4.47)$$

The non-linear mechanical behaviour of a timber frame wall (and of its rheological model) is completely defined.

4.4 Elasto-plastic behaviour of a fully anchored timber-frame wall

A timber-frame wall is defined fully-anchored if the stiffness of the devices which prevent the rigid body motion (i.e. hold-down and angle brackets) can be assumed as infinite. Therefore, according to the model described in the previous section, the only source of deformation is represented by the sheathing-to-framing fastener connection. In this case, the mechanical behaviour of the global sheathing-to-frame connection fastener corresponds to the mechanical behaviour of a fully anchored wall (Figure 4.11).

In this section an analytical relationship between the fastener mechanical properties (strength, stiffness and ductility, Figure 4.9) and the global sheathing-to-frame connection ones (Figure 4.10) is carried out analysing the non-linear behaviour of a fully anchored wall. Particular attention is paid to the ductility parameter because, as described in section 4.2.5, Standards and literature do not suggest any detailed expression for its calculation

The investigation of the non-linear mechanical behaviour of a fully anchored timber frame wall (and hence of global the sheathing-to-frame connection) was carried out by means of an elasto-plastic analysis considering a sequential yielding of the fasteners.

In each step of the analysis the mathematical model proposed by [Girhammar and Kalssner, 2009] for the study of the linear behaviour of a timber frame wall was used. In this model, the wall frame is represented by a pinned frame (the frame is hence not restrained for horizontal loads) whereas the sheathing panel is assumed as a rigid body.

Each sheathing-to-framing fastener is modelled by a bi-directional linear elastic spring. The fastener positioning is usually symmetric (the fasteners are placed along the edge of the panel with an equal spacing). Their geometrical coordinates are related to a referring system with the origin in the centre of the panel. The external horizontal force F is applied on the top corner of the frame. The solution of the mathematical model is characterized by the calculation of the frame rotation, the sheathing panel rotation, the fastener elastic forces and the fastener displacements.

The first step of the elasto-plastic analysis is characterized by an elastic behaviour of all fasteners and by the calculation of value of external force F_1 for which one fastener yields: the wall enters its nonlinear range. Because the elasto-plastic analysis is characterized by a step by step external load increase, each of the later step is analysed still assuming an elastic global behaviour but updating the stiffness matrix of the model, considering that some fasteners have already yielded. In fact, a yielded fastener cannot be considered anymore in the model since its stiffness becomes zero. Hence, a yielded fastener does not behave as an inner constrain and for this reason it must be removed. Because in each step an elastic behaviour of the wall is assumed, the mathematical model proposed by [Girhammar and Kalssner, 2009] can be still used (neglecting the yielded fasteners) for the calculation of the incremental value of the external force for which another fastener yields.

This procedure can be carried on step by step up to the achievement of a kinematic model of the wall. When the number or the disposition of not yielded fasteners cannot guarantee a bracing system for the frame and the mathematical model cannot be used any more: the solution must be achieved by means of the kinematic theory. In order to calculate the ultimate displacement of the fully anchored wall a failure condition is to defined. In this case the condition is defined as the achievement of the ultimate displacement $\delta_{u,c}$ of at least one fastener (fastener failure condition), defined as:

$$\delta_{u,c} = \mu_c \cdot \delta_{y,c} = \mu_c \cdot \frac{f_c}{k_c} \quad (4.48)$$

Referring to the most common-in-practice geometrical properties of timber frame walls, three different kinematic models can be identified. For each of them the layout of the non-yielded fastener is not able to guarantee the lateral stability of the wall.

The first kinematic model is named 'vertical rod' (Figure 4.14, a), because the non-yielded fasteners are placed only along the intermediate vertical stud of the wall. The sheathing panel acts like a vertical rod whose rotation is equal to the rotation of the timber frame.

The second kinematic model is named 'horizontal rod' (Figure 4.14, b). In this case the sheathing panel is connected to the timber frame by means of only two fasteners, placed in the middle point of both perimeter studs. The sheathing panel acts like a horizontal rod characterized by a rigid body horizontal displacement equal to half of the horizontal displacement of the timber frame top beam.

The third kinematic model is defined 'non-restrained panel' (Figure 4.14, c) because no fastener connects the sheathing panel to the frame. For this reason when an external force is applied to the timber frame, the sheathing panel is characterized by no displacement or rotation. The sheathing panel is in fact completely released from the timber framed.

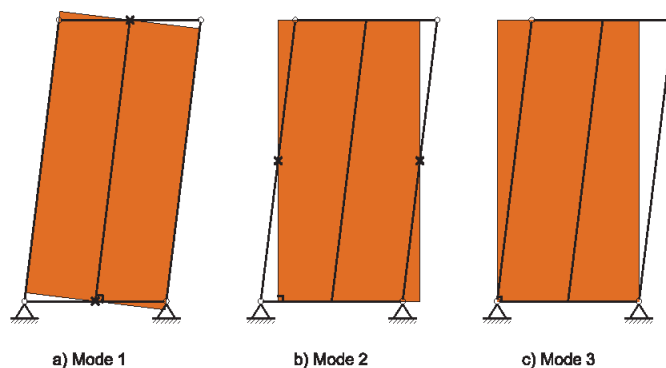


Figure 4.14: Fully anchored wall kinematic mechanisms

The kinematic analysis is carried out by increasing the kinematic degree of freedom (usually represented by the top horizontal displacement of the frame) up to the failure

condition, defined by the achievement of the ultimate displacement of one fastener at least. However the failure condition might be achieved before the kinematic mechanism of model occurs: some fastener might achieve its ultimate displacement when some other fasteners are not yielded yet. This condition usually occurs when the fastener spacing is low.

The force-displacement curve obtained by the elasto-plastic analysis is represented by a piecewise-linear curve. Each line segment is characterized by a gradually decreasing slope. The kinematic mechanism is represented by the last segment, characterized by an horizontal slope.

4.4.1 *Elasto-plastic analysis of a fully anchored wall with E.A.T.W.-1.0*

The study of the non-linear mechanical behaviour of a fully-anchored wall by means of an elasto plastic analysis is surely a very efficiently but time-consuming method since it several mathematical steps are required.

For this reason, a code (*Elasto-plastic Analysis of Timber Walls - EATW*) was implemented in *MatLab* for the analysis of several timber-framed wall typologies characterized by different properties. The analyses were carried out in particular considering three input data, namely: the dimensionless fastener spacing (s/b), the panel geometrical parameter (α) and the fastener ductility (μ_c). The fastener positioning is automatically generated by the code considering a constant spacing along the outer studs and the frame beams (equal to two times the spacing along the inner stud) and a rectangular sheathing panel. The following ranges for the input data were considered:

- $1/25 < s/b < 1/2$
- $h/b=1,2,3$
- $1 < \mu_c < 8$

The output data are represented by all parameters that characterize the mechanical behaviour of the mathematical model for all steps of analysis (displacement of the frame top beam, the increase of the external force, the sheathing panel rotation, the frame rotation, the fastener internal forces, the fastener displacements) and by the wall force vs displacement piecewise-linear curve. All output data are expressed by dimensionless units assuming the strength and the yield displacement of each fastener equal to one.

The piecewise linear curve of the wall was then bi-linearized in order to define strength, stiffness and ductility parameter of the analysed fully anchored wall (or of the global sheathing-to-panel connection).

In Table 4.1, Table 4.2 and Table 4.3, the ductility of the global sheathing-to-panel connection (corresponding to the ductility of a fully anchored frame wall) is reported, depending on the ductility of the fastener, the fastener spacing and the panel geometrical ratio.

Ductility μ_{SH} with $\alpha = 1$

μ_c	s/b					
	1/2	1/4	1/6	1/8	1/12	1/25
1.00	<u>1.00</u>	<u>1.00</u>	<u>1.00</u>	<u>1.00</u>	<u>1.00</u>	<u>1.00</u>
1.50	1.38	1.29	1.27	<u>1.27</u>	<u>1.26</u>	<u>1.26</u>
2.00	1.73	1.63	1.60	1.60	<u>1.60</u>	<u>1.59</u>
2.50	2.07	1.96	1.92	1.92	<u>1.91</u>	<u>1.91</u>
3.00	2.40	2.28	2.23	2.23	2.22	<u>2.22</u>
3.50	2.73	2.59	2.54	2.54	2.53	<u>2.52</u>
4.00	3.05	2.89	2.84	2.84	2.83	<u>2.82</u>
4.50	3.37	3.20	3.14	3.14	3.13	<u>3.12</u>
5.00	3.69	3.50	3.44	3.43	3.42	<u>3.42</u>
5.50	4.00	3.80	3.74	3.73	3.72	<u>3.71</u>
6.00	4.32	4.10	4.03	4.03	4.01	<u>4.01</u>
6.50	4.63	4.40	4.33	4.32	4.31	<u>4.30</u>
7.00	4.94	4.70	4.63	4.62	4.60	<u>4.59</u>
7.50	5.26	5.00	4.92	4.91	4.89	<u>4.89</u>
8.00	5.57	5.29	5.22	5.21	5.19	5.18

Table 4.1: Fully-anchored wall ductility for $\alpha=1$; case which the fastener failure condition occurs before the kinematic model

Ductility μ_{SH} with $\alpha = 2$

μ_c	s/b					
	1/2	1/4	1/6	1/8	1/12	1/25
1.00	<u>1.00</u>	<u>1.00</u>	<u>1.00</u>	<u>1.00</u>	<u>1.00</u>	<u>1.00</u>
1.50	1.39	<u>1.35</u>	<u>1.34</u>	<u>1.34</u>	<u>1.34</u>	<u>1.34</u>
2.00	1.83	1.77	<u>1.76</u>	<u>1.76</u>	<u>1.76</u>	<u>1.76</u>
2.50	2.26	2.18	2.17	<u>2.17</u>	<u>2.17</u>	<u>2.17</u>
3.00	2.69	2.59	2.57	<u>2.57</u>	<u>2.57</u>	<u>2.57</u>
3.50	3.11	2.99	2.97	2.97	<u>2.97</u>	<u>2.96</u>
4.00	3.53	3.39	3.37	3.36	<u>3.36</u>	<u>3.36</u>
4.50	3.94	3.79	3.76	3.76	<u>3.76</u>	<u>3.75</u>
5.00	4.36	4.19	4.16	4.15	4.15	<u>4.15</u>
5.50	4.77	4.58	4.55	4.54	4.54	<u>4.54</u>
6.00	5.18	4.98	4.95	4.94	4.93	<u>4.93</u>
6.50	5.59	5.38	5.34	5.33	5.32	<u>5.32</u>
7.00	6.01	5.77	5.73	5.72	5.71	<u>5.71</u>
7.50	6.42	6.17	6.12	6.11	6.10	<u>6.10</u>
8.00	6.83	6.56	6.52	6.50	6.49	<u>6.49</u>

Table 4.2: : Fully-anchored wall ductility for $\alpha=2$; \underline{n} case which the fastener failure condition occurs before the kinematic model

Ductility μ_{SH} with $\alpha=3$

* μ_c	s/b					
	1/2	1/4	1/6	1/8	1/12	1/25
1.00	1.00	1.00	1.00	1.00	1.00	1.00
1.50	1.43	1.40	1.40	1.40	1.40	1.40
2.00	1.90	1.85	1.85	1.85	1.85	1.85
2.50	2.36	2.30	2.29	2.29	2.29	2.29
3.00	2.82	2.74	2.73	2.73	2.73	2.73
3.50	3.27	3.18	3.17	3.17	3.16	3.16
4.00	3.73	3.62	3.61	3.60	3.60	3.60
4.50	4.18	4.06	4.04	4.04	4.03	4.03
5.00	4.64	4.49	4.48	4.47	4.47	4.47
5.50	5.09	4.93	4.91	4.90	4.90	4.90
6.00	5.54	5.37	5.35	5.34	5.33	5.33
6.50	5.99	5.80	5.78	5.77	5.76	5.76
7.00	6.44	6.24	6.21	6.20	6.20	6.20
7.50	6.89	6.68	6.65	6.63	6.63	6.63
8.00	7.35	7.11	7.08	7.07	7.06	7.06

Table 4.3: Fully-anchored wall ductility for $\alpha=3$; case which the fastener failure condition occurs before the kinematic model

As an example, the elasto-plastic analysis of a fully-anchored wall characterized by $\alpha=2$, $s/b=0.25$ and $\mu_c=3$ is reported (Figure 4.15). For each step of the analysis, the wall force-displacement piecewise-linear curve is obtained, representing in the next picture the fastener layout (from Figure 4.16, to Figure 4.17). Black and red dots for each step represent respectively not yielded and yielded fasteners. In Figure 4.22 the piecewise-linear curve and the bi-linear curve are shown.

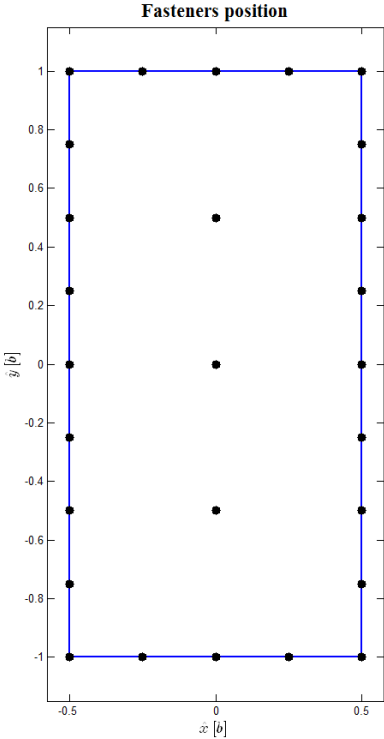


Figure 4.15: Fastener layout

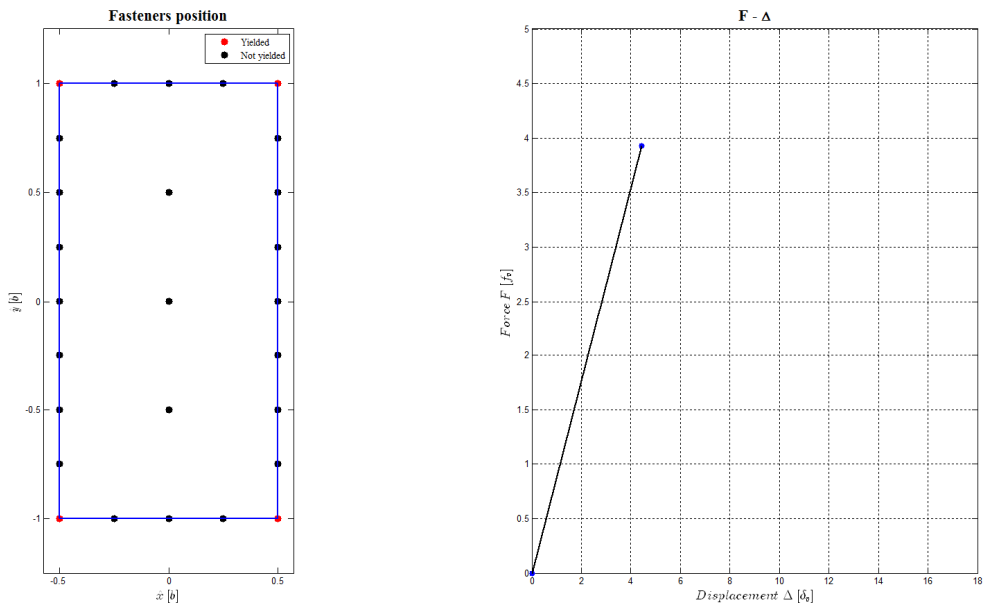


Figure 4.16: 1st step of analysis

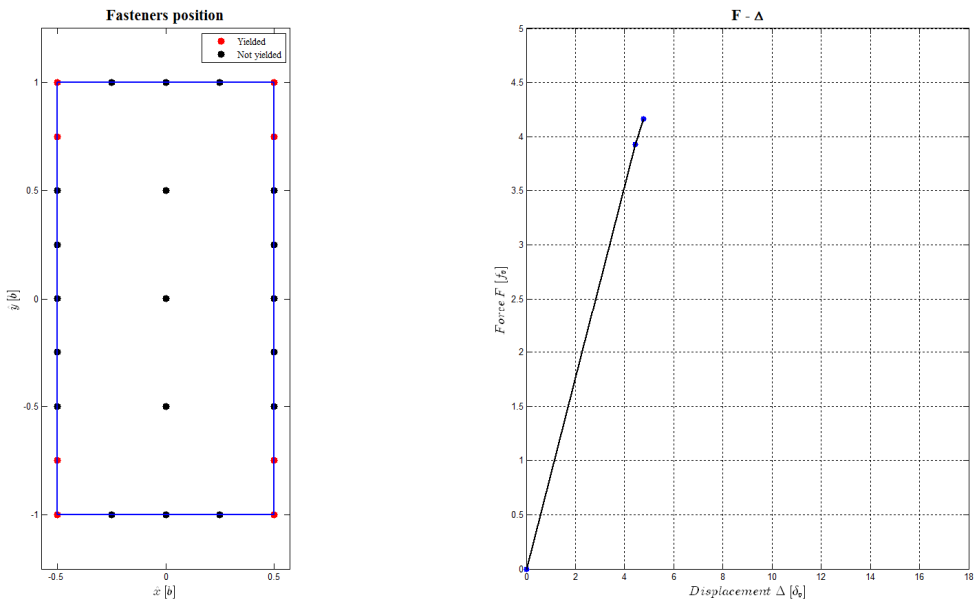


Figure 4.17: 2nd step of analysis

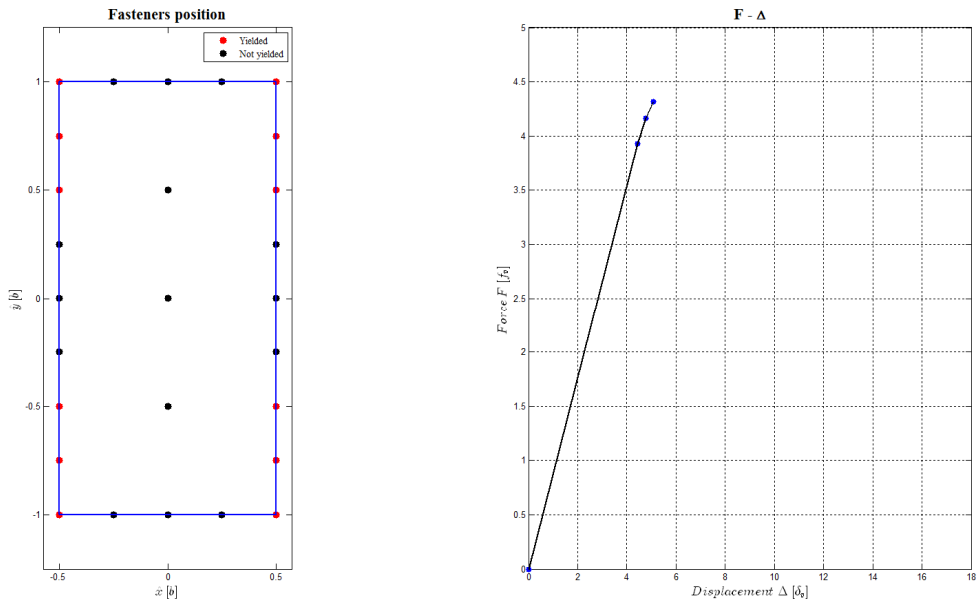


Figure 4.18: 3rd step of analysis

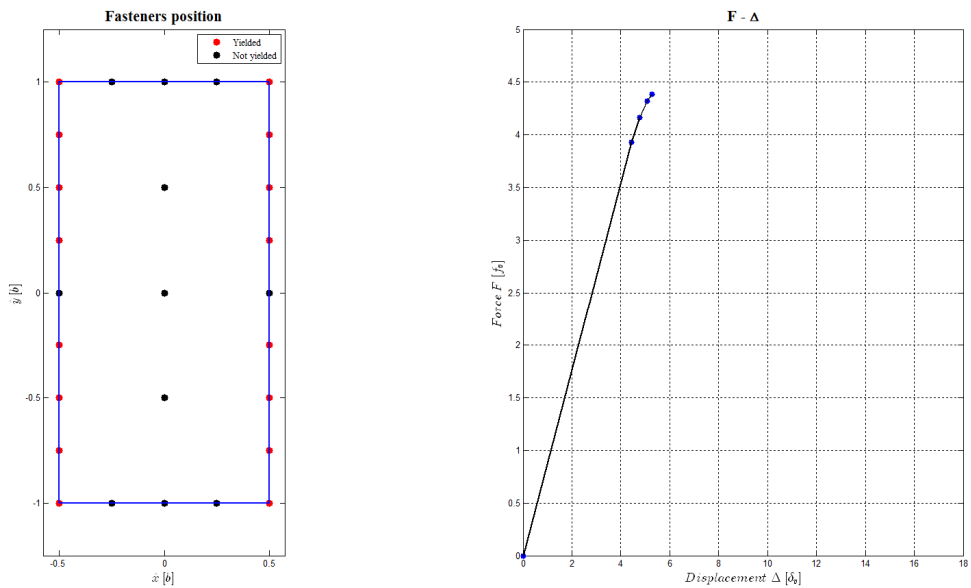


Figure 4.19: 4th step of analysis

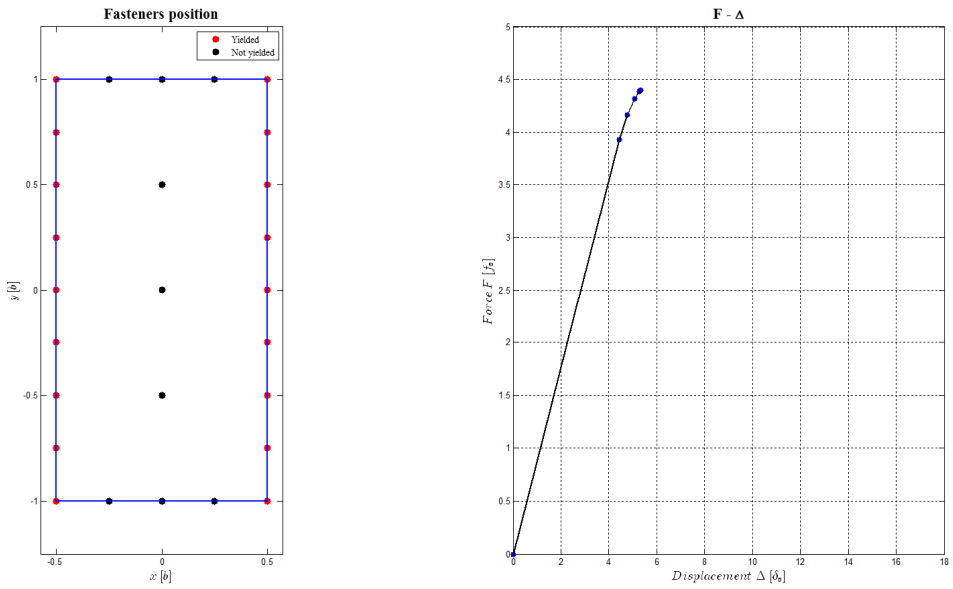


Figure 4.20: 5th step of analysis

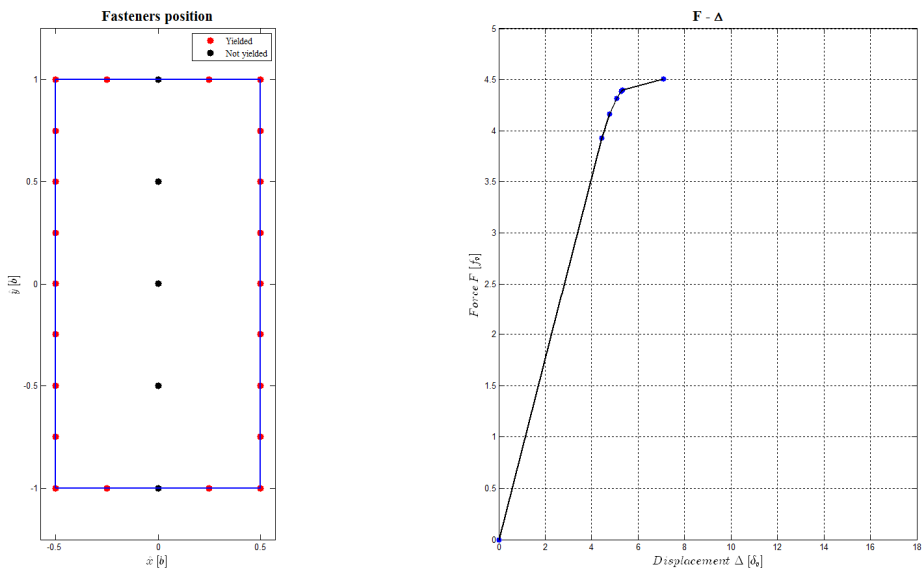


Figure 4.21: 6th step of analysis

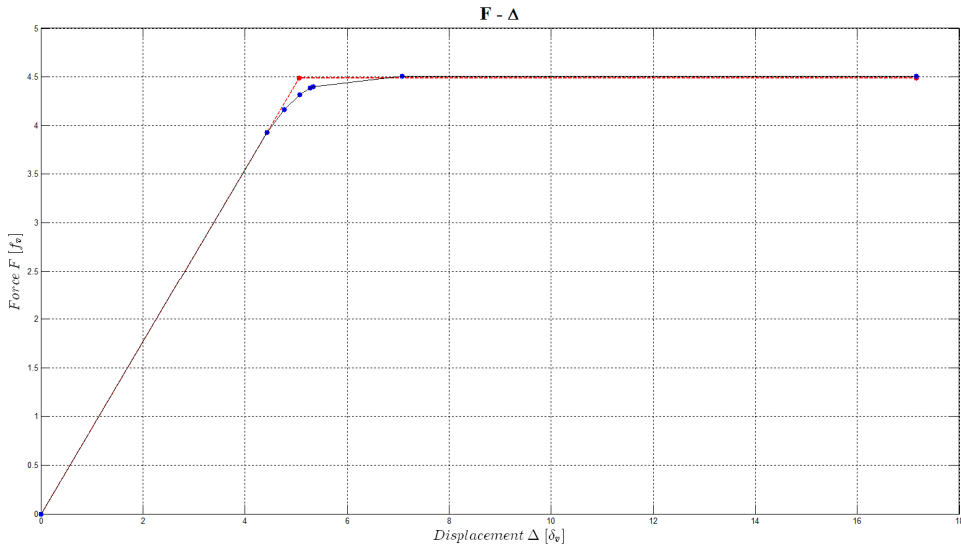


Figure 4.22: *piecewise-linear curve (solid line) and bi-linear curve (dashed line)*

In order to obtain an analytical relationship between the ductility of the global sheathing-to-frame connection μ_{SH} to the ductility of the fasteners μ_{SH} the values of Table 4.1, Table 4.2 and Table 4.3 were plotted. As shown in Figure 4.24, Figure 4.25 and Figure 4.26 a linear relationship can be assumed. The sheathing-to-frame connection ductility μ_{SH} is not significantly influenced by the fastener spacing s/b whereas it increases with the panel geometrical parameter α .

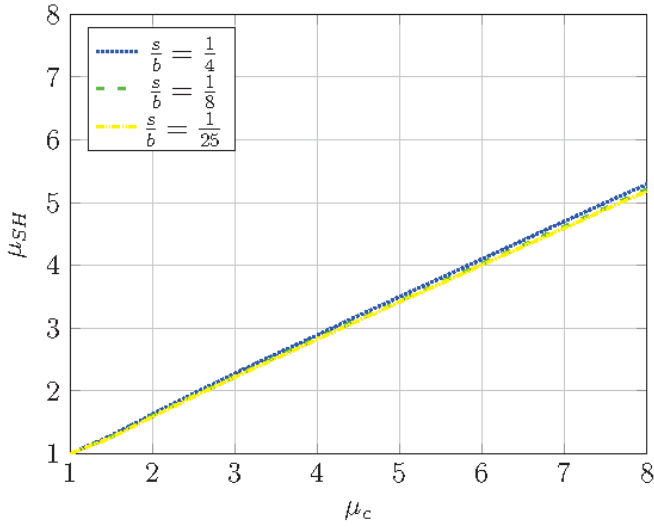


Figure 4.23: μ_{SH} vs. μ_c ($\alpha=1$)

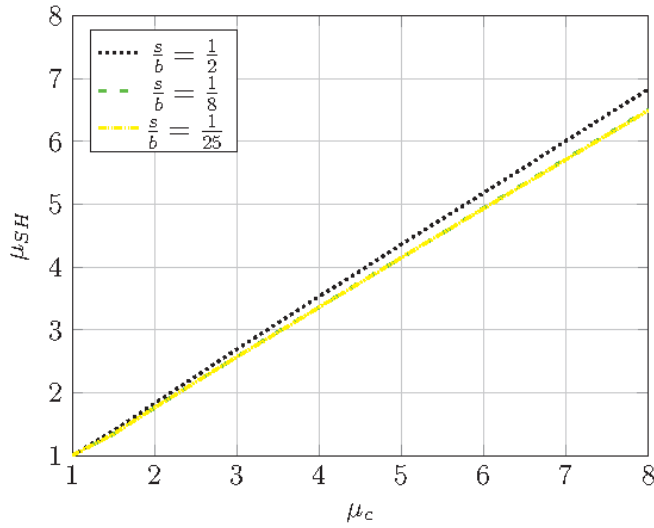


Figure 4.24: μ_{SH} vs. μ_c ($\alpha=2$)

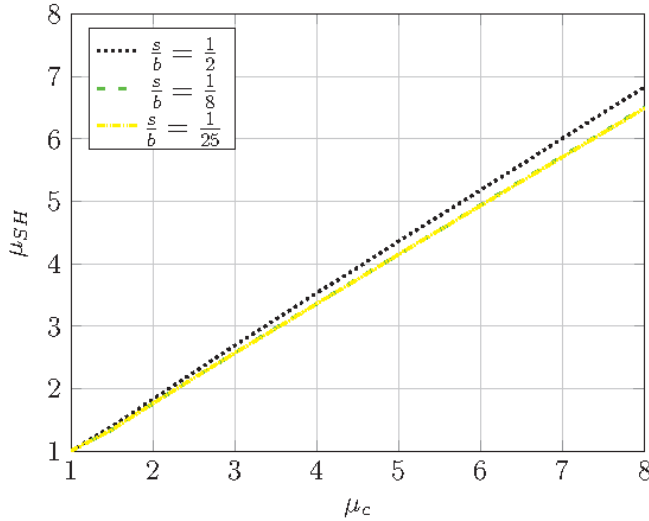


Figure 4.25: μ_{SH} vs μ_c ($\alpha=3$)

Therefore, the analytical relationship between the sheathing to frame connection ductility μ_{SH} and the fastener ductility μ_v can be obtained as:

$$\mu_{SH} = \rho(\alpha) \cdot \mu_c + v(\alpha) \quad (4.49)$$

The parameters ρ and v which depend on the panel geometric parameter α can be obtained by means of an quadratic interpolation from the previous curves:

$$\begin{cases} \rho = -0.054 \cdot \alpha^2 + 0.350 \cdot \alpha + 0.305 \\ v = 0.068 \cdot \alpha^2 - 0.415 \cdot \alpha + 0.753 \end{cases} \quad (4.50)$$

This equation represents the analytical relationship required to complete the definition of the elasto-plastic behaviour of the global sheathing-to-frame connection. Hence, the ultimate displacement $\Delta_{U,SH}$ can be calculated.

4.5 Case study

In this section a common in practice timber-frame wall is analysed describing its idealized elasto-perfectly plastic mechanical behaviour.

The analysed wall has length l and height h respectively equal to 2500 mm and 2400 mm . The timber frame is built with C24 finger-jointed solid construction timber elements and it is braced on both sides ($n_{bs}=2$) by means of two 15 mm thick ($t_p=15\text{ mm}$) and 1250 mm width b OSB3 panels. The sheathing-to-frame connection is obtained by means of 1.8 by 60 mm ring nails placed with a 125 mm constant spacing s . The wall is connected to the ground by 3 angle brackets ($n_a=3$) and a hold-down in both bottom corners ($n_h=1$). The uniform vertical load q is assumed equal to 20.8 kN/m .

The mechanical properties of fasteners, angle brackets and hold downs are obtained, in this case, by the monotonic load tests carried out by the Timber Research Group of the University of Trento. For each experimental curve an idealized elasto-plastic force-displacement curve² was defined in order to define strength, stiffness and ductility of each tested element (Figure 4.26, Figure 4.27, Figure 4.28, Table 4.4, Table 4.5, Table 4.6).

² The idealized elasto-perfectly plastic force-displacement relationship was obtained imposing that the areas under the actual and the idealized curves were equal. The stiffness of the idealized curve was defined by the slope of the line which intersects the actual curve at a force value equal to the 70% of the maximum force. However other methods can be used, provided that the idealized elasto - perfectly plastic force-displacement relationships of connectors (nails, angle brackets and hold down) and the wall are obtained by the same procedure

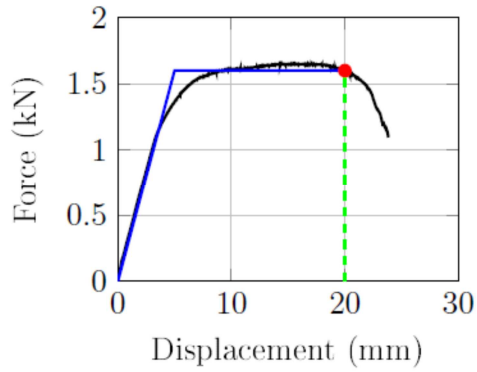


Figure 4.26: Elasto-plastic curve and experimental curve of a fastener ring 2.8x60mm

Fasteners	
f_c	1.6 [kN]
$\delta_{y,c}$	5.3 [mm]
$\delta_{u,c}$	21.3 [mm]
k_c	0.3 [kN/mm]
μ_c	4.00

Table 4.4: Mechanical properties of fasteners

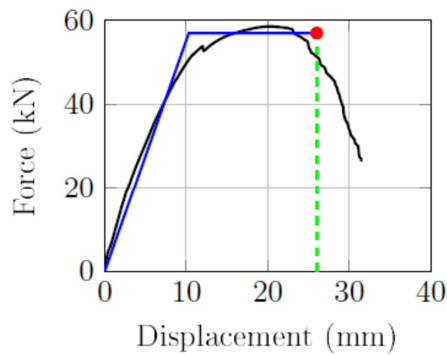


Figure 4.27: Elasto-plastic curve and experimental curve of the hold-down

Hold down	
f_h	56.9 [kN]
$\delta_{y,h}$	10.9 [mm]
$\delta_{u,h}$	27.4 [mm]
k_h	5.2 [kN/mm]
μ_h	2.50

Table 4.5: Mechanical properties of hold downs

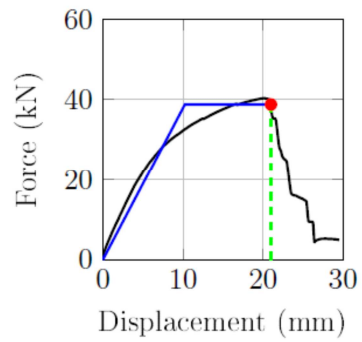


Figure 4.28: Elasto-plastic curve and experimental curve of an angle bracket

Angle bracket	
f_a	38.8 [kN]
$\delta_{y,a}$	10.2 [mm]
$\delta_{u,a}$	21.4 [mm]
k_a	3.7 [kN/mm]
μ_a	2.1

Table 4.6: *Mechanical properties of angle brackets*

According to section 4.2 the mechanical parameters which describe the behaviour of each spring and of the friction block in the rheological model can be calculated (Table 4.7, Table 4.8, Table 4.9, Table 4.10).

F_{SH}	64.0 [kN]
$\Delta_{Y,SH}$	23.2 [mm]
$\Delta_{U,SH}$	77.2 [mm]
K_{SH}	2.7 [kN/mm]
μ_{SH}	3.3

Table 4.7: *Sheathing-to-framing connection mechanical properties*

F_A	116.4 [kN]
$\Delta_{Y,A}$	10.2 [mm]
$\Delta_{U,A}$	21.4 [mm]
K_A	11.4 [kN/mm]
μ_A	2.1

Table 4.8: *Rigid body translation component mechanical properties*

F_H	59.27	[kN]
$\Delta_{Y,H}$	10.5	[mm]
$\Delta_{U,H}$	26.3	[mm]
K_H	5.7	[kN/mm]
μ_H	2.5	

Table 4.9: Rigid body rotation component mechanical properties

F_q	27.1	[kN]
-------	------	------

Table 4.10: Friction block yield curve

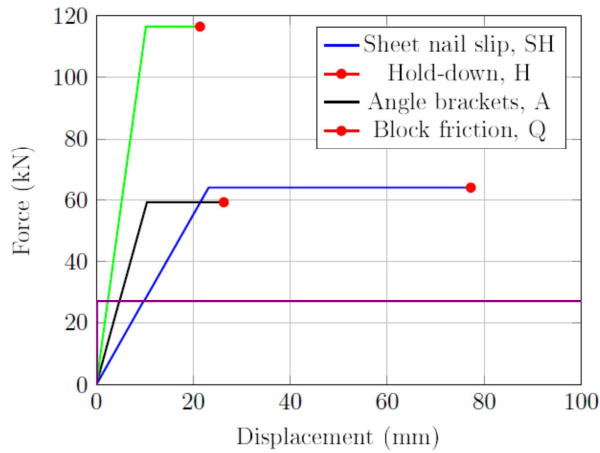


Figure 4.29: Elasto-plastic curves of the rheological model components

The strength of the wall F_w can be obtained by the following expression:

$$F_w = \min (F_H + F_q ; F_A ; F_{SH}) = \min (86.4; 116.4 ; 64.0) = 64.0 \text{ kN} \quad (4.51)$$

The weakest element index is hence defined as:

$$i = SH \quad (4.52)$$

The yield force of the friction block is equal to:

$$F_q = 27.1 \text{ kN} \quad (4.53)$$

The β parameter is hence equal to:

$$\beta = \frac{F_q}{F_w} = \frac{27.1}{64.0} = 0.4 \quad (4.54)$$

Because β is lower than 1, the mechanical behaviour of the wall can be described by a tree-linear force vs. displacement curve.

The wall stiffness $K_{tot,nt}$ is calculated as:

$$K_{tot,nt} = \left(\frac{1}{K_{SH}} + \frac{1}{K_A} \right)^{-1} = \left(\frac{1}{2.8} + \frac{1}{11.4} \right)^{-1} = 2.2 \text{ kN / mm} \quad (4.55)$$

The wall displacement $\Delta_{q,W}$ when the friction block yields hence results equal to::

$$\Delta_{q,W} = \frac{F_q}{K_{tot,nt}} = \frac{27.1}{2.2} = 12.2 \text{ mm} \quad (4.56)$$

The wall stiffness K_{tot} , related to the second segment of the curve, is calculated as:

$$K_{tot} = \left(\frac{1}{K_H} + \frac{1}{K_{SH}} + \frac{1}{K_A} \right)^{-1} = \left(\frac{1}{5.7} + \frac{1}{2.8} + \frac{1}{11.4} \right)^{-1} = 1.6 \text{ kN / mm} \quad (4.57)$$

Hence the wall yield displacement $\Delta_{Y,W}$ is:

$$\Delta_{Y,W} \frac{F_W}{K_{tot}} - \frac{F_q}{K_H} = \frac{64.0}{1.6} - \frac{27.1}{5.6} = 35.3 \text{ mm} \quad (4.58)$$

Therefore the wall secant stiffness K_W results:

$$\begin{aligned} K_W &= \left(\frac{1}{K_{tot}} - \frac{\beta}{K_H} \right)^{-1} = \left(\frac{1}{K_{SH}} + \frac{1}{K_A} + \frac{1-\beta}{K_H} \right)^{-1} = \\ &= \left(\frac{1}{2.7} + \frac{1}{11.4} + \frac{0.42}{5.66} \right)^{-1} = 1.8 \text{ kN/mm} \end{aligned} \quad (4.59)$$

The wall ductility μ_W is obtained by eq. (4.41) as:

$$\mu_W = 1 + \frac{K_W}{K_i} (\mu_i - 1) = 1 + \frac{K_W}{K_{SH}} (\mu_{SH} - 1) = 1 + \frac{1.8}{2.8} (3.3 - 1) = 2.5 \quad (4.60)$$

The ultimate displacement $\Delta_{U,W}$ results:

$$\Delta_{U,W} = \mu_w \cdot \Delta_{Y,W} = 2.5 \times 35.3 = 89.4 \text{ mm} \quad (4.61)$$

The force vs. displacement curve can be plotted as shown in Figure 4.30.

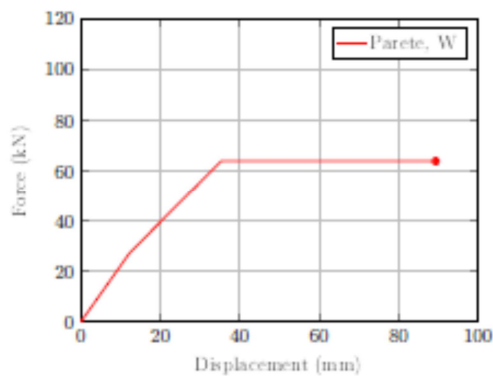


Figure 4.30: Wall elasto-plastic trilinear curve

4.6 Performance based seismic design of a timber-frame wall

The common-in-practice seismic design of a timber frame wall is based on the simple calculation of the design actions on its structural components and respectively verifications. Moreover, with the exception of the application of some simple detailing rules, related to the maximum diameter of fasteners, in most of Standards and Codes no detailed specific assessment of the failure mechanism and of the global ductility is required.

However, as reported in Chapter 2, the choice of the failure mechanism and the calculation of the global ductility of the walls are fundamental in order to guarantee the required ductility of an entire designed building, expressed by the behaviour factor q . Therefore, the current approach for the timber-frame building seismic design cannot be

considered thorough if compared to other structural types and materials. Most of seismic designs of timber-frame buildings require nowadays only resistance verifications, neglecting stiffness and ductility ones .

For this reason, a seismic performance based design method for timber frame walls is presented in this section. The design of each component constituting a timber-frame wall is carried out to satisfy not only the resistance verification, but also to guarantee the required stiffness and ductility demand of the wall.

The first step of the method regards the selection of the wall failure mechanism to which the ductility of the wall is directly related. For this reasons the ductility demand $\mu_{w,sd}$ of the wall is firstly to be imposed and the design of the connections should be carried out so that the following equation is satisfied:

$$\mu_w = 1 + \frac{F_i}{K_i} \cdot \frac{K_w}{F_w} \cdot (\mu_i - 1) > \mu_{w,sd} \quad (4.62)$$

As described in section 4.3, the ductility of the wall does not depend only on the ductility of the weakest connection.

In order to guarantee that selected failure mode of the wall occurs, the capacity design approach should be satisfied so that the stronger elements do not yield, remaining in the elastic range while the weakest element achieves its yielding dissipating the seismic energy. For this purpose the demand of stronger elements is obtained from the strength of the weakest element and not from the analyses.

If the weakest element is represented by the global sheathing-to-frame fastener connection ($i=SH$) or by the rigid body translation connection ($i=A$) (case 1), its design action $F_{Ed,i}$ results equal to the analysis design force F_{Ed} :

$$F_{Ed,i} = F_{Ed} < F_{Rd,i} \quad (4.63)$$

The design action of the elements j which must remain in the elastic range ($j=A$ if $i=SH$ or $j=SH$ if $i=A$) is given by the weakest element i strength multiplied by the over strength factor γ_{Rd} .

$$F_{Ed,j} = \gamma_{Rd} \cdot F_{Rd,i} < F_{Rd,j} \quad (4.64)$$

The design action of the hold down, the contribution of the vertical load should be considered, according to the following equation:

$$F_{Ed,H} = \gamma_{Rd} \cdot F_{Rd,i} - F_q < F_{Rd,H} \quad (4.65)$$

If the weakest element is represented by the rigid body rotation connection ($i=H$) (case 2), its design action $F_{Ed,i} = F_{Ed,H}$ can be calculated as:

$$F_{Ed,H} = F_{Ed} - F_q < F_{Rd,H} \quad (4.66)$$

In this case the global sheathing-to-frame connection and the rigid body translation connection must remain in the elastic range. Their design action is hence equal to:

$$F_{Ed,j} = \gamma_{Rd} \cdot F_{Rd,H} + F_q < F_{Rd,j} \quad (4.67)$$

with $j=A, SJ$.

The stiffness of the wall should be assessed in order to compare its displacement with code-specified displacement limits for the serviceability limit states. The following expression should be satisfied:

$$K_W \geq K_{W,min,SLE} \quad (4.68)$$

4.6.1 Design Example

In this chapter a timber-frame wall is designed according to the performance based seismic approach presented in the previous section.

The wall is subjected to a vertical uniform load q equal to 20 kN/m and an external force F_{Ed} equal to 60 kN for the ultimate limit state and equal to 30 kN for the serviceability limit state. The ductility demand $\mu_{W,Ed}$ is assumed equal to 2.5 whereas the inter-storey drift at the serviceability limit state is to be lower than 0.5% (Table 4.11).

The frame is built with C24 finger-jointed solid construction timber elements and it is braced on both sides ($n_{bs}=2$) by means of two 15 mm thick ($t_p=15 \text{ mm}$) and 1250 mm width ($b=1250 \text{ mm}$) OSB3 panels. The sheathing-to frame fastener connection, the angle brackets and the hold down are characterized by the same geometrical and mechanical properties of the wall considered in section 4.5. According to Standards, experimental properties could not be directly used because the characteristic values of the strength properties and the mean value of stiffness are required. For this reason a complete experimental campaign should be carried out for each connector and device in order to define its properties by means of a statistical approach. After getting the

characteristic value of strength $f_{j,k}$ the design strength $f_{j,d}$ can be obtained considering the safety factor γ_M :

$$f_{j,d} = \frac{f_{j,k}}{\gamma_M} \quad (4.69)$$

On the other hand the design values of stiffness and of ductility can be assumed equal to the respectively mean values.

The design yield displacement and the design ultimate displacement hence can be obtained as:

$$\delta_{y,j,d} = \frac{f_{j,d}}{k_j} \quad (4.70)$$

$$\delta_{u,j,d} = \mu_j \cdot \delta_{y,j,d} \quad (4.71)$$

In this case study, in order to simplify the presentation of the method the characteristic values are considered equal to the mean values and a safety factory equal to 1 is assumed. The design mechanical properties of each connector and devices are reported in Table 4.12, Table 4.13 and in Table 4.14).

$F_{Ed,SLV}$	60	[kN]
$F_{Ed,SLD}$	30	[kN]
l	2500	[mm]
b	1250	[mm]
h	2400	[mm]
q	20	[kN/m]
n_{bs}	2	
γ_{rd}	1.2	
γ_M	1.0	
$\mu_{W,Ed}$	2.5	
$\Delta_{lim,SLD}$	0.005h	

Table 4.11: Geometrical characteristics, loads, ductility and stiffness demand

Ring nails		
$f_{c,d}$	1.6	[kN]
k_c	0.3	[kN/mm]
μ_c	4.0	
$\delta_{y,c,d}$	5.3	
$\delta_{u,c,d}$	21.3	

Table 4.12: Ring nail 2.8 x 60 mm mechanical properties

Angle brackets		
$f_{a,d}$	38.8	[kN]
k_a	3.8	[kN/mm]
μ_a	2.1	
$\delta_{y,a,d}$	10.2	
$\delta_{u,a,d}$	21.4	

Table 4.13: Angle bracket mechanical properties

Hold down	
$f_{h,d}$	56.9 [kN]
k_h	5.2 [kN/mm]
μ_h	2.5
$\delta_{y,h,d}$	10.9
$\delta_{u,h,d}$	27.4

Table 4.14: Hold down mechanical properties

In order to satisfy the ductility demand of the wall, the global sheathing-to-frame connection was selected as the weakest element. The index i is hence equal to SH :

$$i = SH \quad (4.72)$$

The design action of the global sheathing-to-frame connection is equal to the analysis external force F_{Ed} of the wall:

$$F_{Ed,SH} = F_{Ed,SLV} = 60 \text{ kN} \quad (4.73)$$

The maximum spacing of the nails can be obtained as:

$$s_{max} = \frac{n_{bs} \cdot f_{c,d} \cdot l}{F_{Sd,SH}} \cdot \tau = \frac{2 \times 1.6 \times 2.5}{60} \times 1 = 133 \text{ mm} \quad (4.74)$$

Assuming a 90 mm spacing the strength of the global sheathing-to-frame connection $F_{rd,SH}$ results:

$$F_{Rd,SH} = F_{Rd,W} = \frac{n_{bs} \cdot f_{c,d} \cdot l}{s} \cdot \tau = \frac{2 \times 1.6 \times 2.5}{0.09} \times 1 = 88.9 \text{ kN} > F_{Sd,SH} = 60 \text{ kN} \quad (4.75)$$

The verification is satisfied.

The design action of the rigid body translation connection can be evaluated from the eq. (4.64) with $j=A$ (in fact $i=SH$):

$$F_{Ed,A} = \gamma_{Rd} \cdot F_{Rd,SH} = 1.2 \times 88.9 = 106.7 \text{ kN} \quad (4.76)$$

The minimum number of angle brackets hence results:

$$n_{a,min} = \frac{F_{Sd,A}}{f_{a,d}} = \frac{106.7}{38.8} = 2.8 \quad (4.77)$$

A number n_a equal to 4 is assumed.

The strength of the rigid body translation connection can be hence obtained as:

$$F_{Rd,A} = n_a \cdot f_{a,d} = 4 \times 38.8 = 155.2 \text{ kN} > F_{Sd,A} = 106.7 \text{ kN} \quad (4.78)$$

The strength verification is satisfied.

The design action of the rigid body rotation $F_{Ed,H}$ should be obtained from equation (4.65) after calculating the yield force of the friction block F_q :

$$F_q = \frac{q \cdot l^2}{2 \cdot h} = \frac{20 \times 2.5^2}{2 \times 2.4} = 26.0 \text{ kN} \quad (4.79)$$

$$F_{Ed,H} = \gamma_{Rd} \cdot F_{Rd,SH} - F_q = 1.2 \times 88.9 - 26.0 = 80.6 \text{ kN} \quad (4.80)$$

The required number of hold downs $n_{h,min}$ for each corner of the wall hence results:

$$F_{Ed,H} = n_{h,min} \cdot f_{h,d} \cdot \frac{l}{h} \quad (4.81)$$

$$n_{h,min} = \frac{F_{Ed,H}}{f_{h,d} \cdot h} \cdot l = \frac{80.7}{56.9 \times 2.4} \times 2.5 = 1.5 \quad (4.82)$$

The number of hold down n_h is hence assumed equal to 2:

$$n_h = 2 \quad (4.83)$$

The strength of the rigid body rotation connection $F_{Rd,H}$ can be calculated as:

$$F_{Rd,H} = n_h \cdot f_h \cdot \frac{l}{h} = 2 \times 56.9 \times \frac{2.5}{2.4} = 118.0 > F_{Sd,H} = 80.6 \text{ kN} \quad (4.84)$$

The verification is satisfied.

The stiffness demand of the wall $K_{W,min,SLE}$ can be obtained as the ratio between the serviceability limit states external force $F_{Ed,SLE}$ and The serviceability limit states limiting value $\Delta_{lim,SLD}$.

$$K_{W,min,SLE} = \frac{F_{Sd,SLE}}{\Delta_{lim,SLE}} = \frac{30}{12} = 2.5 \text{ kN/mm} \quad (4.85)$$

The stiffness of the rigid body rotation connection K_H can be calculated according to equation (4.5) as:

$$K_H = n_h \cdot k_h \cdot \left(\frac{l}{h}\right)^2 = 2 \times 5.2 \times \left(\frac{2.5}{2.4}\right)^2 = 11.3 \text{ kN/mm} \quad (4.86)$$

The stiffness of the rigid body translation connection K_A is given by (equation (4.12)) :

$$K_A = n_a \cdot k_h = 4 \times 3.8 = 15.2 \text{ kN/mm} \quad (4.87)$$

The stiffness of the global sheathing-to-frame connection K_{SH} is obtained from equation(4.15):

$$K_{SH} = \frac{n_{sb}}{\frac{1}{k_c} \cdot \lambda(\alpha) \cdot \frac{s}{l}} = \frac{2}{\frac{1}{0.3} \times 4.4 \times \frac{90}{2500}} = 3.8 \text{ kN/mm} \quad (4.88)$$

where:

$$\alpha = \frac{h}{b} = \frac{2.4}{1.25} = 1.92$$

$$\lambda(\alpha) = 0.810 + 1.855 \cdot \alpha = 0.810 + 1.855 \times 1.92 = 4.4$$

In this case, the wall strength $F_{Rd,W}$ is greater than the yield force of the friction block F_q and hence the elasto-perfectly plastic curve of the wall is tree linear.

$$\beta = \frac{F_q}{F_{W,Rd}} = \frac{26.0}{88.9} = 0.3 < 1 \quad (4.89)$$

By means of equations (4.22) and (4.24) the wall secant stiffness of the wall K_W can be compared with the required stiffness.

$$K_{tot} = \left(\frac{1}{K_{SH}} + \frac{1}{K_A} + \frac{1}{K_H} \right)^{-1} = \left(\frac{1}{3.8} + \frac{1}{15.2} + \frac{1}{11.3} \right)^{-1} = 2.4 \text{ kN/mm} \quad (4.90)$$

The verification is satisfied.

Because the weakest element is represented by the global sheathing-to-frame connection ($i=SH$), to calculate the ductility of the wall μ_w , the ductility of the sheathing-to-frame connection must be calculated by eq. (4.49):

$$\left\{ \begin{array}{l} \rho = -0.054 \times 1.92^2 + 0.350 \times 1.92 + 0.305 = 0.778 \\ \nu = 0.068 \times 1.92^2 - 0.415 \times 1.92 + 0.753 = 0.207 \\ \mu_{SH} = 0.778 \times 4.0 + 0.207 = 3.33 \end{array} \right. \quad (4.91)$$

The ductility of the wall results:

$$\mu_w = 1 + \frac{K_w}{K_i} \cdot (\mu_i - 1) = 1 + \frac{2.6}{3.8} \cdot (3.3 - 1) = 2.6 > \mu_{w, sd} = 2.5 \quad (4.92)$$

The verification is satisfied.

5 LINEAR ANALYSIS OF TIMBER-FRAME MULTI-STOREY WALLS UNDER HORIZONTAL FORCES

After introducing in chapters 3 and 4 the mechanical behaviour (linear and non-linear) of a timber frame wall under a horizontal force, in this chapter multi-storey wall series are analysed. The main aim of this study is the assessment of horizontal force distribution of timber-frame walls by means of a simplified analysis model. Particular attention is paid to the seismic analysis. Only elastic linear analyses are investigated: these in fact are the most common-in-practice in the phase design of timber frame buildings.

5.1 A backup numerical modelling for multi-storey walls under horizontal forces

In this section a backup numerical modelling for the linear analysis of a multi-storey series $(m \times n)^3$ of a timber frame walls subjected to horizontal forces is presented. The main objective is the assessment of the internal actions for each level of each wall by means of a suitable but simplified analysis model. This model is a natural evolution of the 1-storey wall model presented in chapter 3 because the same sources of deformations are considered. Firstly, a singular multi-storey wall $(m \times 1)$ is analysed; secondly the behaviour of a 1-storey series of walls $(1 \times n)$ is investigated; lastly a general modelling for the analysis of multi-storey series of walls $(m \times n)$ is proposed.

5.1.1 Backup numerical modelling for a vertically-aligned wall $(m \times 1)$

The analysis model for a vertically-aligned timber frame wall can be obtained a simple superimposition of the 1-storey wall model presented in chapter 3. At each level j^{th} , the timber frame wall is represented by a pinned frame braced by a horizontal spring with stiffness $K_{SP,j}$. Each bottom corner is connected to the lower wall by means of a vertical elastic spring with stiffness $k_{h,j}$, modelling the in-tension hold down, and a pinned axially rigid beam on the other corner. Moreover, a horizontal spring with stiffness equal to $K_{A,j}$ is used to simulate the source of deformation from devices which prevent the rigid body translation of the walls (Figure 5.1). A uniform vertical load q_j may be used to simulate dead and live loads on the wall.

³ A series of multi-storey walls can be defined as a mathematical matrix whose rows represent the levels and each column represent a singular vertically-aligned wall. Hence a series of wall can be represented by two indexes: j for the j^{th} level and i for the i^{th} wall).

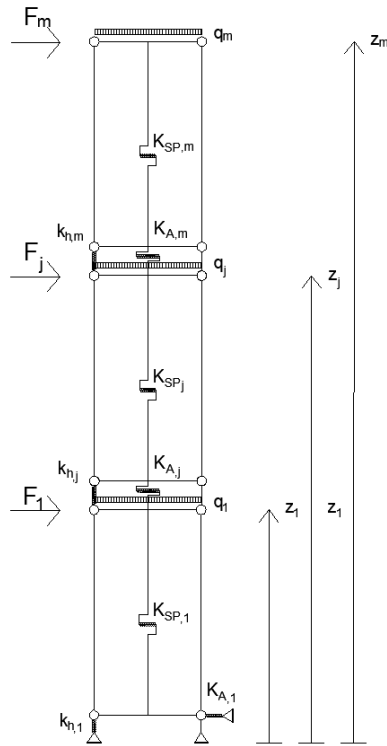


Figure 5.1: $m \times 1$ wall modelling

As for 1-storey wall, the sources of deformation are represented by the sheathing panel shear, the global sheathing-to-frame connection, the rigid body rotation and the rigid body translation. However, as shown in Figure 5.1, the influence of the rigid body rotation increases with the height of the wall because it is linear related to the level height z_j . Hence, according to the observations reported in Chapter 1, the non-linearity between the stiffness of the wall and its length becomes remarkable.

When the hold-down tensile force $T_{h,j}$ is negative, the hold-down is not in tension. For this reason, the vertical spring with stiffness $k_{h,j}$ is to be replaced by a pinned axially rigid beam. The analysis model in fact must be consistent with the obtained solution.

5.1.2 Study of 1-storey series of walls (1 x n)

A model for 1-storey series of walls can be obtained by connecting each 1-storey wall i_{th} to the next one, $i+1_{th}$, with a horizontal axially rigid pinned beam (Figure 5.2). This beam is used to simulate the usual diaphragm behaviour of the floor which impose the same horizontal displacements of the walls.

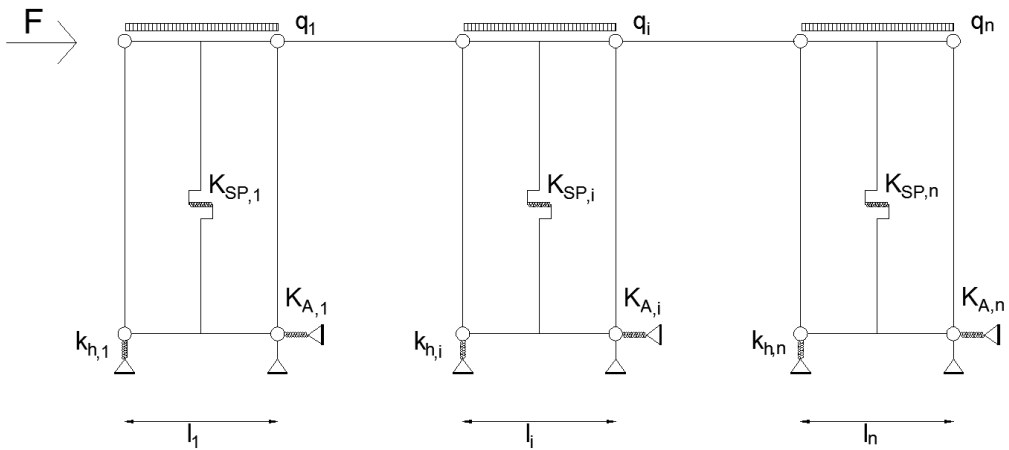


Figure 5.2: 1-storey 1 x n series of wall

To get the solution of the analysis model, represented by the horizontal force of each wall F_i and the horizontal system Δ , a numerical or an analytical approach can be performed.

In order to study the influence of the source of deformation on the internal force distribution, the constitutive law of the system, the equilibrium law and the compatibility law must be considered.

The constitutive law of the system is represented by the expression which relates the force acting on a wall F_i to its horizontal displacement Δ_i , as reported in chapter 3:

$$F_i = K_{tot,i} \cdot (\Delta_i + \Delta_{N,i}) \quad (5.1)$$

The equilibrium of the system is represented simply by the sum of the forces actin on each wall,

$$\sum_{i=1}^n F_i = F \quad (5.2)$$

while the compatibility law imposes the same horizontal displacement for all the walls:

$$\Delta_i = \Delta \quad (5.3)$$

By some simple mathematical operations, the horizontal displacement Δ and the forces acting on each wall F_i can be calculated as:

$$\Delta = \frac{F - \sum_{i=1}^n (K_{tot,i} \cdot \Delta_{N,i})}{\sum_{i=1}^n K_{tot,i}} \quad (5.4)$$

$$F_i = \frac{K_{tot,i}}{\sum_{j=1}^n K_{tot,j}} \cdot \left[F - \sum_{j=1}^n (K_{tot,j} \cdot (\Delta_{N,j} - \Delta_{N,i})) \right] \quad (5.5)$$

Equation 5.5 shows how the forces acting on each wall F_i depends on the stiffness $K_{tot,i}$ of the wall (which, according to the parametric study presented in Chapter 3, is not linear to the wall length) and its influenced by the vertical loads of all walls.

The tensile force of hold-down of the i_{th} wall can be calculated as:

$$T_i = \frac{F_i \cdot h}{l_i} - \frac{q_i \cdot l_i}{2} \quad (5.6)$$

If the i_{th} hold-down is not in tension, the wall stiffness $K_{tot,nt,i}$ must be used: the rigid body rotation source must be neglected. Moreover the horizontal displacement given by the vertical load $\Delta_{N,i}$ results equal to zero. In this case the analysis must be performed again, according to the new consistent model. The analysis process is hence iterative.

The same results can be carried out with the numerical model, previously described. Also in this case an iterative process may be required. When a hold-down force is negative, the vertical spring must be replaced with a vertical axially rigid pinned beam and a new analysis must be performed.

5.1.3 Case study

A numerical example is presented to assess the force distribution for a 1×2 series of walls (*Figure 5.3*) under a horizontal force F of 30 kN. The geometrical and mechanical properties of both walls are reported in *Table 5.1*.

The stiffness of each equivalent spring of the simplified model is:

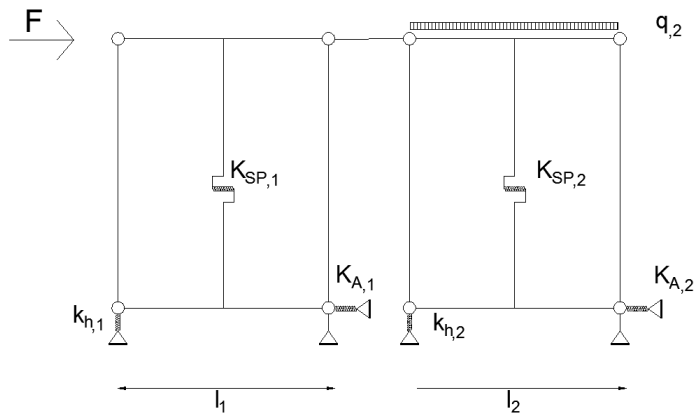


Figure 5.3: 1×2 series of wall

	Wall n.1	Wall n.2
Length l [mm]	2500	2500
Height h [mm]	2500	2500
Vertical load q [kN/m]	0	20
Braced sides n_{bs}	2	2
Sheathing panel shear modulus G_p [MPa]	1000	1000
Shathing panel thickness t_p [mm]	15	15
Shathing panel length b [mm]	1250	1250
Fastener stiffness k_c [N/mm]	500	500
Fastener spacing s_c [mm]	100	100
Hold down stiffness k_h [N/mm]	5000	5000
Angle bracket stiffness k_a [N/mm]	3000	3000
Angle bracket number n_a [N/mm]	4	4

Table 5.1: Properties of walls

$$K_{P,1} = \frac{G_{p,1} \cdot n_{bs,1} \cdot t_{p,1} \cdot l_1}{h} = 30000 \frac{N}{mm}$$

$$K_{P,2} = \frac{G_{p,1} \cdot n_{bs,2} \cdot t_{p,2} \cdot l_2}{h} = 30000 \frac{N}{mm}$$

$$K_{SH,1} = \frac{n_{bs,1} \cdot k_{c,1} \cdot l_1}{\lambda_1 \cdot s_{c,1}} = 5531 \frac{N}{mm}$$

$$K_{SH,2} = \frac{n_{bs,2} \cdot k_{c,2} \cdot l_2}{\lambda_2 \cdot s_{c,2}} = 5531 \frac{N}{mm}$$

$$K_{A,1} = k_{a,1} \cdot n_{a,1} = 12000 \frac{N}{mm}$$

$$K_{A,2} = k_{a,2} \cdot n_{a,2} = 12000 \frac{N}{mm}$$

$$K_{H,1} = \frac{k_{h,1} \cdot l_1^2}{h^2} = 5000 \frac{N}{mm}$$

$$K_{H,2} = \frac{k_{h,2} \cdot l_2^2}{h^2} = 5000 \frac{N}{mm}$$

The first iteration is carried out assuming that both the hold-downs are in tension. The stiffness of each wall results:

$$K_{TOT,1} = \left(\frac{1}{K_{P,1}} + \frac{1}{K_{SH,1}} + \frac{1}{K_{A,1}} + \frac{1}{K_{H,1}} \right)^{-1} = 2010 \frac{N}{mm}$$

$$K_{TOT,2} = \left(\frac{1}{K_{P,2}} + \frac{1}{K_{SH,2}} + \frac{1}{K_{A,2}} + \frac{1}{K_{H,2}} \right)^{-1} = 2010 \frac{N}{mm}$$

The displacements caused by the vertical load is:

$$\Delta_{N1} = \frac{q_1 \cdot h}{2 \cdot k_{h,1}} = 0mm$$

$$\Delta_{N2} = \frac{q_2 \cdot h}{2 \cdot k_{h,2}} = 5mm$$

From equation (5.5) the forces acting on each wall are:

$$F_1 = \frac{K_{tot,1}}{\sum_{j=1}^2 K_{tot,j}} \cdot \left[F - \sum_{j=1}^2 \left(K_{tot,j} \cdot (\Delta_{N,j} - \Delta_{N,1}) \right) \right] = 9.98kN$$

$$F_2 = \frac{K_{tot,2}}{\sum_{j=1}^2 K_{tot,j}} \cdot \left[F - \sum_{j=1}^2 \left(K_{tot,j} \cdot (\Delta_{N,j} - \Delta_{N,2}) \right) \right] = 20.02kN$$

The total displacement is:

$$\Delta = \frac{F - \sum_{i=1}^2 \left(K_{tot,i} \cdot \Delta_{N,i} \right)}{\sum_{i=1}^2 K_{tot,i}} = 4.96mm$$

The hold-down axial forces can be calculated as:

$$T_1 = \frac{F_1 \cdot h}{l_1} - \frac{q_1 \cdot l_1}{2} = 9.98kN$$

$$T_2 = \frac{F_2 \cdot h}{l_2} - \frac{q_2 \cdot l_2}{2} = -4.98kN$$

The hold-down of the second wall is not in tension. The solution is hence not consistent with the analysis model. For this reason the stiffness $k_{h,2}$ must be imposed equal to infinity:

$$k_{h,2} \rightarrow \infty$$

The total stiffness of the wall 1 $K_{tot,nt,1}$ hence results equal to

$$K_{TOT,2} = \left(\frac{1}{K_{P,2}} + \frac{1}{K_{SH,2}} + \frac{1}{K_{A,2}} \right)^{-1} = 3362 \frac{N}{mm}$$

while the horizontal displacement due to the vertical load results equal to zero:

$$\Delta_{N2} = \frac{q_2 \cdot h}{2 \cdot k_{h,2}} = 0mm$$

Solving the updated model of analysis we get:

$$F_1 = 11.2kN$$

$$F_2 = 18.78kN$$

$$\Delta = 5.58mm$$

The updated hold-down axial forces are:

$$T_1 = \frac{F_1 \cdot h}{l_1} - \frac{q_1 \cdot l_1}{2} = 11.2 \text{ kN}$$

$$T_2 = \frac{F_2 \cdot h}{l_2} - \frac{q_2 \cdot l_2}{2} = -6.22 \text{ kN}$$

Because T_2 is negative the solution is consistent.

5.1.4 Modelling for a series of walls ($m \times n$)

The analysis model of a m -storey series of n walls is a natural development of the two previous models presented in sections 5.1.2 and 5.1.3. Each wall is considered as m -storey vertically aligned wall connected to other walls at each level by means of horizontal axially rigid pinned beam. These are used also in this case to represent the diaphragm behaviour of the floors and hence to impose the same horizontal displacement of the walls. Each wall is characterized by an internal horizontal spring with stiffness equal to $K_{SP,ji}$ (where j is related to the j -th level and i to the i -th wall) and connected to the lower wall with a vertical spring $k_{h,ji}$, a vertical axially rigid pinned beam and a horizontal spring $k_{a,ji}$. Each wall may be loaded by a uniform vertical load $q_{,ji}$. An external horizontal force F_j is assigned at each level (Figure 5.4).

Exactly as in the previous cases, the solution obtained by the analysis must be consistent with the adopted model. If the hold down axial force T_{ji} is positive (hold down in tension) a vertical spring $k_{h,ji}$ must be used. On the contrary, when T_{ji} is negative (hold down not in tension) the vertical spring must be replaced with a vertical axially rigid pinned beam. For this reason the process is iterative and it can be stopped when the compatibility is achieved.

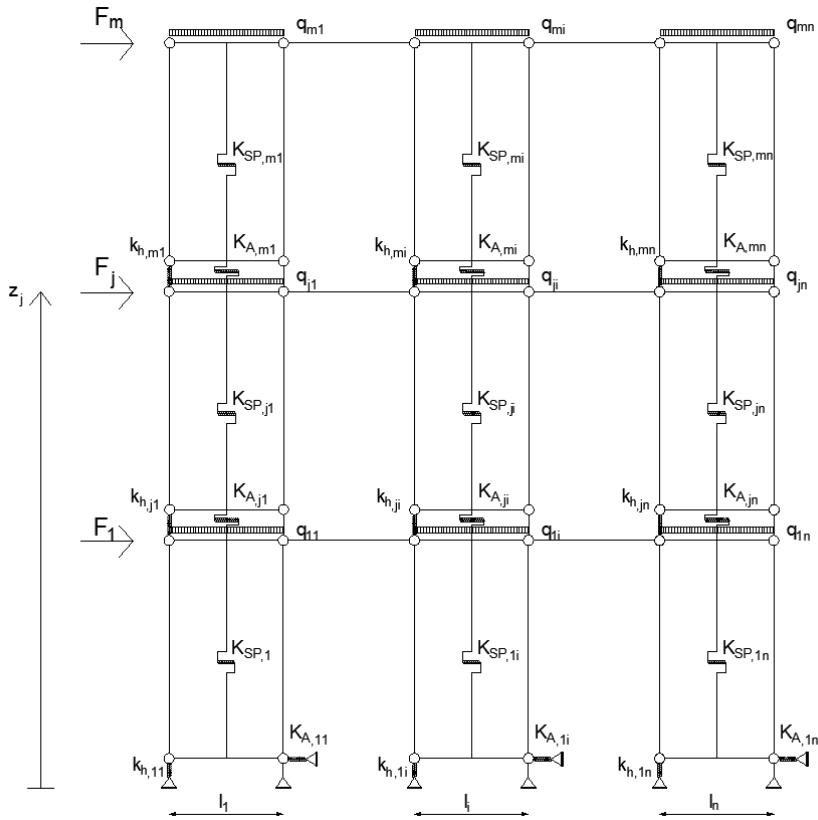


Figure 5.4: $m \times n$ series of walls

5.1.5 Case study

A 3×2 series of wall under horizontal forces is studied in this section. The mechanical and geometrical properties of the walls are reported in Table 5.2 while the external forces in Table 5.3. In the first iteration all hold-downs on the left corner of the walls are supposed in tension (Figure 5.5).

LINEAR ANALYSIS OF T.-F. MULTI-STOREY WALLS UNDER HORIZONTAL FORCES

	Wall n.1 i=1			Wall n.2 i=2		
	j=1	j=2	j=3	j=1	j=2	j=3
Length l [mm]		2500			1250	
Height h [mm]	2500	2500	2500	2500	2500	2500
Vertical load q [kN/m]	15	15	10	0	0	0
Braced sides n_{bs}	2	2	2	2	2	2
Sheathing panel shear modulus G_p [MPa]	1000	1000	1000	1000	1000	1000
Shathing panel thickness t_p [mm]	15	15	15	15	15	15
Shathing panel length b [mm]	1250	1250	1250	1250	1250	1250
Fastener stiffness k_c [N/mm]	500	500	500	500	500	500
Fastener spacing s_c [mm]	100	100	100	100	100	100
Hold down stiffness k_h [N/mm]	5000	2500	2500	5000	2500	2500
Angle bracket stiffness k_a [N/mm]	3000	2000	2000	3000	2000	2000
Angle bracket number n_a [N/mm]	4	4	4	2	2	2

Table 5.2: Properties of 3 x 2 series of walls

	j=1	j=2	j=3
F [kN]	5	10	10

Table 5.3: External horizontal forces

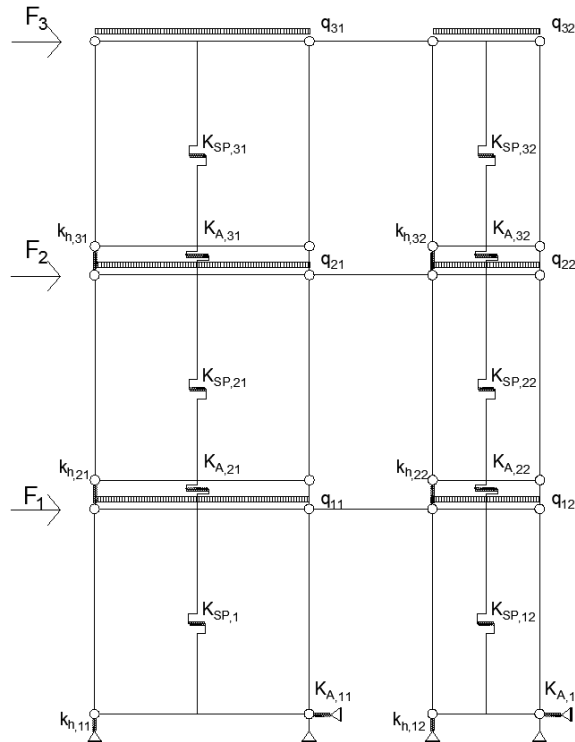


Figure 5.5: 3 x 2 model: 1st iteration

The internal shear of each wall at each level, the axial forces at the left and right bottom corners of the walls are reported in Table 5.4.

	Wall n.1 i=1			Wall n.2 i=2		
	j=1	j=2	j=3	j=1	j=2	j=3
Shear [kN]	20.8	18.5	11.0	4.2	1.5	-0.1
Left corner axial force [kN]	0.3	-1.8	-1.6	9.4	1.1	-1.9
Right corner axial force [kN]	-100.2	-60.7	-23.5	-9.4	-1.1	+1.9

Table 5.4: Results of 1st iteration (inconsistent values are underlined)

Because hold-down axial forces $T_{2,1}$ and $T_{3,1}$ are negative (-1.8 kN and -1.6 kN) and the vertical pinned beam axial force $N_{3,2}$ is positive (+1.9), the solution is not consistent. All hold down axial forces should be positive (in tension) and all vertical pinned beam ones negative (in compression). For this reason a model updating is required, substituting the

two in-compression hold-downs with two vertical axially rigid pinned beam and the in-tension vertical pinned beam with a vertical spring (Figure 5.6).

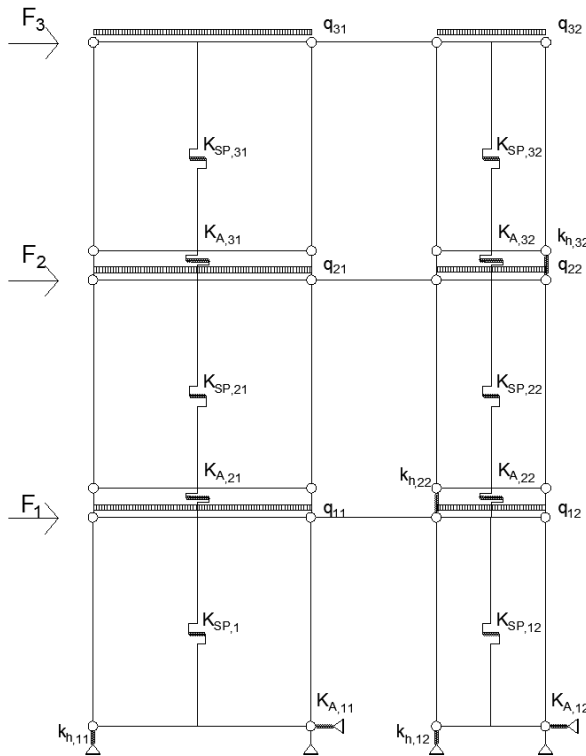


Figure 5.6: 3 x 2 model: 2nd iteration

It is important to highlight how at the 3rd level of the wall n.2 the side in tension is the right-one while at the 1st and 2nd level is the left-one: the vertical springs have different positions.

The solution of the new model is reported in Table 5.5.

	Wall n.1 i=1			Wall n.2 i=2		
	j=1	j=2	j=3	j=1	j=2	j=3
Shear [kN]	21.0	18.5	11.0	4.0	1.5	-0.1
Left corner axial force [kN]	0.2	-2.1	-1.9	9.7	1.7	1.4
Right corner axial force [kN]	-100.1	-60.4	-23.2	-9.7	-1.7	-1.3

Table 5.5: results of 1st iteration

All results are consistent. The horizontal displacements for both iterations are reported in Table 5.6.

	j=1	j=2	j=3
Δ (1 st) [mm]	6.6	11.9	14.3
Δ (2 nd) [mm]	6.3	12.6	16.2

Table 5.6: *horizontal displacements*

5.2 Linear seismic analysis of timber frame walls

In section 5.1.4 a model for the analysis of multi-storey walls under static horizontal loads was introduced. Horizontal forces may represent equivalent seismic actions and therefore this model can be used to carry out linear seismic analyses too. Depending on the structural properties of the building two types of analyses are usually suggested by Standards: the lateral force method of analysis (LFM) and the modal response spectrum (MRS) analysis.

5.2.1 Lateral force method

The Lateral Force Method (LFM) of analysis for the seismic design of a timber frame building can be assumed as a particular case of the analysis method introduced in section 5.1.4. The LFM in fact supposes that the seismic action is represented by equivalent static horizontal forces applied to the building storeys.

The magnitude of each force can be calculated assuming that the building dynamic response is not significantly affected by contribution from higher modes of vibration. In most cases the distribution of the horizontal equivalent seismic forces are calculated supposing that the first mode horizontal displacements increase linearly with the of the building. For these two reasons, the LFM is usually used only when the structure meets the regular in elevation criteria. The fundamental period of the structure is generally assessed by means of a simplified expression, without a modal analysis of the structure, depending on its height.

Also for this type of analysis, an iterative process might be required in order to obtain a consistent solution with the adopted model. Wall shears, hold-down axial forces and horizontal displacements can be calculated.

5.2.2 Modal Response Spectrum analysis

When the dynamic behaviour of a structure does not depend only by its first mode of vibration, a modal response spectrum (MRS) analysis is required. The seismic action is represented also in this case by equivalent horizontal static forces but all significant modes of vibration are considered in the analysis. For this reason, a dynamic modal analysis should be performed in order to assess the period, the mode shape and the effective modal mass for each significant mode of vibration. The effects produced by each equivalent force distribution are the combined according to procedures suggested by Standards (i.e. SRSS, CQC, etc.).

The application of the MRS analysis to a series of timber frame walls ($m \times n$) requires first of all the study of its dynamic behaviour by means of a suitable model. For this purpose the backup model presented for the static analysis can be used.

Referring to a 1-storey single timber frame wall, a concentrated mass m is added on the top framing beam of the model presented in Chapter 3.

The equation of motion can be obtained from the equilibrium of the concentrated mass subjected to its inertial force F_{in} and to the wall elastic force F :

$$F_{in} + F = 0 \quad (5.7)$$

The inertial force can be expressed as

$$F_{in} = m \cdot \ddot{\Delta} \quad (5.8)$$

where $\ddot{\Delta}$ is the acceleration of the wall.

The wall elastic force, according to Chapter 3, is given by⁴:

$$F = K_{tot} \cdot (\Delta + \Delta_N) \quad (5.9)$$

Substituting equations (5.8) and (5.9) in (5.7) we get:

$$m \cdot \ddot{\Delta} + K_{tot} \cdot (\Delta + \Delta_N) = 0 \quad (5.10)$$

Or:

$$m \cdot \ddot{\Delta} + K_{tot} \cdot \Delta = -K_{tot} \cdot \Delta_N \quad (5.11)$$

Dividing each term of equation (5.11) by the mass m , a second order differential equation can be obtained:

$$\ddot{\Delta} + \omega^2 \cdot \Delta = -\omega^2 \cdot \Delta_N \quad (5.12)$$

where the circular frequency is defined as:

$$\omega^2 = \sqrt{\frac{K_{tot}}{m}} \quad (5.13)$$

The solution can be obtained considering both the homogeneous and the particular terms as:

⁴ If the source of deformation caused by the hold-down is not considered the equation (5.9) is rewritten as: $F = K_{tot,nt} \cdot \Delta$

$$\Delta(t) = A \cdot e^{(i \cdot \omega \cdot t + \vartheta)} + \Delta_N \quad (5.14)$$

where A and ϑ are respectively the amplitude and the phase of the motion.

When the rigid body contribution is not considered equations (5.12),(5.13) and (5.14) and are rewritten as:

$$\ddot{\Delta} + \omega_{nt}^2 \cdot \Delta = 0 \quad (5.15)$$

$$\omega_{nt}^2 = \sqrt{\frac{K_{tot,nt}}{m}} \quad (5.16)$$

$$\Delta(t) = A \cdot e^{(i \cdot \omega_{nt} \cdot t + \vartheta)} \quad (5.17)$$

The modal analysis for a multi-storey series of walls can be performed similarly to the 1-storey singular wall. Referring to the backup model proposed in section 5.1.4 a concentrated mass m_j is assigned to the j^{th} storey⁵. The mass matrix M is hence defined as:

$$[M] = \begin{bmatrix} m_1 & 0 & 0 & 0 \\ 0 & m_j & 0 & 0 \\ 0 & 0 & m_{j+1} & 0 \\ 0 & 0 & 0 & m_m \end{bmatrix} \quad (5.18)$$

Therefore a modal analysis of the model can be performed, obtaining the r -th natural period T_r and the relative mode shape $\{\phi\}^r$.

⁵ The concentrated mass is not assigned to each wall because the horizontal displacements are supposed the same.

If the hold-down source of deformation for the $wall_{ji}$ is not considered, the vertical spring $k_{h,ji}$ must be replaced by a vertical axially rigid pinned beam. For this reason, for a series of wall several different dynamic properties (periods and mode shapes) can be assessed, depending on the hold-down state (tension or not in tension).

After calculating the dynamic properties of a series of walls the MRS analysis can be performed. Assuming a design horizontal pseudo-acceleration response spectrum the equivalent horizontal static force array $\{F\}^r$ for the r -th mode of vibration is given by:

$$\{F\}^r = S_d(T_r) \cdot \Gamma_r \cdot [M] \cdot \{\phi\}^r \quad (5.19)$$

where $S_d(T_r)$ is the design response spectrum value for the period T_r and Γ_r the modal participation factor defined as:

$$\Gamma_r = \frac{\{\phi\}^{rT} \cdot [M] \cdot \{\tau\}}{\{\phi\}^{rT} \cdot [M] \cdot \{\phi\}^r} \quad (5.20)$$

where τ is the $m \times 1$ ones array, with m equal to the number of storeys.

The equivalent static forces obtained by equation (5.19) are applied to the backup model to assess, for the r -th mode of vibration, the force F_{ji}^r acting on each wall and the relative effects E_{ji}^r (shear V_{ji}^r and overturning moment M_{ji}^r) characterizing the $wall_{ji}$.

In this case the effects on structure are calculated without considering the effects of vertical loads. In fact is not possible to know a priori the directions of horizontal forces of each mode force array because they change its direction during an earthquake. For this reason vertical loads are considered only for the calculation of the tensile force of the hold-downs.

The maximum global effect E_{ji} of the seismic action may be calculated assuming that the maximum effect for each mode of vibration does not occur concurrently. Standards suggest some combination procedures, such as the Square Root of Sum of Squares (SRSS):

$$E_{ji} = \sqrt{\sum_{r=1}^m (E_{ji}^r)^2} \quad (5.21)$$

As in the case of static analyses, the results must be consistent with the adopted model and hence the hold-downs must be characterized by in-tension axial forces.

The maximum global tensile force T_{ji} can be calculated as:

$$T_{ji} = \frac{M_{ji}}{l_i} - \frac{q_{ji} \cdot l_i}{2} \quad (5.22)$$

When T_{ji} is greater than zero the solution is consistent. On the contrary when T_{ji} is negative the analysis model must be updated, replacing the vertical linear spring $k_{h,ji}$ with a vertical axially rigid pinned beam.

5.2.3 Case study

The MRS analysis of the 3 x 2 series of wall of section 5.1.4 is presented. The modal analysis and the first iteration is performed assuming all hold-down are in tension.

The mass matrix is defined as:

$$[M] = \begin{bmatrix} 600 & 0 & 0 \\ 0 & 600 & 0 \\ 0 & 0 & 600 \end{bmatrix} kg$$

The periods and the relative mode shapes (see Figure 5.7, Figure 5.8 and Figure 5.9) results:

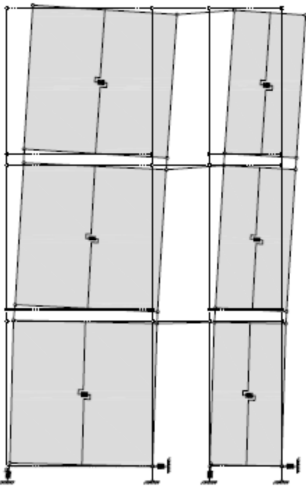


Figure 5.7: 1st mode
($T_1=0.34s$)

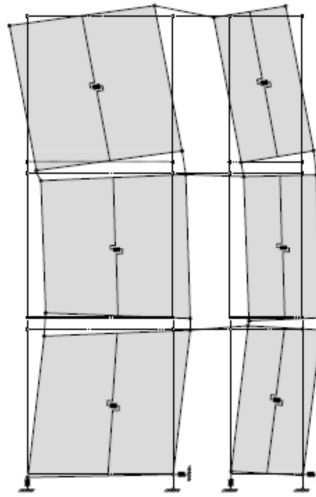


Figure 5.8: 2nd mode
($T_1=0.09s$)

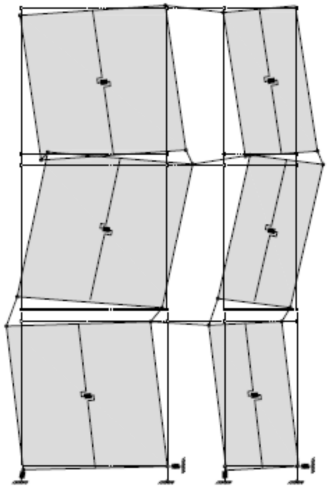


Figure 5.9: 3rd mode
($T_1=0.05s$)

$$\begin{array}{l}
 T_1 = 0.34s \\
 T_2 = 0.09s \\
 T_3 = 0.05s
 \end{array}
 \left\{ \phi^1 \right\} = \begin{Bmatrix} 0.21 \\ 0.59 \\ 1.00 \end{Bmatrix}
 \left\{ \phi^2 \right\} = \begin{Bmatrix} 1.00 \\ 0.77 \\ -0.66 \end{Bmatrix}
 \left\{ \phi^3 \right\} = \begin{Bmatrix} 1.00 \\ -0.95 \\ 0.29 \end{Bmatrix}$$

The design response spectrum is shown in Figure 5.10.

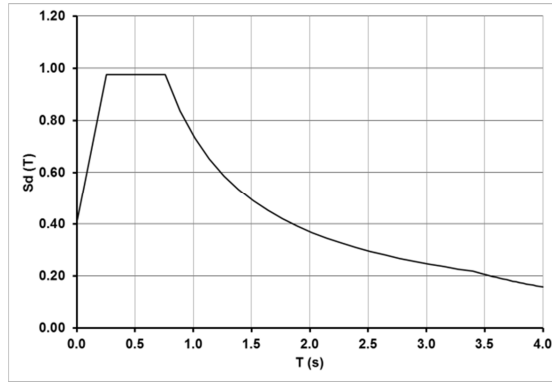


Figure 5.10: Design acceleration response spectrum

The modal participation factors can be calculated as:

$$\Gamma_1 = 1.30 \quad \Gamma_2 = 0.55 \quad \Gamma_3 = 0.17$$

The response spectrum values for the three modes of vibration are:

$$S_d(T_1) = 0.97g \quad S_d(T_2) = 0.60g \quad S_d(T_3) = 0.45g$$

The horizontal force arrays $\{F\}^r$ results:

$$\{F\}^1 = \begin{Bmatrix} 1.55 \\ 4.16 \\ 7.42 \end{Bmatrix} kN \quad \{F\}^2 = \begin{Bmatrix} 1.94 \\ 1.50 \\ -1.28 \end{Bmatrix} kN \quad \{F\}^3 = \begin{Bmatrix} 0.45 \\ -0.43 \\ 0.13 \end{Bmatrix} kN$$

For each force array, a static analysis can be performed calculating the shear forces V and the overturning moment M .

$$[V]^1 = \begin{bmatrix} 9.75 & 3.38 \\ 9.02 & 2.56 \\ 6.04 & 1.38 \end{bmatrix} kN \quad [V]^2 = \begin{bmatrix} 1.57 & 0.59 \\ 0.17 & 0.05 \\ -0.96 & -0.32 \end{bmatrix} kN \quad [V]^3 = \begin{bmatrix} 0.10 & 0.05 \\ -0.22 & -0.08 \\ 0.09 & 0.04 \end{bmatrix} kN$$

$$[M]^1 = \begin{bmatrix} 62.03 & 18.30 \\ 37.65 & 9.85 \\ 15.10 & 3.45 \end{bmatrix} kN \quad [M]^2 = \begin{bmatrix} 1.95 & 0.80 \\ -1.98 & -0.68 \\ -2.40 & -0.80 \end{bmatrix} kN \quad [M]^3 = \begin{bmatrix} -0.08 & 0.03 \\ -0.33 & -0.10 \\ 0.23 & 0.10 \end{bmatrix} kN$$

Effects are then combined by means of the SRSS procedure, getting:

$$[V]^{tot} = \begin{bmatrix} 9.88 & 3.43 \\ 9.02 & 2.56 \\ 6.12 & 1.42 \end{bmatrix} kN \quad [M]^{tot} = \begin{bmatrix} 62.06 & 18.32 \\ 37.70 & 9.87 \\ 15.29 & 3.54 \end{bmatrix} kN$$

In order to validate the results, the tensile forces of the hold-downs must be calculated. They result as:

$$[T]^{tot} = \begin{bmatrix} -25.18 & 14.66 \\ -16.17 & 7.90 \\ -6.38 & 2.83 \end{bmatrix} kN$$

From results, the compatibility is not satisfied since all 1st wall hold-downs are in compression. The numerical model must be updated fixing all 1st wall hold-downs and a new model analysis must be performed to calculate the new dynamic properties:

$$\begin{array}{l} T_1 = 0.18s \\ T_2 = 0.06s \\ T_3 = 0.04s \end{array} \quad \{\phi^1\} = \begin{Bmatrix} 0.40 \\ 0.77 \\ 1.00 \end{Bmatrix} \quad \{\phi^2\} = \begin{Bmatrix} 1.00 \\ 0.52 \\ -0.80 \end{Bmatrix} \quad \{\phi^3\} = \begin{Bmatrix} -0.86 \\ 1.00 \\ -0.42 \end{Bmatrix}$$

The modal participation factors are calculated:

$$\Gamma_1 = 1.24 \quad \Gamma_2 = 0.38 \quad \Gamma_3 = -0.15$$

The response spectrum values for the three updated modes of vibration are:

$$S_d(T_1) = 0.78g \quad S_d(T_2) = 0.48g \quad S_d(T_3) = 0.42g$$

The horizontal force arrays $\{F\}^r$ results:

$$\{F\}^1 = \begin{Bmatrix} 2.27 \\ 4.38 \\ 5.68 \end{Bmatrix} kN \quad \{F\}^2 = \begin{Bmatrix} 1.02 \\ 0.53 \\ -0.81 \end{Bmatrix} kN \quad \{F\}^3 = \begin{Bmatrix} 0.31 \\ -0.36 \\ 0.15 \end{Bmatrix} kN$$

For each force array, a static analysis can be performed calculating the shear forces V and the overturning moment M .

$$[V]^1 = \begin{bmatrix} 10.33 & 2.00 \\ 9.41 & 0.65 \\ 5.98 & -0.30 \end{bmatrix} kN \quad [V]^2 = \begin{bmatrix} 0.57 & 0.17 \\ -0.26 & -0.02 \\ -0.74 & -0.07 \end{bmatrix} kN \quad [V]^3 = \begin{bmatrix} 0.07 & 0.03 \\ -0.16 & -0.05 \\ 0.12 & 0.03 \end{bmatrix} kN$$

$$[M]^1 = \begin{bmatrix} 64.30 & 5.88 \\ 38.48 & 0.88 \\ 14.95 & -0.75 \end{bmatrix} kN \quad [M]^2 = \begin{bmatrix} -1.08 & 0.20 \\ -2.5 & -0.23 \\ -1.85 & -0.18 \end{bmatrix} kN \quad [M]^3 = \begin{bmatrix} 0.08 & 0.03 \\ -0.10 & -0.05 \\ 0.30 & 0.08 \end{bmatrix} kN$$

The effects are the combined by means of the SRSS procedure getting:

$$[V]^{tot} = \begin{bmatrix} 10.35 & 2.01 \\ 9.41 & 0.65 \\ 6.03 & 0.31 \end{bmatrix} kN \quad [M]^{tot} = \begin{bmatrix} 64.31 & 5.88 \\ 38.56 & 0.90 \\ 15.07 & 0.77 \end{bmatrix} kN$$

In order to validate the results, the tensile forces of the hold-downs must be calculated as:

$$[T]^{tot} = \begin{bmatrix} -24.28 & 4.70 \\ -15.83 & 0.72 \\ -6.47 & 0.62 \end{bmatrix} kN$$

The results are consistent with the updated backup model. The iterative process can be stopped.

6 3-STOREY TIMBER-FRAME BUILDING SHAKE TABLE TEST

In this chapter a 3-storey timber-frame building full scale shake table test, performed at the laboratory TreesLab Eucentre (see, Figure 6.1) in Pavia (Italy), is described. This work characterizes the third and last phase of the research project Chi-Quadrato with the aim, as stated in chapter 1, to assess the seismic performance of a timber-frame building.

6.1 Geometry and Design of the specimen

The test specimen was characterized by a rectangular 5 x 7 m footprint and three stories with a maximum height equal to 7.65 m. The footprint dimensions of the building were chosen in relation to the size of the shaking table (5.6 x 7 m). The anchoring system with the shake table was made with a rigid steel base. The in-plane wall layout was selected considering the interactions between the structural elements and, therefore, analysing different mechanisms of transfer of internal forces. The structure is symmetrical along the longitudinal direction (Y) and it is characterized by an asymmetry in the transverse direction (X). Since the shaking table is characterized by a single

3-STOREY TIMBER-FRAME BUILDING SHAKE TABLE TEST

translational degree of freedom, the building has been subjected to a seismic input parallel to its longitudinal direction (Y). In order to study more clearly the distribution of the seismic internal forces in the direction of the specimen (Y), only two different lengths of the walls (2500 and 1250 mm) were adopted (see,

Figure 6.2). These walls run without interruption from the ground to the top of the building: for this reason the structure may be considered regular in elevation. The floors were formed by box section elements 140 mm height, to which were superimposed and nailed 15 mm thick OSB panel 15 mm in order to guarantee a rigid diaphragm behaviour. The floor elements were arranged in the longitudinal direction and therefore supported by the transverse walls. This choice was taken with the purpose of minimizing the stabilizing contribution, given by gravitational loads, on the walls parallel to the direction of the seismic input. The roof (two pitches characterized) was made by solid timber beams and a timbered plank with stiffened perforated metal strips. The framed walls were braced by OSB panels 15 mm thick, placed on both sides and connected to the timber frame by ring nails (2.8 x 60 mm). Studs and beams of the walls were made with solid timber, section 160 x 60 mm and 160 x 100 mm.



Figure 6.1: *Test specimen*

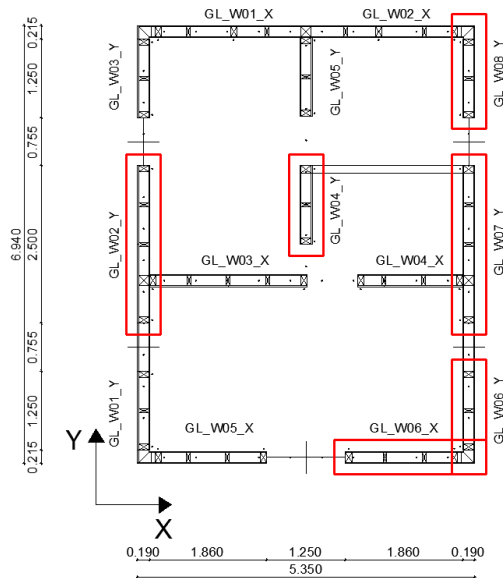


Figure 6.2: Building structural plan and instrumented walls

The shake table, characterized by a single translational degree of freedom (Y), had plan dimensions of 5.6 x 7.0 m and a mass of 42 tons. The steel basement was made with European Standard Channels HEA 300 and HEB 300, anchored to the shake table by means of steel bars in order to ensure a sufficiently rigid support. Solid timber beams were positioned on the top of the steel base which to the steel beams were connected by means of M16 class 8.8 bolts (see, Figure 6.3 a). The bolt spacing (500 mm) was chosen with the aim of making the relative displacement between the base and the timber beam negligible. In order to validate this hypothesis during the test phases a displacement transducer was installed. The connection of the walls to the base was obtained by means of two different devices. With reference to the tensile forces at the corners of each walls, Hold-Down devices were used, connected by bolts to the top flange of the steel beams (Figure 6.4). Moreover, in order to avoid their slippage the walls were screwed to base timber beam (Figure 6.5).

3-STOREY TIMBER-FRAME BUILDING SHAKE TABLE TEST



Figure 6.3: *Base timber beam and steel basement*



Figure 6.4: *Hold-downs*



Figure 6.5: *Inclined screws connection*

The design of the structure was carried out in accordance with Italian and European Standards NTC 08, Eurocode 5 and Eurocode 8. The design analysis, as well as checks on structural elements and connections, were carried out with traditional methods of calculation, without referring to experimental results obtained from the investigation of previous campaigns. The fundamental aim of the test was in fact also to validate the current calculation methods adopted for the timber-framed building design. It is assumed that the building placed in Ferla (Syracuse province, Italy), as this site is characterized by the maximum reference ground acceleration a_g equal to 0.27g for a return period of 475 years under Italian law. The choice of the behaviour factor was carried out in accordance with the Eurocode 8, which suggests a factor equal to 5, as reported in chapter 2. With reference to some suggestions in the literature, a prudential factor q equal to 4 was adopted. The viscous damping was assumed equal to 5%

The design floor dead load was assumed equal to 2.5 kN/m^2 , whereas the live load 2 kN/m^2 and the snow load 0.95 kN/m^2 .

The building mass was equal to 367 kN (37.43 tons) whereas the specimen mass (considering also the steel base mass) was equal to 407 kN (41.51 tons), lower than the shake table payload, equal to 140 tons.

6.2 Specimen assembly and description of instrumentation

All primary structural elements with the exception of the roof were prefabricated. During the assembly in the laboratory only the placement of structural elements and their connection were performed. The phases of assembly were completed in 3 days by 5 workers.



Figure 6.6: *Phases of assembly at Eucentre TreesLab*

The building was tested without finish and non-structural elements. In order to simulate additional mass relative to the dead loads and live loads, the entire stratigraphy of the roof and the insulation of the walls, some concrete blocks on the floors, some tiles on the roof and additional materials within the walls were placed.

The behaviour of the building was monitored by an suitable set-up of measuring characterized of 103 instruments and an optical acquisition system, capable of detecting

continuously the absolute displacement of control points on the eastern façade of the building itself. The arrangement of the instruments was carried out taking into account the unidirectional motion of the shake table, thus positioning majority instruments on the walls parallel to the input seismic. In particular, the behaviour of 6 walls (5 in the longitudinal direction and 1 in the transverse direction) were monitored both on the ground floor and first one as reported in Figure 6.2. Otherwise second floor walls were not instrumented as expected deformations had been not significant. On each monitored wall on the ground floor 2 load cells were placed with the aim of measuring the tensile force in the Hold-Down. On each Tie-Down (the first floor hold-down) two strain gauges with the same aim were used .



Figure 6.7: Wire potentiometers (26), uplift LVDT (10) and Tie-down strain gauges

In order to measure the shear deformation of each monitored walls monitored two diagonal wire potentiometers wire were positioned. The wall corner uplift and wall rigid translation were measured by means of linear potentiometers (LVDT).



Figure 6.8: *Corner uplift and rigid translation LVDTs*

The arrangement of the markers on the eastern façade of the building allows the knowledge of the floor absolute displacement. These measures are fundamental to assess the inter story drifts of the building during the seismic tests. In order to validate the hypothesis that floors and roof can be considered as wire potentiometers were used in order to measure the floor in-plane deformation. In particular only the second floor was instrumented since it is characterized, according to the numerical model, by the highest seismic force. In addition to the instruments described, some displacement transducers (LVDT) were placed between adjacent floor box elements in order to monitor any reciprocal sliding in the direction of motion (Figure 6.9).



Figure 6.9: *Floor box element LVDTs*

Twenty-three unidirectional accelerometers were used with the aim of monitoring the accelerations at various levels of the building. The obtained measurements have allowed both to evaluate the accelerations reached at different levels during seismic tests (and thus the inertia forces of the floors) and to carry out the dynamic identification of the building. In order to check that the connection system with the shaking table avoided relative displacements between the base of the building and the shaking table itself, displacement transducers were placed (Figure 6.10): the motion of the table is to be transferred to the base of the building without any alteration.



Figure 6.10: *LVDT for the measure of the relative displacement of the steel basement and the base timber beam*

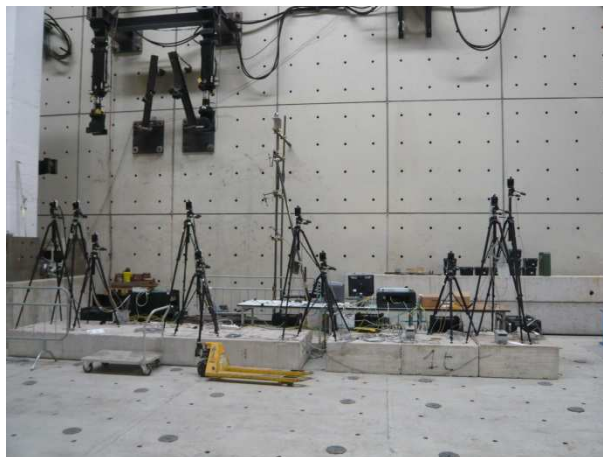


Figure 6.11: *Infrared cameras*



Figure 6.12: *Optical system marker arrangement*

All seismic tests were preceded and followed by a dynamic test identification, performed at low intensity, by means of a low amplitude 0.2-40 Hz clipped-band flat white noise, characterized by RMS amplitude of 0.05g. The sampling frequency was equal to 256Hz. The dynamic identification was carried out with the aim of identify the dynamic properties of the structure after each seismic test. Some possible variations of the fundamental period of the structure are in fact excellent signs of any damage of the structure. The seismic tests were carried out scaling appropriately the selected ground motion to reference PGA values. The sampling frequency for seismic tests was equal to 1024 Hz.

6.3 Test design

In order to properly design the shake table test, the assessment of the specimen suitability, its dynamic properties and its performance was carried out. With this aim a suitable numerical model was made (Figure 6.13), according to analysis model propose in Chapter 5.

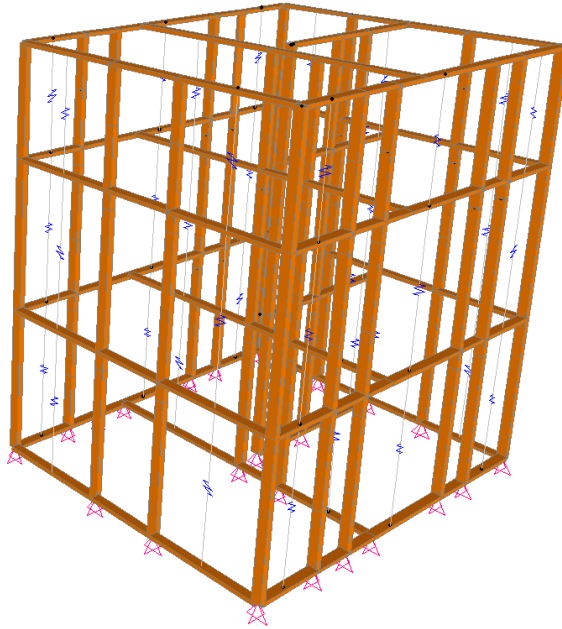


Figure 6.13: *Timber-frame building analysis model*

Three different building numerical models were carried out to consider separately the deformation components namely the sheathing panel deformation K_P , the sheathing-to-framing fastener K_{SH} , the rigid body translation K_A and rigid body rotation deformation contribution K_H . The first model (Model A) only the sheathing panel deformation contribution K_P was considered whereas in the second one (Model B) also the contribution of the sheathing-to-framing connection stiffness K_{SH} was implemented. Lastly, an additional numerical model (Model C) was developed: the behaviour of Hold-Down k_h was added. The modelling of the floors and the roof was carried out by assigning a horizontal diaphragm constrain to each story. Each floor mass was concentrated in the each floor centre of mass. The properties of the three adopted analysis models are reported in Table 6.1.

	K_A	K_{SH}	K_P	k_h
Model A	∞	∞	yes	∞
Model B	∞	yes	yes	∞
Model C	∞	yes	yes	yes

Table 6.1: *Stiffness contributions for the numerical models*

The evaluation of the dynamic properties of the test building was performed using only the Model A and the Model B. This choice was taken as identification dynamic tests are usually performed at very low input levels and hence the contribution of translation and rigid body rotation may be negligible. The vibration mode shapes were obtained directly from the model referring to each centre of mass. In Table 6.2 the fundamental periods for both main direction (X and Y) are reported.

Natural period [s]		
First mode shape	Model A	Model B
Transversal direction (x)	0.106	0.297
Longitudinal direction (y)	0.297	0.295

Table 6.2: *Natural periods in transversal and longitudinal directions*

The ratio between the fundamental periods of the two models is approximately equal to 3. The stiffness K_P was in fact approximately 9 times the stiffness K_{SH} . The structure can be considered regular in elevation in both directions and for both models. The modal mass of the first translational mode shape is in fact in all cases greater than 90%. The regularity in plan, as expected, occurs only in the longitudinal direction (y). The modal mass associated with the rotational mode shape is in fact significant only in transversal direction (47 and 51% for the two models). Moreover, the modal shapes show how the roof is much stiffer than the lower levels due to a reduced height of the walls and a considerable reduction of the seismic mass.

The choice of the ground motion (input signal) was taken so that the frequency content of the signal is significant in the range of the structure estimated frequencies. For this purpose the 1979 Hotel Albatros-Ulcinj Montenegro Earthquake (M_w 6.9) y-direction ground motion (Figure 6.14) was selected. The peak ground acceleration PGA is equal to 0.224 g (equivalent to 2,199 m/s²).

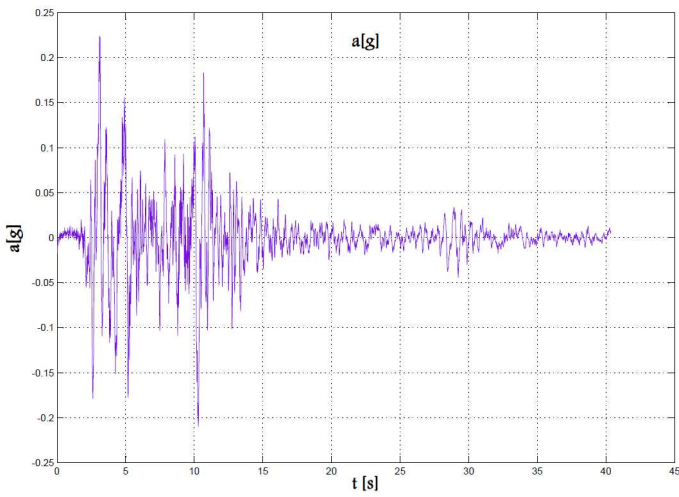


Figure 6.14: Acceleration Time-History of unscaled Hotel Albatros-Ulcinj Montenegro Earthquake *y*-direction ground motion

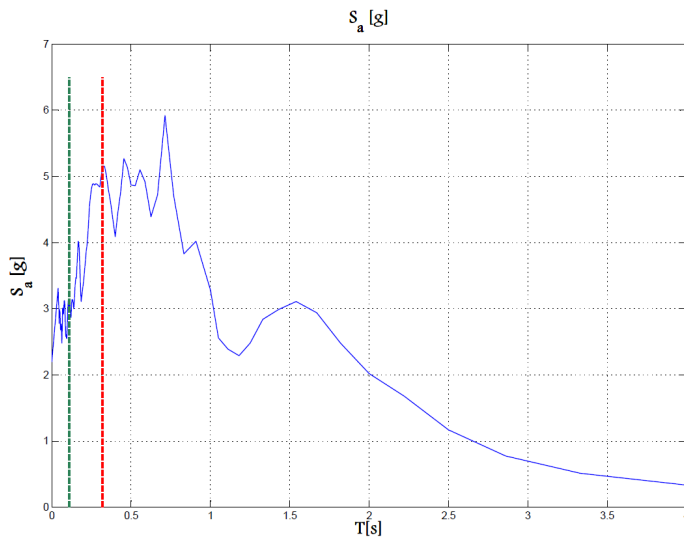


Figure 6.15: Pseudo-acceleration elastic response spectrum (5%) of unscaled Hotel Albatros-Ulcinj Montenegro Earthquake *y*-direction ground motion

As shown in Figure 6.15 the pseudo-acceleration elastic spectrum is characterized by a wide amplification band (constant energy band), ranging approximately between a 0.20

s to 0.70 s. For this reason, an incorrect assessment of the building fundamental period do not produce high variations of the spectral values. Moreover, because after seismic tests a building damage, and thus a structural period increase, might be expected, the wide spectrum amplification band guarantee that the building is subjected to similar acceleration spectrum values for all seismic tests. As reported in Figure 6.15, the period of the model B (red vertical line) falls in the amplification band, otherwise the model A (green vertical line) one falls in the high frequency band, characterized by a smaller amplification. However, as reported in the shake table fidelity paragraph, the feedback recorded signal response spectrum is characterized by an amplification band that extends up to the high frequency values.

The assessment of the structure seismic capacity, defined in terms of base shear strength V_b and base overturning moment strength M_r , was carried out to select the amplitude scaling factors of the seismic input signal, in relation with the limit states which are to be achieved during the seismic tests.

With this aim, the capacity curve of the structure was obtained, plotting the relation between the base shear force V_b and the control displacement d_c according to the nonlinear static analysis method (pushover). Two different load patterns: the uniform pattern and the modal pattern. For this purpose the same numerical model of the linear elastic analysis was used, selecting conveniently which structural elements (represented by the springs) should have been considered in the non-linear range. This choice was taken regarding to the results obtained from Chi-Quadrato experimental campaign on the connection components and on the timber-frame walls and to the expected structural behaviour. From this, only the sheathing-to-framing connection contributions (K_{SH}) and the hold down (k_h) at the ground floor were represented by a non-linear curve. All other contributions (wall translation K_A , panel deformation K_P and hold-down of the upper floors k_h) are taken in the linear range. The properties for each element were obtained by laboratory tests carried out during the Chi-Quadrato experimental campaign. The control point was taken at the centre of mass of the building. The ultimate displacement of the capacity curve was selected assuming the following criteria: the hold-down tensile deformation equal to 30 mm for the model C and the wall shear deformation (K_{SH}) equal to 100 mm (corresponding to an inter-story drift of 4%) for the model B.

3-STOREY TIMBER-FRAME BUILDING SHAKE TABLE TEST

According to the results provided in Table 6.3 and Figure 6.16, for both models the capacity curve related to the modal pattern is characterized by a less strength than the mass pattern one, but by a comparable ultimate displacement.

In the model B the ultimate displacement is obtained by the maximum acceptable shear deformation (100 mm) of the 2.5 m length ground floor wall GL_W07_Y. In model C failure occurs by achieving ultimate Hold down deformation (30 mm) in the ground floor wall GL_W06_Y.

As expected, the maximum base shear of the model B is much higher than the model C one.

Model	Pattern	Base shear strength [kN]	Ult. disp. [mm]	OTM [kNm]
B	uniform	471	123	2104
B	modal	472	133	2306
C	uniform	176	122	787
C	modal	157	121	787

Table 6.3: Non-linear analysis results

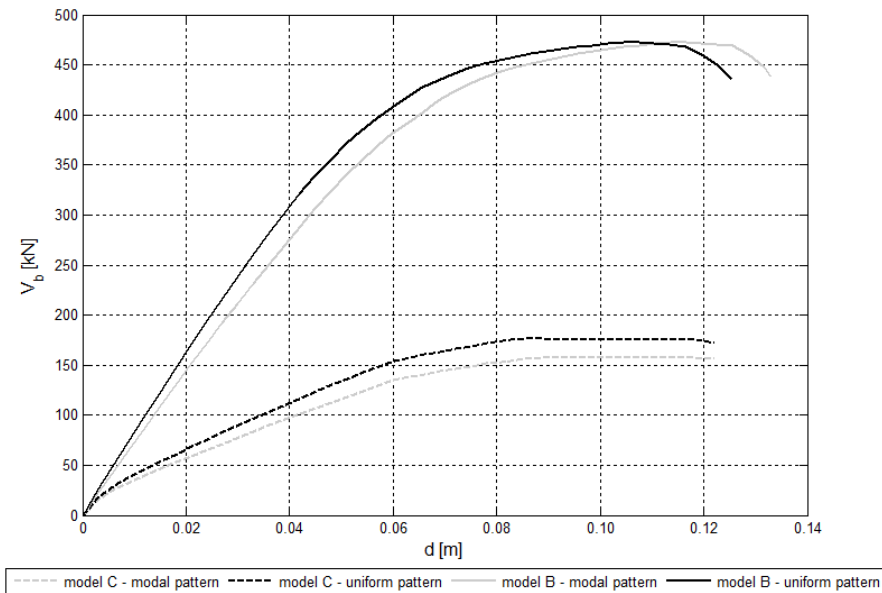


Figure 6.16: Nonlinear analysis base shear vs roof displacement curves

In order to study the response of the structure for different levels of seismic input, the peak ground accelerations and the scale factors of ground motion, required are to be selected to reach different limit states of the structure. After obtaining the capacity curve the seismic displacement demand it is to be selected. The analysis method used for this purpose is the so-called *N2 method* or modified capacity spectrum method (MSCM) proposed by [Fajfar,2000] and also suggested in both Italian and European Standards. The displacement seismic demand is obtained by the intersection of the equivalent SDOF scaled capacity curve of the structure and the ADRS capacity spectrum, given by reduction of the elastic ADRS spectrum by means of the behaviour structure factor, depending on the period and the ductility of the structure (see Figure 6.17). The analyses were carried out referring only to the “uniform” lateral pattern (a failure interests of ground floor walls is expected). PGAs and ground motion scale factors were calculated referring to the structure ultimate displacement and structure “yield” displacement (Table 6.4).

Modello	PGA _y [g]	PGA _u [g]	q*
B	0.71	1.09	1.55
C	0.27	0.48	1.81

Table 6.4: Yield and ultimate displacement PGAs

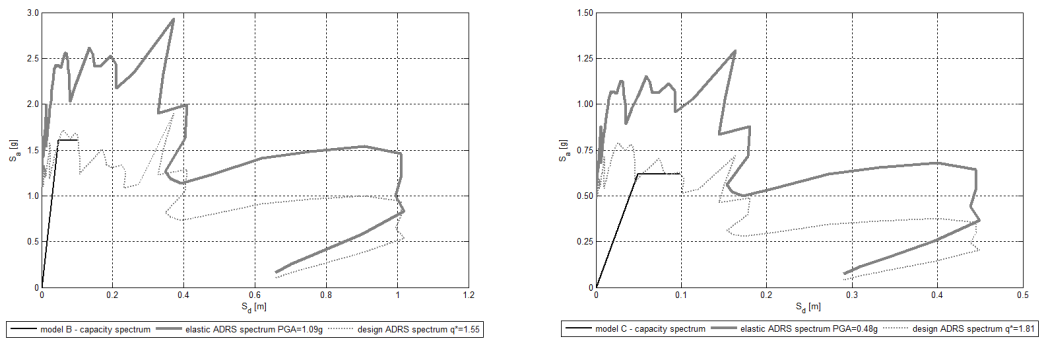


Figure 6.17: Structural ultimate displacement capacity spectra for model B and model C

After defining the acceleration values which represent yield and collapse structural limit states limit, the sequence of seismic tests was decided. Firstly the design PGA values (equal to 0.07 g and to 0.28 g) were firstly selected. The choice of the following seismic

levels was taken in order that it was significant for both analysis models according to the assessed PGA values in Table 6.5: Seismic test sequence.

Seismic test	Ground motion	Scale factor	PGA (g)
1	Montenegro	0.31	0.07
2	Montenegro	1.25	0.28 (I)
3	Montenegro	1.25	0.28 (II)
4	Montenegro	2.23	0.50
5	Montenegro	3.13	0.70
6	Montenegro	4.46	1.00

Table 6.5: *Seismic test sequence*

6.4 Analysis of results

The acquisition and sampling of signals were performed with an anti-aliasing filter, in order to restrict the bandwidth of a signal to a Nyquist frequency equal to half the desired sampling frequency. All signals acquired during seismic tests were appropriately filtered in order to eliminate noises present at high frequencies and not arising from the excitation of the structure tested. For this reason it was decided to use a low-pass Infinite Impulse Response (IIR) filter and in particular a Butterworth filter characterized by a cutoff-frequency (value for which the attenuation is 3 dB) equal to 25.5 Hz and a stop-band-frequency (value for which the attenuation is 40 dB) equal to 50 Hz.

All seismic tests were preceded by a tuning phase of the shaking table control system (very low-intensity vibrations applied to the structure) by means of an iterative process (adaptive inverse control) in which the reference signal and the shaking table feedback signal were compared, in order to obtain a response function as close as possible to unit magnitude and zero phase over the entire range of frequencies of interest. During this phase was also possible to acquire the data needed to dynamical identification of the structure.

To investigate the fidelity of the motion reproduced from the shake table, in Figure 6.18 are reported the pseudo-acceleration response spectra (damping of 5%.) of the reference signal (imposed to the system) and of the signal imposed by the table (feedback signal), registered by the accelerometer placed on the table (A37).

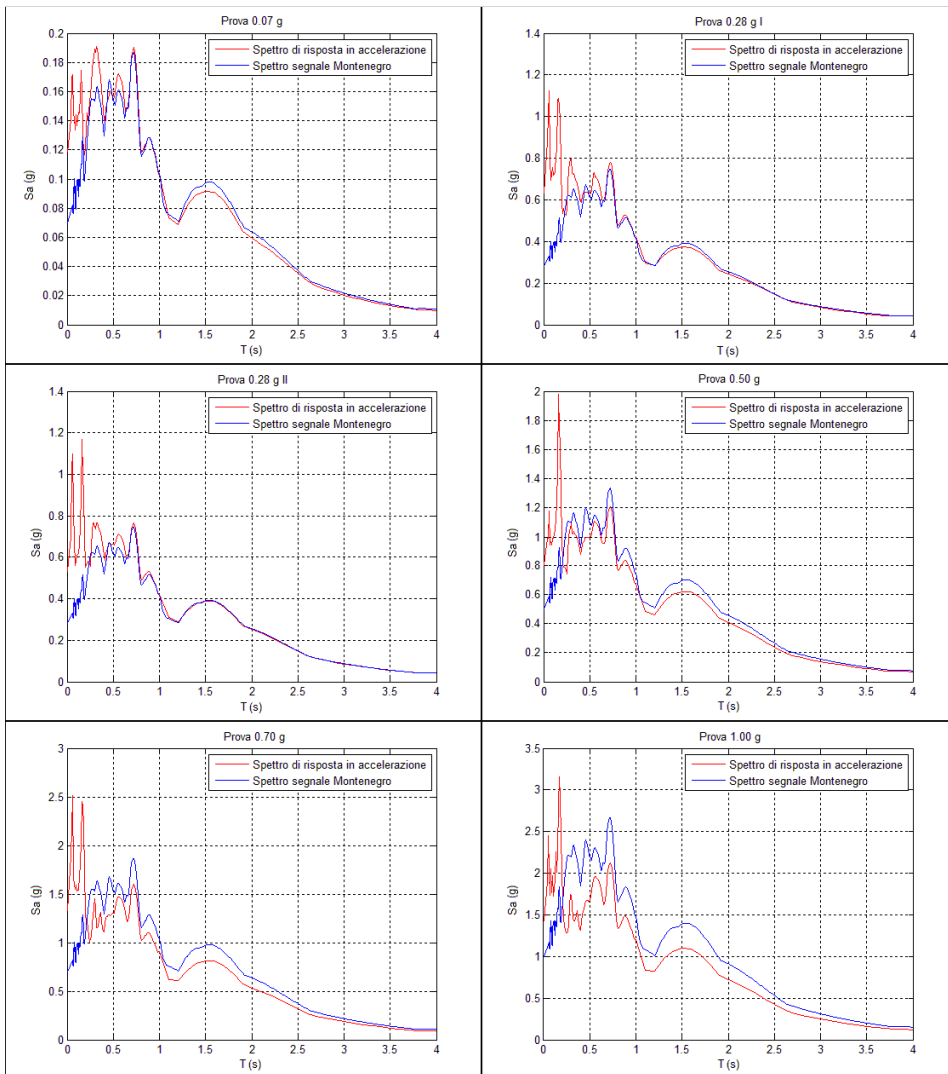


Figure 6.18: Comparison of the pseudo acceleration response spectra of the shaking table input for each test (feedback signal in red line) with the Montenegro record (blue line) scaled at the same nominal PGA (reference signal in black line).

The analysis of the data recorded by the accelerometers during seismic tests is really useful for understanding both the entity of the accelerations, to which are subjected the various floors of the building the structural and non-structural elements and occupants, both to assess the possible amplification resulting from the dynamic characteristics of the structure and the frequency content of the input signals.

3-STOREY TIMBER-FRAME BUILDING SHAKE TABLE TEST

Position	Accelerometer	Direction	0.07 g	0.28 g I	0.28 g II	0.50 g	0.70 g	1.00 g
Shake table	A37	Y	0.12	0.63	0.53	0.80	1.33	1.43
1°	A1	Y	0.08	0.36	0.43	0.69	1.05	1.15
	A3	Y	0.08	0.34	0.43	0.68	1.06	1.27
	A9	Y	0.08	0.35	0.43	0.69	1.06	1.26
2°	A16	Y	0.10	0.38	0.44	0.73	1.12	1.38
	A22	Y	0.10	0.37	0.45	0.74	1.13	1.45
	A24	Y	0.10	0.37	0.44	0.73	1.09	1.35
3°	A31	Y	-	-	0.51	0.82	1.24	1.64
	A33	Y	-	-	0.50	0.82	1.27	1.54
	A35	Y	-	-	0.50	0.81	1.29	1.52
Roof ridge	A27	Y	-	-	0.63	0.89	1.44	1.68

Table 6.6: *Maximum accelerations recorded during seismic tests*

The most important parameter for understanding the response of a structure subjected to seismic action is undoubtedly the inter-storey drift. As a matter of fact, according to Performance Based Seismic Design Method, damage to structural and non-structural elements can be related to this parameter, with the aim to define a relationship between seismic demand and expected performance of the building. The inter-storey drift is defined as the ratio between the relative horizontal displacement between two floors and the height inter-storey. In Figure 6.19 and Figure 6.20 the relation between the maximum acceleration at the shake table level and the maximum interstorey drift recorded during each test is shown respectively for the first and the second floor. A linear trend is observed up to the 0.7 g PGA seismic test (maximum shake table recorded acceleration equal to 1.33g): in the subsequent 1 g PGA test a significant slope softening of trend confirmed once again the transition to the non reversible phase of the structure.

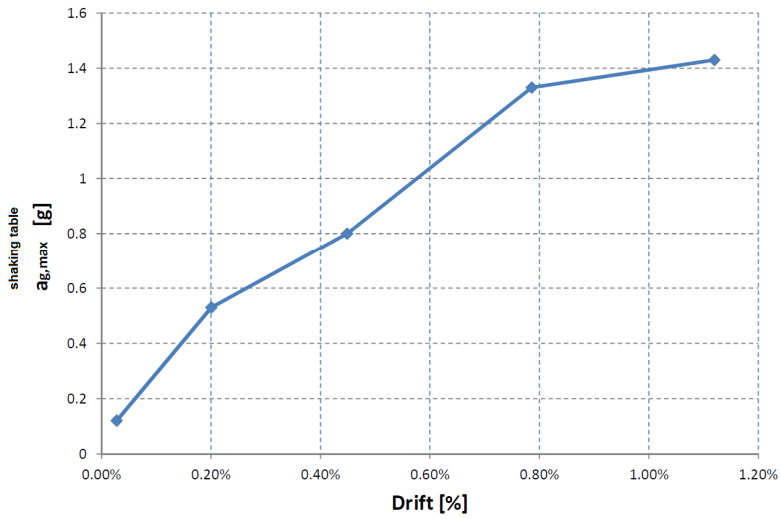


Figure 6.19: Inter-storey drift related to the first floor

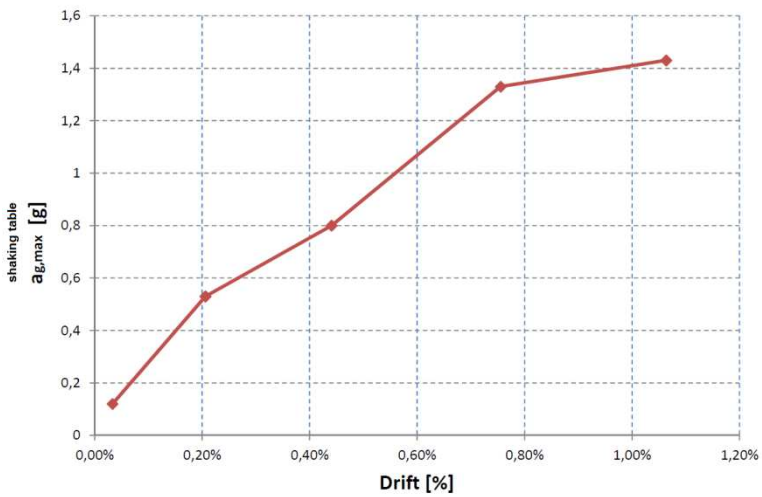


Figure 6.20: Inter-storey drift related to the second floor

3-STOREY TIMBER-FRAME BUILDING SHAKE TABLE TEST

The obtained results confirmed that for values of inter-story drift of the order of 1.5 - 2% not visible structural damage could be associated. In order to assess the effect of the overturning forces on each single timber frame wall, load cells have been positioned to monitor the tensile force acting on each Hold-Down. In Table 6.7 the maximum values recorded for each load cell are reported.

Wall	Seismic test					
	0.07 g	0.28 g I	0.28 g II	0.50 g	0.70 g	1.00 g
GL_W06_Y	0.0	0.0	0.0	0.2	0.9	2.4
GL_W06_Y	0.0	0.0	0.0	3.7	9.7	26.4
GL_W07_Y	0.0	0.0	0.0	0.9	5.0	9.6
GL_W07_Y	0.0	3.9	3.8	14.4	25.6	28.4
GL_W08_Y	0.0	2.7	2.5	8.8	19.4	27.6
GL_W08_Y	0.0	0.0	0.0	3.8	16.1	27.9
GL_W04_Y	0.0	1.8	1.3	4.2	13.2	20.1
GL_W04_Y	0.0	2.5	1.6	7.7	24.8	38.8
GL_W06_X	0.0	0.0	0.0	1.8	3.4	5.2
GL_W06_X	0.0	2.5	2.0	5.2	10.2	16.3
GL_W02_Y	0.0	0.0	0.0	0.7	4.5	9.4
GL_W02_Y	-	-	-	13.4	31.5	36.0

Table 6.7: Maximum values of traction forces registered by the Hold-Down load cells (kN)

From Table 6.7 can be deduced that, for the first three test phases, the forces can be considered non-significant. On the contrary, in the test phase characterized by the maximum magnitude (1 g), the role of the Hold-Down is evident.

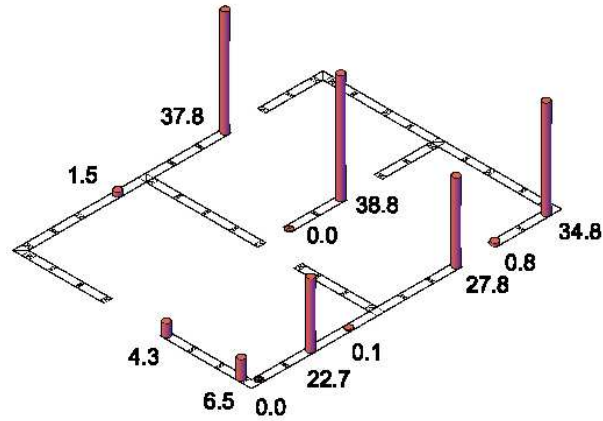


Figure 6.21: Vertical force values [kN] recorded by the Hold-down load cells when the maximum value is reached at the right corner

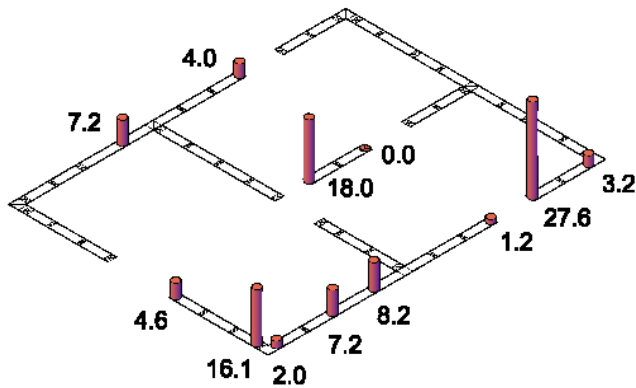


Figure 6.22: Vertical force values [kN] recorded by the Hold-down load cells when the maximum value is reached at the left corner

The activation of the Hold-Down placed to the right corner of each wall corresponds to a very low value of force in the Hold-Down placed to the left corner of the same wall

(Figure 6.21): similar behaviour is observed when the Hold-Down positioned in the left corner are activated (Figure 6.22). Moreover, it is possible to observe that the hold-down on the wall GL_W06_X are always activated by the motion in the both directions.

Concerning with the force measured in the Tie-Down elements, only in the last two test phases (0.7 g and 1 g) they were significantly activated (thus demonstrating their usefulness), while in the first three test phases they recorded a force value near to zero was recorded.

The wall rigid motion (sliding and overturning) during the test phases was monitored by the optical system on the east façade, and by some LVDTs appropriately arranged.

Figure 6.23 shows, for seismic test at 1 g, the maximum slippage recorded values at each wall (the outer wall GL_W07_Y registered the maximum slip of 4.2 mm at the first floor and of 2.2 mm at the second floor). The recorded values can be considered virtually zero for seismic test with nominal PGA lower than 0,28 g.

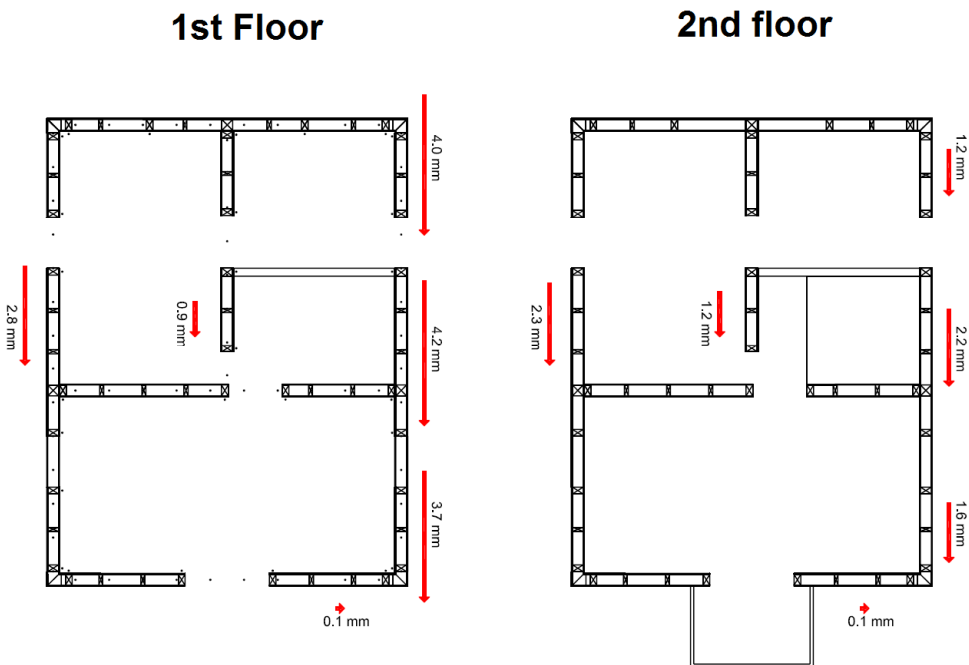


Figure 6.23: Slippage values of the walls for seismic test at 1.00 g

Figure 6.24 shows the values of uplift at the ground floor for seismic test at 1 g. These values are consistent with the value of the maximum force measured in the Hold-Down.

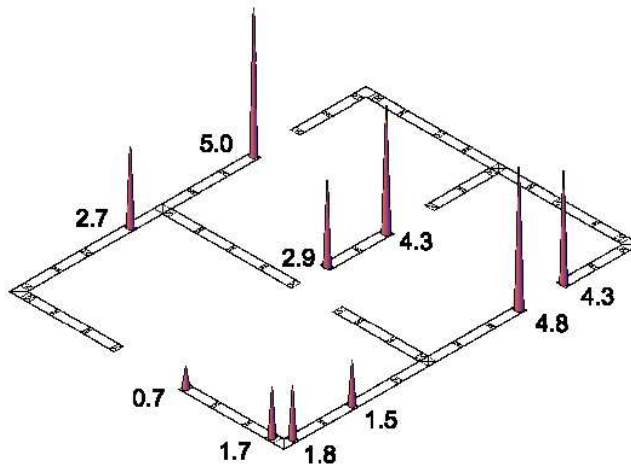


Figure 6.24: Hold-down uplift values (mm) of the walls on the ground floor to the test at 1.00 g

The wall shear deformation was measured by wire potentiometers and optical markers, measuring the variation of the wall diagonal length. Since the instruments were positioned on the panel and not on the frame of the wall, the most significant contribution due to the nail deformation is non “visible” for walls formed by a single panel (e.g. 1250 mm length walls). On the contrary, for “multi-panel” walls (e.g. 2500 mm length walls), the nail slip contribution is part of the recorded deformation, but cannot be directly deducted from the sheathing panel shear deformation.

In plane deformation of the horizontal diaphragms was measured by a couple of diagonal wire potentiometers crossed arranged. We can consider the deformation of the intermediate floors negligible since the maximum elongation recorded was equal to 1 mm. In the case of the roof diaphragm instead, the maximum elongation recorded was equal to 4.1 mm over a total length of about 3.70 m, resulting in a deformation that is equal to 0.1%. It is interesting to highlight this difference of the in plane deformation

3-STOREY TIMBER-FRAME BUILDING SHAKE TABLE TEST

registered for the roof during all stages of the, symptom, as expected, a lower stiffness of the diaphragm.

The slippage between the box floor elements was monitored by a couple of LVDT transducers placed parallel the floor span. From the maximum values recorded can be noted that such displacement can be considered negligible for all stages of the test.

After each seismic test the entire structure was visually inspected in order to assess any structural damage. It is observed how the structure, in agreement with the data obtained from the instrumentation arranged, showed no damage typically observed in this structural typology in the laboratory test (residual rotation of the panels, rupture of the panels near the corners, unthreading of the nails of the Hold-Down, etc..). The value of the calculated maximum inter – storey drift was equal to 1.24% and consistent with findings from the visual survey. This drift value, as observed in the laboratory tests previously carried out on individual walls as well as reported by the studies in the literature, is generally not associated with any type of structural damage.



Figure 6.25: *Visual inspection of the building*

6.4.1 *Global hysteretic response*

The hysteretic response global building is described by the curve of the total force to the base as a function of the relative displacement of the centre of the roof and has been evaluated for all the seismic tests subsequent to the test at 0.28 g I. The force at the base of the building was calculated by summing the contributions of inertial forces relative to the three planes, obtained by multiplying the mass of the deck of reference for the respective absolute accelerations measured by the accelerometers placed in proximity of the centre of gravity of the decks. It is important to emphasize how the force calculated represents the total inertial force of the structure and not the base shear. The inertial forces in fact, in a damped system, are equal to the sum of the elastic forces (cut) and those viscose. The relative displacement of the control point s was derived as the difference between the absolute displacement of the ridge x_{A27} and the absolute displacement of the vibrating table x_{A37} . The absolute displacement signals were obtained through a double integration of the signals recorded by the accelerometers placed on the table (A37) and on the top (A27), filtered in the frequency band between 0.2 Hz and 40 Hz. Figure 6.26 shows, for the four seismic tests considered, the force-displacement diagrams obtained.

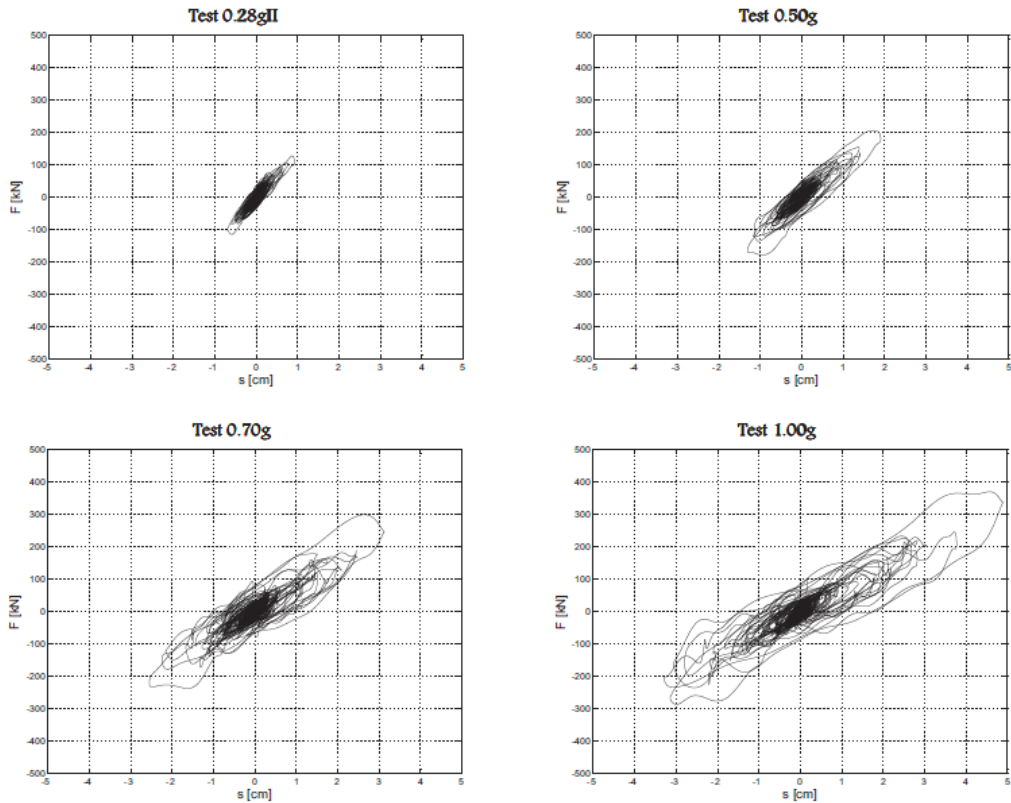


Figure 6.26: Global hysteretic response curves

Analysing the previous pictures no stiffness variation for the first three phases of the test can be observed, while a slight degradation in the last seismic test, confirmed also by the dynamic identification results, appears. The hysteresis loops increase with the displacement of the structure, showing an energy dissipation also in the early stages of testing. The maximum inertial force recorded for the test to 1.00 g is equal to 368 kN, in correspondence of a relative displacement of 4.9 cm.

In Figure 6.27 the peak base force achieved in each of the hysteretic cycles versus the corresponding peak roof relative displacement and the capacity curve obtained by the numerical model B is reported. The behaviour of the tested structure is almost linear up to the displacement reached in the test at 0.70 g and then undergoes an abrupt decay of stiffness in the next test (1.00 g). Comparing the tested structure capacity curve to the model one, an higher stiffness of the tested building can be observed. Moreover it would

appear that the peak force of tested structure is lower the model one. However this does not be stated for certain as no significant damages were observed after 1.00 g seismic test. Likely the structure could have been tested for higher seismic input achieving the failure conditions for higher base force peak values.

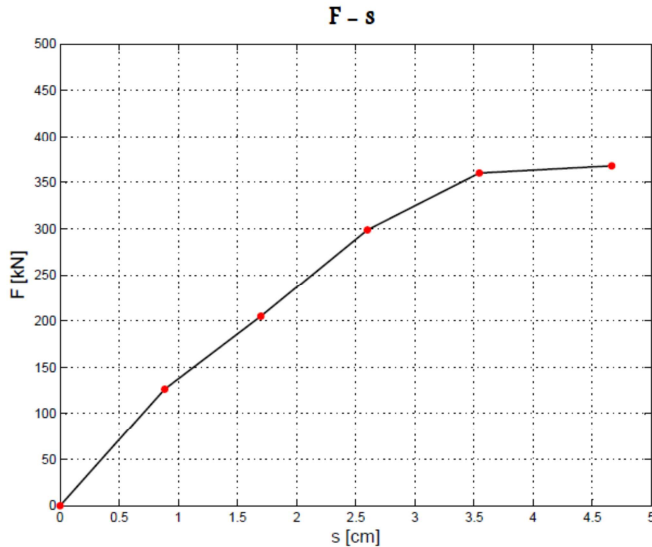


Figure 6.27: Peak base force vs roof displacement curve

6.4.2 Modal testing

Modal test analysis was carried out to identify the dynamic properties of the specimen, and evaluate the relation between dynamical parameters variation and damage occurred to the building prototype. In fact an increase of the period may be related directly to the decrease of structural stiffness of the building and hence to its damage.

During the experimental campaign two type of modal testing were performed: ambient noise vibration tests before the first and after the last seismic test, by means of a limited number of geophones (Figure 6.28) positioned according the configuration illustrated in Figure 6.29; random vibration tests during the shaking table tuning phase, using data

3-STOREY TIMBER-FRAME BUILDING SHAKE TABLE TEST

collected by the accelerometers (Figure 6.30) configuration shown in Figure 6.31. The techniques used for signal analysis were made in both cases in the frequency domain.

In the case of ambient noise vibration test Output-Only techniques were adopted since the acquisition involved only the response of the structure due to an unknown input noise. Basic Frequency Domain (BFD) and Frequency Domain Decomposition (FDD) techniques were adopted in this case. On the contrary, for random vibration tests during the shaking table tuning phase, the input signal recorded by the accelerometers on the shaking table itself was available, and in this case was possible to consider a input-output system and therefore directly calculate the Frequency Response Functions (*FRFs*).

In both methods the analysed signal can be assumed as random. For this reasons, in order to reduce leakage, the Welch method with a Hanning window was employed. The frequency resolution resulted equal to 0.0625 Hz.



Figure 6.28: *Geophones used for the dynamical identification of the structure*

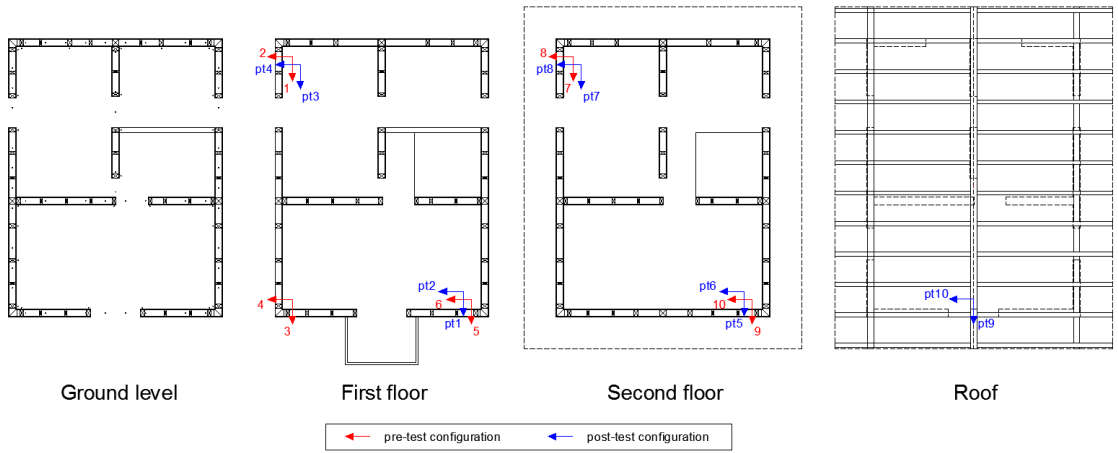


Figure 6.29: Geophones layout



Figure 6.30: Accelerometer

3-STOREY TIMBER-FRAME BUILDING SHAKE TABLE TEST

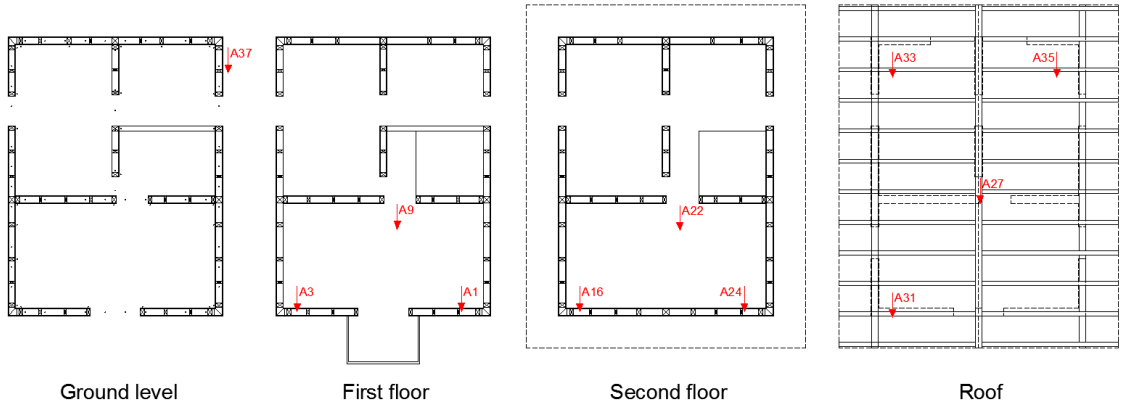


Figure 6.31: Accelerometer layout

In order to identify the frequencies of the system, taking into account that the main vibration modes are related to the flexural deformation in two different directions, the Cross Spectra (X Spectra) of two channel pairs referring to the same direction were analysed, reporting the amplitude, phase and coherence parameters in function of the frequency (according to the BFD technique the peaks of amplitude of cross-spectra are associated to the modes of the structures).

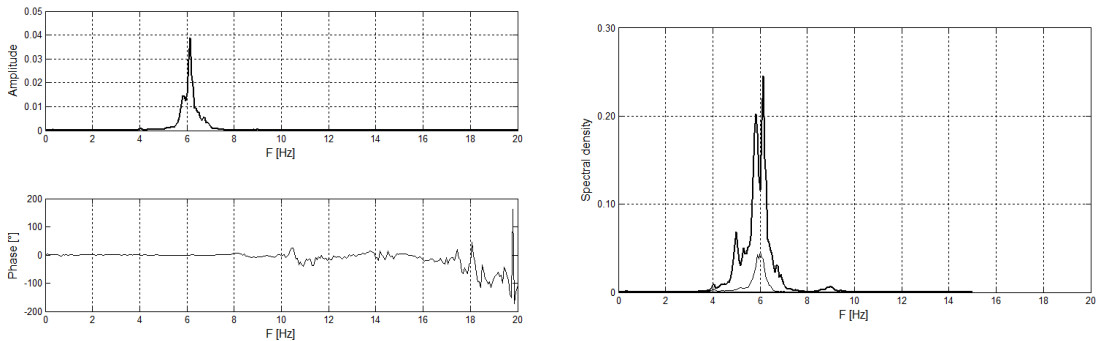


Figure 6.32: Analysis made with BFD (a) and FDD (b) methods before the first seismic test

Referring to ambient noise vibration test performed before the seismic sequence, the amplitude and phase of the cross-spectrum between the channels 5 and 9 (longitudinal

direction) show a peak amplitude for a frequency equal to 6.125 Hz (Figure 6.32,a). The phase equal to 0° confirmed that the motion is actually of fundamental flexural mode shape. Similarly, analysing the cross-spectra relative to the transversal direction, a first flexural mode was observed at the frequency of 5 Hz. Less information is instead provided from the graphs regarding the second flexural mode.

In order to validate the results obtained from the BFD the FDD method was employed. In Figure 6.32 (b) is reported the Singular Value Decomposition (SVD) of the Power spectral density (PSD) matrix of the response. It is possible to note the presence of three peaks in correspondence of the following frequency values 5, 5.875 and 6.125 Hz. The study of the modal shapes revealed that the frequencies 5 Hz and 6,125 Hz, as observed with the BFD method, are actually associated with the two bending modes respectively in the transversal and longitudinal directions. The peak corresponding to the frequency of 5,875 Hz is not associated with any significant mode shape.

Referring to ambient noise vibration test performed after the last seismic test, a geophone was also positioned on the roof ridge of the building, according to configuration shown in Figure 6.33. As in the previous case, the process of dynamic identification was carried out both through the BFD and FDD methods.

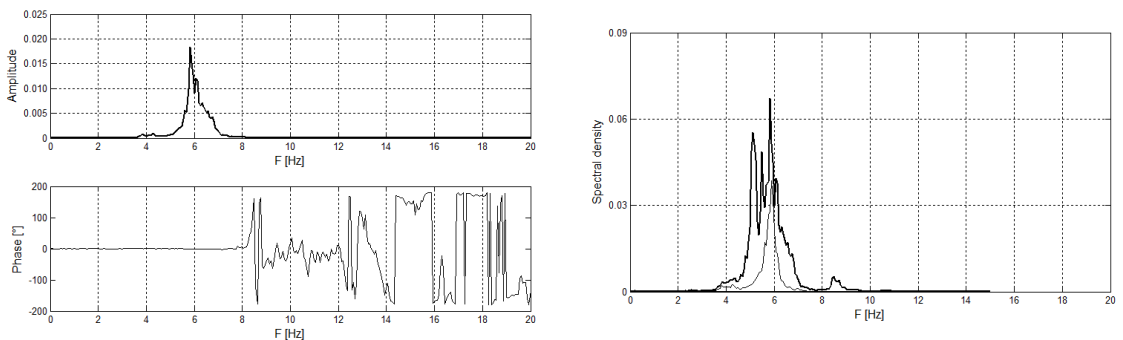


Figure 6.33: Analysis made with BFD (a) and FDD (b) methods after the last seismic test

The amplitude and phase of the cross-spectrum between the channels 5 and 9 (longitudinal direction) show a peak amplitude at a frequency equal to 5.813 Hz (Figure 6.33,a , highlighting a slight decrease of the fundamental frequency in the longitudinal

direction of the building, and hence the achievement of the non-linear behaviour during seismic tests.

On the contrary, the results of cross-spectra relative to the transversal direction did not show any variation of the dynamic properties of structures: in fact the peak value frequency remained equal to 5 Hz, the same measured before the seismic tests.

The same results were confirmed by the FDD technique (Figure 6.33, b).

The analysis method used to performed the dynamic identification of the structure in case of random vibration tests belongs to input-output methods. In fact, unlike the ambient vibration test, in this case the input signal measured by accelerometer on the shake table was available. A FRF function was obtained for each channel, monitored by an accelerometer, as the ratio in the frequency domain between the output signal (referred to the considered degree of freedom) and the input signal (referred to the shake table). This process can be classified as single-input multiple-output (SIMO): the Peak Peaking amplitude method (PP), where the natural frequencies are taken from the observation of the peaks of the amplitude of the frequency responses function, was adopted.

Since the structure was excited along its symmetric axis in the longitudinal direction, no significant information was recorded by the accelerometers referred to transversal and vertical direction. For this reason only the ten longitudinal accelerometers were considered. However, taking into account the output only results, no transversal natural frequency variation was expected. An example of FRF function for the identification test after 0,7 g seismic test, referred to the accelerometer A27 located on the top of the roof, is reported in Figure 6.34.

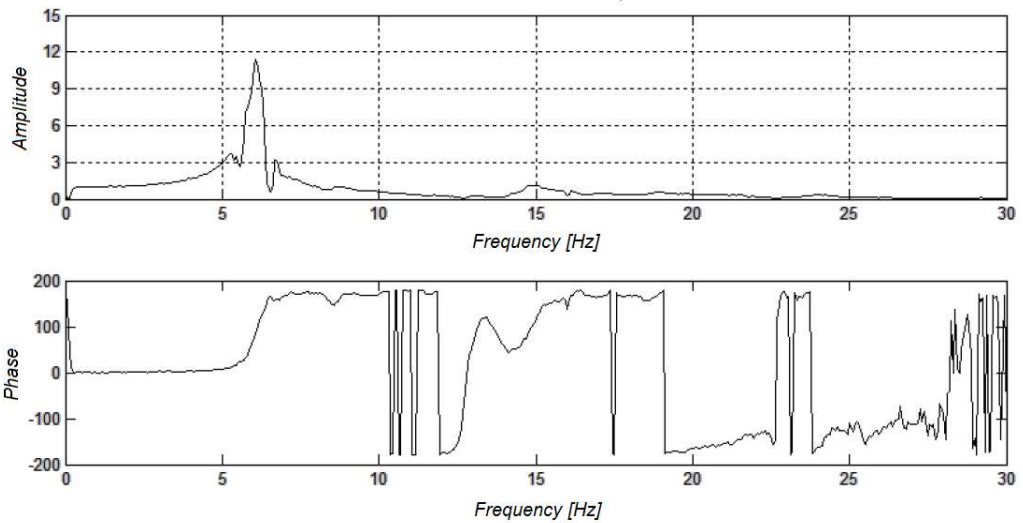


Figure 6.34: FRF function for the accelerometer A16 placed on the second floor for identification test after 0.7 g seismic test

Only for the longitudinal direction in the various identification tests are reported in Table 5 the period and the frequency, and in figures 19, 21 and 24 the mode shapes.

Modal test	Instruments	T_1 [s]	f_1 [Hz]	Analysis method
before 0.07 g	geophons	0.1633	6.1250	Output only BFD/FDD
after 0.28 g I	accelerometers	0.1633	6.1250	Input/output PP
after 0.28 g II	accelerometers	0.1633	6.1250	Input/output PP
after 0.50 g	accelerometers	0.1649	6.0625	Input/output PP
after 0.70 g	accelerometers	0.1649	6.0625	Input/output PP
after 1 g	geophons	0.1720	5.8125	Output only BFD/FDD

Table 6.8: Frequency and the fundamental period in the longitudinal direction in the various tests

The variation of the fundamental period after each seismic test is shown in Figure 6.35.

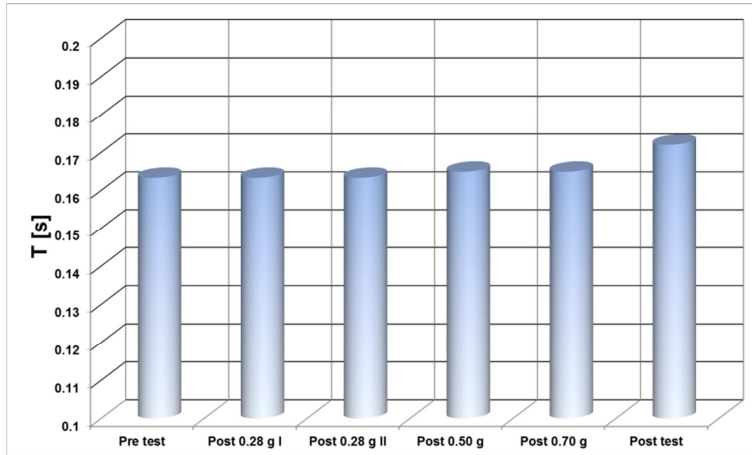


Figure 6.35: Variation of the period in the longitudinal direction after each seismic test

From Figure 6.35 and Table 6.8 no variation of the natural frequency can be observed after the seismic tests with a PGA lower than 0.28 g, and a very small change can be associated to 0.5 g and 0.7 g seismic test. After the last test at 1 g PGA a more significant natural frequency variation was obtained. On the contrary the mode shapes seem not to be changed significantly for all test stages.

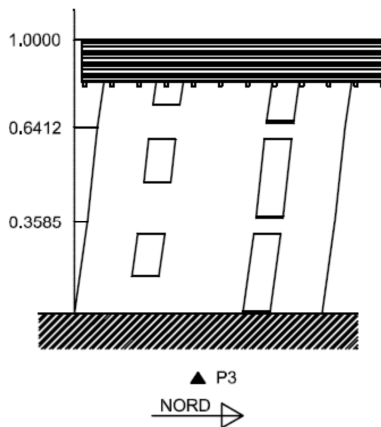


Figure 6.36: Fundamental mode shapes of the building at a frequency of 6,125 Hz in transversal direction (Y)

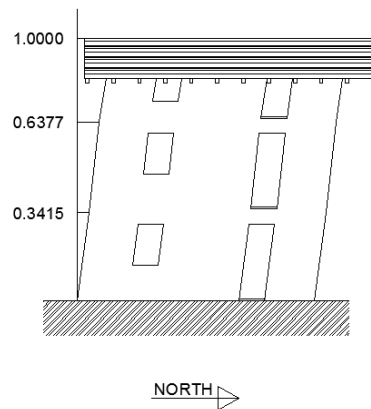


Figure 6.37: *Lateral and from above view of the mode shapes of the building at a frequency of 5.813 Hz - Method FDD*

The experimental results suggest that the dynamic behaviour of the structure can be considered linear and elastic for all the seismic test stages performed, except for the last one at 1 g PGA, where, as confirmed by measured reported in the previous chapter, the structure seems to enter in the non - elastic range.

The equivalent viscous damping characteristics of the test structure can be determined from a FRF function using the half-power bandwidth method. This method was performed from the frequency response, previously determined through the accelerometers for all seismic tests performed. The damping coefficient remains approximately constant at around 4% during the tests carried further confirmation of the fact that the structure has not suffered damage and deformation remained in the elastic range.

6.5 Analysis of results

In this section the main results are discussed concerning with different recorded physical parameters.

From Table 6.6 the amplification of the maximum acceleration can be obtained. This can be defined as the ratio between the peak recorded values and the peak table acceleration:

$$\alpha = \frac{a_{i,max}(g)}{a_{shake\ table, max}(g)} \quad (6.1)$$

Referring to the acceleration recorded in the centre of floors ($i=9$ and 22) and of the roofs ($i=27$) an average equal to 0.82 and 0.88 respectively for the first and the second floor can be calculated up to the test of 0.70 g. These values increased respectively to 0.88 and 1.01 for the test at 1.00 g. The maximum amplification of the roof is between 1.08 and 1.19.

The distribution of the horizontal accelerations registered for each storey for all the seismic tests, except for the 1.00 g test, is uniform, which is consistent with the symmetry of the building. The absence of torsional effects is also confirmed by very low values of acceleration in the transverse direction of the building.

The acceleration values are increasing with the height of the building. The peak measured acceleration is equal to 1.68g. Although the structure did not damage during seismic tests, very high acceleration values were recorded. Therefore, particular attention should be paid in the arrangement of furniture to avoid that they may fall over the occupants. Advanced techniques could be designed, such as the increasing of structural damping, in order to limit the accelerations at the top floors.

The feed-back pseudo acceleration response spectrum is consistent with the reference response spectrum for structural periods greater than 0.8 s but in the high frequency range the former values are greater (Figure 6.18). At the value of the building fundamental period the feed-back response spectrum is characterized by high peaks.

For the seismic tests before 0.70 g test, the peak drift was lower than 0.8%: the structure may have been in the elastic range with high probability. The 1.00g seismic test was characterized by a peak inter-story displacement of 31 mm corresponding to a drift of 1.24% (Figure 6.19).

For the seismic tests before 0.50 g test no significant Hold – Down tensile force was measured so that they can be considered not in-tension (Table 6.7). The 0.50 g test is characterized by hold-down tensile force lower than 15 kN. In the last two seismic tests (0.70 g and 1.00 g) all Hold downs worked significantly. The peak measured forced was of 38.8 kN, corresponding to an uplift of 4.4 mm (Figure 6.24). The in-plan hold down force distribution suggests that each wall behaves likes a cantilever with high tensile forces. Moreover, observing the tensile forces in the building corners (Figure 6.21 and Figure 6.22), it is assumed that the two orthogonal wall collaborate. In conclusion, from the measurements recorded in the load cells, the positioning of the hold downs in the proximity of door or window openings is suggested in order to prevent the rigid-body rotation of each wall.

The dynamic identification, carried out by means of different techniques in the frequency domain processing the signals recorded by the geophone and by the accelerometers, allowed to assess the natural frequency of the undamaged structure in the input seismic direction: 6.125 Hz (Table 6.2). This value is associated with a modal shape almost linear with height (Figure 6.36). The estimated frequency remains constant for the seismic tests with a nominal peak ground acceleration lower than 1.00 g (variation of about 1%). After the 1.00 g test the natural frequency decreased up to a value equal to 5,813 Hz (5% variation). That obtained results shows that the structure remained in the elastic range until the last test. The variation in the last phase suggests that the structure entered the inelastic range even if no visible damage were observed. The calculation of the equivalent modal damping was carried out in the frequency domain by means of the semi amplitude method. The average value obtained from the various channels is equal to 4% and is almost constant for all the tests, confirming no structural damage.

The base timber beam slippage was almost zero for all test phases, confirming the effectiveness of the adopted connection. The building did not suffer, therefore, horizontal displacements resulting from a horizontal rigid motion. The timber wall sliding on the ground floor results lower than 1 mm up to the 0.28 g test. The maximum peak value, equal to 4 mm, was recorded in the last test on the outside wall at the first floor (Figure 6.23). The sliding values of the first floor walls were always lower than the ground floor wall ones, with a maximum peak value equal to 2.3 mm.

3-STOREY TIMBER-FRAME BUILDING SHAKE TABLE TEST

Regarding to the floor in plane deformation, the signals recorded by the instruments wire potentiometers were characterized by peak values lower than 1 mm for all seismic tests. This confirms a diaphragm behaviour of the floors according to the design hypothesis. The elongation recorded on the roof was higher, reaching a value of 4.1 mm. The in plane stiffness of the roof is adequate anyway, although lower, as expected, than the floor one. The recorded sliding between the box elements of the floor (lower than 0.6 mm) confirm the diaphragm behaviour assumption .

The base force vs displacement curve confirms that the structure remained in the elastic range up to the 0.70 g test . In fact the global building stiffness remained unchanged. A decrease is shown during the 1.00 g test

7 CONCLUSIONS

The work presented in this thesis dealt with the study of the timber frame building seismic behaviour by means of numerical modelling and a full scale shake table testing. Three were the main objectives of the work, namely: *a)* the introduction of a suitable numerical model for the linear analyses of timber frame buildings under horizontal loads, *b)* the study of the nonlinear behaviour of 1-storey timber frame wall by means of an analytical approach capable to relate the local ductility of connectors to the global ductility of the wall and lastly, *3)* the investigation of the seismic response of a timber frame building, subjected to increasing seismic input levels, by means of the processing and the analysis of several data recorded during a full scale shake table test. For each of them the main conclusions are reported.

7.1 Linear backup numerical modelling (*a*)

In Chapter 5 an analysis model for the prediction of the linear behaviour of a series of timber frame walls under horizontal forces was proposed. The model is based on the simplified numerical model of a 1-storey timber frame single wall presented in Chapter 3

and it considers all significant sources of deformation, namely: sheathing panel, sheathing-to-frame fastener global connection, rigid body translation and rigid body rotation. The model can be used for both linear static analyses (i.e. wind load analyses) and linear seismic analyses, such as the lateral force method (LFM) of analysis and the modal response spectrum method (MRS). The three main characteristics of the proposed analysis model are summarized in this section.

Firstly, the distribution of the horizontal forces is carried out considering the real stiffness of timber frame walls and not assuming that the wall stiffness depends only on its length. It was demonstrated that the contribution of the rigid body rotation linearly depends on the squared length of the wall. The more significant this contribution is (flexible hold-down), the greater the non-linearity between the wall stiffness and the wall length is. Moreover, the horizontal seismic forces are not distributed storey by storey but a complete model is required. For this reason a different distribution of forces can occur along the height of the structure.

Secondly, it was shown that the distribution of horizontal forces strongly depends on vertical loads, since this produces a stabilizing moment on the walls. This aspect becomes more important for high buildings where the horizontal displacement, caused by the rigid rotation of the wall, is significant. For this reason in the analysis model the vertical load on the walls must be defined. If a hold-down is characterized by a compression axial force, an updating of the model is required. The hold-down must be substituted by a vertical axially rigid pinned beam because the rigid-body contribution must be neglected in the analysis. When the stabilizing moment (of the vertical loads) on the wall is greater than the overturning moment caused by horizontal loads, the wall is in fact not subjected to a rigid rotation. For this reason an iterative process of analysis may be necessary to get a consistent solution.

Thirdly, the application of the MRS analysis to timber frame walls was presented. In common practice, in fact, most seismic designs of timber frame buildings are performed by a LFM analysis, even when non regular in elevation.

7.2 Analytical analysis model of 1-storey timber frame wall nonlinear behaviour (b)

In chapter 5 an analytical approach for the prediction of elasto-plastic behaviour of a 1-storey timber frame wall under a horizontal force was presented. The strength, the stiffness and the ductility of the wall can be calculated from the mechanical and geometrical properties of structural elements and connection devices by means of some simple equations.

The main goal of this study was the definition of the relationship between the local ductility of connectors (sheathing-to-frame fastener, hold-down and angle brackets and the global ductility of the wall as required in common seismic design of structures. By means of the proposed expressions the structural components of the wall can be design to satisfy the ductility demand depending on the q factor used to calculate the seismic force of the structure.

The key aspect of the study is without any doubt the representation of the global nonlinear behaviour of sheathing-to-frame fasteners by means of a singular elasto-plastic horizontal spring, which properties (strength, stiffness and ductility) are defined depends on the mechanical properties of fasteners, their spacing the geometrical ratio of the sheathing panels. The analytical expressions used for the definition of the horizontal spring mechanical properties were obtained performing several elasto-plastic analyses of fully anchored walls, considering the sequential yielding of the sheathing-to frame fasteners. A code in MatLab was implemented.

The substitution of the sheathing-to-frame global connection with a simple elasto-plastic horizontal spring reduces considerably the number of degrees of freedom of a single wall numerical model. For this reason this representation can be implemented in order to carry out static nonlinear analyses of series of walls, exactly as in case of multi-storey series of wall linear analyses. On the contrary, a complete modelling of all fasteners nonlinear behaviour might be time-consuming.

7.3 Full scale 3-storey timber frame building shake table test (c)

In chapter 6 the design, the execution and the analysis of the results of a full scale 3-storey timber frame building shake table test was presented. According to the results reported in chapter 6, conclusions have been drawn regarding the expected and the shown behaviour of the tested building. The key results obtained are summarized below.

- a) The visual inspections showed that the building was not visible damaged during all seismic tests. However the analysis of the results (dynamic identification, capacity spectrum, inter storey drift) confirmed that during the 1.00 g test the structure went beyond its linear elastic limit. The increase , even if modest, of the fundamental period of the structure, the variation of slope of the force-displacement curve, the values of the peak forces measured in the Hold- Down load cells and the inter storey drift peak values confirm this assumption.
- b) The building was designed for a peak ground acceleration equal to 0.28 g (return period of 475 years). The behaviour factor q was assumed equal to 4 (high energy dissipation). A safety factor of 1 was used for all structural verifications both for materials and for connections. The sizes of the building structural elements , the type and the number of the connection devices were chosen in order to minimize the structural over strength but in accordance with the traditional construction practice. In order to properly comment the relationship between the expected response of the structure and that showed one, it may be interesting to report the over-strength values obtained in the design phase. The longitudinal direction wall at the ground floor subjected to the maximum action was the GL_W02_Y wall .

Structural component	Over strength
Sheathing to framing connection	$\frac{F_{v,Rd}}{F_3} = \frac{33.1 \text{ kN}}{12.8 \text{ kN}} = 2.59$
Wall rigid body translation: inclined screws	$\frac{F_{v,Rd}}{F_3} = \frac{19.3 \text{ kN}}{12.8 \text{ kN}} = 1.51$
Wall rigid-body rotation: hold down	$\frac{F_{t,Rd}}{F_{Pterra}} = \frac{31.4 \text{ kN}}{12.3 \text{ kN}} = 2.59$
Stud instability	$\frac{F_{c,0,d}}{K_{crit} \cdot f_{c,0,d}} = 6.67$

Table 7.1: *Over strength factors*

c) According to the results of Table 7.1 the building design over-strength can be assumed equal to 1.51. The design peak ground acceleration which for the structure reaches its ultimate limit state should be obtained multiplying the design peak ground acceleration (0.28 g) by the building design over strength (1.51), getting 0.42 g. According to the assumed high behaviour factor value ($q=4$) a significant structural damage is expected. The building was tested by nominal peak ground accelerations up to 1.00 g. The building showed no damage which can be compared with the ultimate limit state expected ones .

d) A further comparison may be made observing the prediction results obtained by the push over analysis . This analysis was performed taking account of both the real strength of materials and connections (obtained from experimental data). According to the obtained results the second building analysis model (model B), in which the Hold-Down are fixed, is assumed the most suitable. The structural elastic limit was obtained for a PGA of 0.70 g whereas the structure failure PGA was assessed equal to 1.00 g.

e) The seismic tests showed that an acceleration close to 1.00 g identifies the transition from the elastic to the inelastic range. Hence the real seismic performance of the structure can be considered higher than the predicated one. The main reasons in the author's opinion are given in the following:

- the design analysis method is based on simple assumptions about the seismic behaviour of the building. The distribution of horizontal forces, the study of the influence of orthogonal walls and the dynamic study of the structure, are just

CONCLUSIONS

some of the aspects that need to be investigated more accurately in order to make the design more accurate;

- The timber frame walls are characterized by a cantilever behaviour. The tensile forces measured at each hold down are representative of the significant rigid-rotation contribution;
- The over-strength of the structural components of the building is not due to an inaccurate design but to common detailing constructive rules that guarantee a good behaviour of the structure (the maximum spacing of connectors, the sizes of structural elements and so on).

The design and verification criteria adopted assured the safety of the tested building since no damage was observed for acceleration values much higher than the design ones. However this statement cannot be generalized to the analysed structural type. The reliability of the design criteria (especially of the behaviour factor) cannot be judged without separating and quantifying the contributions of each structural element. An extended campaign on several buildings characterized by different properties (the number and the positioning of the walls, failure mechanism, etc.) should be carried out in order to compare the role of each contribution

REFERENCES

1. Andreolli, M., Grossi, P., Sartori, T., Tomasi, R. [2013] Design and production of an heavy timber reaction frame for a laboratory test set-up. ICSA
2. Andersen, P., Brincker, R., Zhang, L., [2001] Modal identification of output-only systems using frequency domain decomposition. Smart material e structures 10, pag. 441-445
3. Armanini, A. [2011] Prova su tavola vibrante di un edificio in legno a pareti portanti intelaiate: progetto ed esecuzione. Master's thesis, Dipartimento di Ingegneria Meccanica e Strutturale, University of Trento
4. Bendat, J. S., Piersol, A. G., [1986] Random Data: Analysis and Measurement Procedures, John Wiley & Sons
5. Clough, R. W. and Penzien, J. [1975] Dynamics of structures, McGraw Hill Book Co., NY

6. Conte, A., Piazza, M., Sartori, T., Tomasi R. [2011], Influence of sheathing to framing connections on mechanical properties of wood framed shear walls. In Congresso Ingegneria Sismica Anidis
7. Conte, A., Piazza, M., Tomasi, R., Sartori, R. [2010] Indagine sperimentale su collegamenti tra fondazione in calcestruzzo e pareti intelaiate lignee. Technical report, Dipartimento di Ingegneria Meccanica e Strutturale, University of Trento
8. Christovallis, I.P., Filiatrault, A., Wanitkorkul, A. [2007] Seismic testing of a full-scale two-story light frame wood building: NEESWood benchmark test, NEESWOOD report NW-01, University at Buffalo
9. CSA 086-01:2005 [2005], Engineering design in wood, CSA, Canadian Standard Association, Toronto (Canada)
10. Daudeville, L., Richard, M., Yasamura, M. [2004] Seismic response of timber frame structures: experiment and finite element modelling, Engineered wood products association, 132
11. Dolan, J.D., Foschi O.R. [1991], Structural analysis model for static loads in timber shear walls, Journal of Structural Engineering, 117(3):851-861
12. Dujic, B., Zaranic, [2004] R. Method for mode model dynamic response of timber frame buildings, Engineered wood products association, 295
13. Ehlbeck, J., Kreuzinger, H., Steck, G., Blaß, H.J., [2005] DIN 1052 Erläuterungen. Bruderverlag
14. EN 1995-1-1/A1 [2008] Eurocode 5. Design of timber structures Part 1-1: General-common rules and rules for building. Brussels, Belgium: CEN, European Committee for Standardization
15. EN 1998-1/A1 [2013] Eurocode 8. Design of structures for earthquake resistance - Part 1: General rules, seismic actions and rules for buildings. Brussels, Belgium: CEN, European Committee for Standardization

16. Ewins, D.J., [2000] Modal testing: theory, practice, and application, Research Studies Press
17. Fajfar, P. A [2000] Nonlinear Analysis Method for Performance-Based Seismic Design, Earthquake Spectra, 16 (3), pp. 573-592
18. Filiatrault, A., Isoda, H., Folz, B. [2003] Hysteretic damping of wood framed buildings, Engineering Structures, 25(4):461-471
19. Filiatrault, A. and Fischer, D. [2001]. Shake table tests of a two-storey woodframe house. Technical Report, CUREE Publication No. W-06
20. Filiatrault, A., Fischer, D., [2001]. Shake table tests of a two-storey woodframe house. Technical Report, CUREE Publication No. W-06
21. Filiatrault, A., Uang, C-M., and Seible, F. [2000] Ongoing seismic testing and analysis program in the CUREE-Caltech woodframe project in California, Proc. of World Conference on Timber Engineering WCTE 2000, Whistler, Canada
22. Folz, B., Filiatrault, A. [2002] Seismic analysis of woodframe structures: model formulation, Journal of structural engineering, 130(9):1353-1360
23. Girhammar, U. A., Kallsner, B. [2009] Analysis of fully anchored light-frame timber shear walls-elastic model, Materials and Structures, 42 p. 301-320
24. Grossi, P., Sartori, T., Tomasi, R. [2014] test on timber frame walls under in-plane forces: Part 1. Proceedings of the Institution of Civil Engineers Structures and Buildings 2014; Special Issue on Seismic test on Timber Buildings:xx
25. Gupta A. K., Kuo, G.P. [1985], Behaviour of timber-framed shear walls, Journal of Structural Engineering, 111(8):1722-1733
26. Gupta, A. K., Kuo, G.P. [1987] Timber-framed shear walls with uplifting. Journal of structural engineering, 113(8):241-259

27. Judd, J., Fonseca, F. [2005] Analytical model for sheathing-to framing connections in wood shear walls and diaphragms, *Journal of structural engineering*, 131(8): 345-352
28. Kallsner, B., Girhammar, U.A. [2004] A plastic lower bound method for design of timber-framed shear walls. *WCTE*, pages 129-134
29. Kallsner, B., Girhammar, U.A. [2009] Plastic models for analysis of fully anchored light-frame timber shear walls *engineering Structures* 31(9):2171-2181, pages 129-134
30. Kasal, B., Leichti, R., Itani, R. [1994] Nonlinear finite-element model of complete light-frame wood structures, *Journal of Structural Engineering*, 120(1):100-119
31. Kessel, M.H., Kammer Z.K. [2004] Three-dimensional load-bearing behaviour of multi-storey timber frame buildings, *WCTE*
32. Loss, C., Zonta, D., Piazza, M. [2012] Analytical model to evaluate the equivalent viscous damping of timber structures with dowel-type fastener connections, *WCTE*
33. Mischi, G. [2012] Comportamento non lineare di una parete intelaiata in legno: proposta di un approccio analitico
34. Modena, R., Piazza, M., Tomasi, R., [2006] *Strutture in legno*, Hoepli
35. NTC08 [2008] "Norme tecniche per le costruzioni," Ministero delle Infrastrutture e dei Trasporti, Decreto Ministeriale del 14 gennaio 2008, Supplemento ordinario alla G.U. n. 29 del 4 febbraio 2008 (in Italian)
36. NZS 3603 [1993], *Timber Structures Standard*. NZS, Wellington, New Zealand
37. Porteous, J., Kermani, A., [2008] *Structural Timber Design to Eurocode 5*, John Wiley & Sons
38. Rossi, S. [2012] Formulazioni analitiche, modelli numerici e metodologie di calcolo per l'analisi di edificio in legno soggetti a forze orizzontali, Master's thesis, Dipartimento di Ingegneria Meccanica e Strutturale, University of Trento

39. Salenicovich, A.J. [2000] The racking performance of lighthframe shear walls. Ph.D. thesis, Wood Science and Forest Product, Virginia Polytechnic Institute and State University,VA
40. Sartori T., Piazza M., Tomasi R., Grossi P. [2012b] Characterization of the mechanical behaviour of light-frame timber shear walls through full-scale tests, Proc. of World Conference on Timber Engineering WCTE 2012, Auckland, New Zealand
41. Sartori T., Tomasi R. [2013] Experimental investigation on sheathing-to-framing connections in wood shear walls, Engineering Structures, v. 56, (2013), p. 2197-2205
42. Sartori, T. [2012] Structural behaviour of timber framed buildings, PhD Thesis, University of Trento (Italy)
43. Silva J.M., Maia N.M. [1999] Modal Analysis and Testing, Proc. of the NATO Advanced Study Institute on Modal Analysis and Testing, Sesimbra, Portugal, 3-15 May, 1998, Springer Verlag
44. Sullivan T. J., Pinho R., Pavese, A. [2004] An Introduction to Structural Testing Techniques, Earthquake Engineering Research Report Rose School
45. Tarabia, A.M., Itani R.Y., [1997] Static and dynamic modeling of light-frame buildings, Computers & Structures, 63(2):319-334
46. Tomasi R., Sartori T. [2013] Mechanical behaviour of connections between wood framed shear walls and foundations under monotonic and cyclic load, Construction and Building Materials, v. 44, (2013), p. 682-690
47. Van de Lindt J.W. , Rosowsky D.V, Filiatrault A. , Symans M.D., Davidson R.A. [2006] Development of a Performance-Based Seismic Design Philosophy for Mid-Rise Woodframe Construction: Progress on the NEESWood Project, Proceedings of WCTE 2006 – World Conference on Timber Engineering – August 6-10, 2006, Portland, OR, US

PUBLICATIONS

- I. **D. Casagrande**, S. Rossi, T. Sartori, R. Tomasi, "Analytical and numerical analysis of timber framed shear walls" in World Conference on Timber Engineering 2012, WCTE 2012, Auckland, New Zealand: [WCTE 2012], 2012, p. 497-503. Proceedings of: WCTE, Auckland, New Zealand, 2012. - URL: <http://www.scopus.com/inward/record.url?eid=2-s2.0-84871990992&partnerID=40&md5=1e83875ec17c44d53d51b4c8f7b91c21>
- II. **D. Casagrande**, P. Grossi, T. Sartori, R. Tomasi, "Seismic behaviour of timber frame multi-storey buildings" in COST Action FP1004 , Zagabria: University of Bath, 2012. Proceedings of: COST, Zagabria, Croazia, April 19-20, 2012
- III. T. Sartori, **D. Casagrande**, R. Tomasi, M. Piazza, "Shake table test on 3-storey light-frame timber building" in World Conference on Timber Engineering 2012, Auckland, New Zealand: [WCTE2012], 2012. Proceedings of: WCTE2012, Auckland, New Zealand, 2012. - URL: <http://www.scopus.com/inward/record.url?eid=2-s2.0-84871969766&partnerID=40&md5=9b01423080c8df89ea5a3d907f520ccf>

- IV. M. Andreolli, **D. Casagrande**, M. Piazza, A. Polastri, T. Sartori, R. Tomasi, "Test sismici su tavola vibrante di un edificio a tre piani in legno a pannelli portanti intelaiati" in Conference proceeding XIV Convegno ANIDIS , Bari: Anidis , 2011. - ISBN: 9788875220402. Proceedings of: Anidis2011, Bari, 18 - 22 settembre 2011
- V. R. Tomasi, T. Sartori, **D. Casagrande**, M. Piazza, " Shaking table test on a full scale three-storey timber framed building" in Journal of Earthquake Engineering, *submitted*
- VI. **D. Casagrande**, S. Rossi, T.Sartori, R. Tomasi, "Analytical and backup numerical modelling for linear elastic response of single-storey timber shear walls subjected to horizontal force: a unified-iterative approach" in Engineering Structures, *submitted*
- VII. R. Tomasi, **D. Casagrande**, P. Grossi, T.Sartori, "Shaking table test on a three-storey timber building with OSB sheathing panels" in Insitution of Civil Engineers – ICE, *submitted*